aquifers was examined by taking account of the following conditions;

The Lower Ajlun (A1-6) ; Hydrochemistry of the groundwater basin has not been studied except for a limited area in the southern part of the Jafr basin.

The Amman - Wadi Sir (B2/A7) ; The aquifer is believed to satisfy the quality requirements.

The Rijam (B4) ; Part of this aquifer has been contaminated by irrigation return with high salinity.

5.4.2 Lower Ajlun (A1-6) aquifer

The lower Ajlun (A1-6) has not been regarded as a promising aquifer due to the lack of information on both hydrogeology and hydrochemistry.

In 1985 NRA carried out a series of chemical analysis on the water samples from seven project boreholes. The boreholes, which penetrate the whole of the lower Ajlun (A1-6) in and around the Shidiya area in the southern part of the Jafr basin, is composed of alternating sandstones and shales with rather low apparent resistivities of less than 100 ohm-m. The values of E.C are in the range between 1,000 and 2,750 micromho/cm and of T.D.S between 700 and 2,000 mg/l, which follow the slightly saline water environment and/or the stagnant water environment. At the southwestern edge of the A1-6 aquifer where the narrow bands of outcrop receive rainfall, the groundwater is fresh with T.D.S of 600 to 700 mg/l, while the water salinity increases up to 1,728 to 2,048 mg/l towards the east basin boundary.

The spatial variation of water salinity (T.D.S) in the carbonate rocks is dependent on the aquifer characteristics such as formation lithology, recharge area and distance of groundwater flow. North of the Salwan fault, the groundwater in the lower Ajlun (A1-6) aquifer is mainly derived from the A4 formation which is arenaceous consisting of medium to coarse homogeneous sandstones with a very high aquifer pressure of 30 kg/cm^2, which explains the very low range in water salinity such as T.D.S of 326 mg/l. The sand layer in the A4 acts as a sand filter to percolating groundwater flow in the lower Ajlun. The following is a summary of the chemical analysis of a water sample from JT-3;

Well No.	E.C m.mho/cm	T.D.S mg/l	pH -	Ca^{++} mg/l	Mg^{++} mg/l	Na^{++} Mg/l	K^{+} mg/l	Cl^{-} mg/l	$SO4^{--}$ mg/l	$CO3^{--}$ mg/l	$HCO3^{-}$ mg/l
JT-3	0.510	326	7.3	46.5	21.2	20.7	14.9	25.9	33.6	0.0	235.5

The above result is figured on a Piper's tri-linear diagram. JT-3 is plotted in the area of "carbonate hardness" as seen in Fig.5.11. The quality is excellent in meeting drinking water standards, and is suitable for most uses.

A water salinity (E.C) map of the lower Ajlun (A1-6) is shown in Fig.5.21.

5.4.3 Amman - Wadi Sir (B2/A7) aquifer

The Amman - Wadi Sir (B2/A7) has been identified as a promising aquifer to satisfy the water requirements of the Study area. The hydrochemistry of this aquifer has been examined more detail than any other aquifers except for the areas of the northeastern part of the Jafr basin and the eastern part of the upper Hasa basin where no drillings were carried out before this study. The water samples of the B2/A7, which were collected from the test wells such as at JT-1, JO-3 and JO-5, were analyzed at WAJ's chemical laboratory in Amman. The following is a summary of the chemical analysis of the water samples;

Well No.	E.C m.mho/cm	T.D.S mg/l	pH -	Ca^{++} mg/l	Mg^{++} mg/l	Na^{++} Mg/l	K^{+} mg/l	Cl^{-} mg/l	$SO4^{--}$ mg/l	$CO3^{--}$ mg/l	$HCO3^{-}$ mg/l
JT-1	0.620	397	7.4	53.1	28.6	27.6	3.5	52.5	20.2	0.0	257.5

JO-3	1.000	653	7.2	86.2	46.6	62.1	5.9	105.3	129.7	0.0	340.5
JO-5	1.830	1,171	8.1	163.1	54.2	190.9	9.4	141.5	532.2	0.0	339.9

The regional E.C values in the B2/A7 aquifer are less than 700 micromho/cm in the Western Highlands, 1000 to 1,400 micromho/cm in the central part of the Jafr basin, and 4,000 to 6,000 micromho/cm in the east of the "Karak Wadi Al Fiha fault". The E.C value is as low as 400 to 1,100 micromho/cm in the northern part of the Salwan fault, while it rises to 1,800 micromho/cm in the east of the "Karak - Wadi Al Fiha" fault. The values of T.D.S follow the same pattern, showing T.D.S of 390 mg/l at JT-1, 635 mg/l at JO-3, and 1,171 mg/l at JO-5. Three groups of the quality types are plotted on the Piper's tri-linear diagram, including i) "carbonate hardness" at Western Highlands and western part of upper Hasa basin, ii) "no one cation-anion pair exceeds 50 %" at central part of the Jafr basin and eastern part of upper Hasa basin, iii) "non carbonate alkali exceeds 50 %" at eastern part of Jafr basin. Groundwaters are pure and fresh in the Western Highlands, slightly saline in the central part of the Jafr basin, and saline in the eastern part of the Jafr basin. The regional water salinity (E.C) of the B2/A7 is mapped in the Fig.5.22.

5.4.4 Rijam (B4) aquifer

Flood flows, which are impounded temporarily in the lower reaches of wadis on the B4 formation, are the main source of groundwater recharge. Water salinity in the flood water is as low as less than 400 micromho/cm of E.C, while it increases from west to east in B4 aquifer. The E.C value is 600 micromho/cm in the recharging area and 1,800 micromho/cm in and around the eastern aquifer limit.

In the central Rijam groundwater basin, where intensive groundwater irrigation has been carried out by local farms in and around the Al Jafr town since 1966, the E.C increased from 500 micromho/cm to 2,000-5,200 maximum. The VLF survey was carried out in and around the irrigated land, to delineate the areal extent of the contamination by irrigation return flow. The apparent resistivity in the shallow Rijam (B4) aquifer is as low as less than 10 ohm-m in and around J-1 and J-17 where intensive groundwater irrigation has been performed using the wells in the farms, while it is as high as more than 100 ohm-m in the surrounding areas where no intensive irrigation has been carried out. From the resistivity map in Fig.4.61, it is interpreted that the polluted area and/or aquifer has a limited extent which corresponds to the areal limit of the irrigated land. Fig.5.23 shows the regional water salinity (E.C) of the Rijam (B4).

5.5 Potential Wellfields

5.5.1 General

The potential wellfields are found in the confined areas in the Lower Ajlun (A1-6) and Amman - Wadi Sir (B2/A7) aquifers, while very limited groundwater potential is evaluated in the shallow Rijam (B4) aquifer.

5.5.2 Lower Ajlun (A1-6) aquifer

In the southern part of the Jafr basin below the Palestine grid N=930 to N=940, the A1-6 is thin as less than 100 m thick and it is unsaturated, while it is confined in the central and northern parts of the study area. (see Fig.5.14)

The A1-6 formation outcrops a few kilometers to the west of the watershed along the slope on the Western Highland, where rather higher rainfalls replenish the aquifer. Flood runoff in the wadis, which intersects the narrow bands of the A1-6 outcrops on the steep slopes, is another source of the groundwater recharge. The arenaceous and argillaceous sediments of the A1-6 does not include any fracturing and/or caving structures on the outcrops along the cliffs. The recharge from the flood waters in the wadis may not a significant source of the groundwater recharge.

The lower Ajlun (A1-6) underlies the Amman - Wadi Sir (B2/A7), which consists of alternating sandstones, sandy silts, silty marls, marls and clay/shale units. Main productive aquifer is sandstone layer of A4 which is interbedded by the impervious formations of A5/6 and A3. The A4 is pervious but very thin being about 20 m thick.

The regional groundwater flows in the A1-6 aquifer are confined by the three major fault systems such as the "Arja - Uweina" flexure, "Salwan" fault and "Karak - Wadi Al Fiha" fault. The faults act as impervious barrier, where displacements exceed the thickness of the A4 formation as seen in Fig.5.12. In the western highland, the groundwater flows from southwest to northeast in and along the "Arja - Uweina" flexure. The groundwater is in a stagnant environment in the area between Salwan fault and east of the "Arja - Uweina" flexure, where water salinity is high and piezometric elevation is as low as about 740 m. In the northern part of the study area between the "Salwan" fault and the "Karak - Wadi Al Fiha" fault, the groundwater flows from the west to the east with very low water salinity and higher piezometric elevation at about 890 m.

The potential wellfield in the A1-6 is regionally confined in the area between "Salwan" fault and "Karak - Wadi Al Fiha" fault. The experimental wellfield is selected in and along the wadi Rigl, which is located to the northwest of the JT-3. Simulation mesh model of the A1-6 which includes the experimental well field of the "East Hasa" is shown on Fig.5.24.

5.5.3 Amman - Wadi Sir (B2/A7) aquifer

In the south and the southeastern part of the Jafr basin below the Palestine grid N=940 to N=960, the B2/A7 varies from 0 to 100 m in thickness and it is unsaturated. In the central part of the study area, the B2/A7 aquifer is in a confined condition, while it is unconfined in the surrounding areas as seen in Fig.5.17.

The B2/A7 formation outcrops on the Western Highland along the divide of the western boundary of the Jafr basin, where higher rainfall of 200 to 300 mm per annum replenish the aquifer. The flood waters in the wadis on the outcrops of the B2/A7 formation which are highly fractured with caves, fissures and cracks, are also important source of the groundwater recharge. Average annual recharge through the wadi beds in the outcrop area is estimated at 6.7 MCM/y in total.(Refer to chapter 3 of surface hydrology)

The Amman - Wadi Sir (B2/A7) formation underlies the Muwaqqar (B3) formation, which consists of two aquifer units of B2 and A7. For the purpose of the modeling study, the Amman - Wadi Sir (B2/A7) aquifer is assumed to be a single hydraulic system with hydraulic conductivity.

The regional groundwater flows in the B2/A7 aquifer are confined by two major faulting structures such as "Arja - Uweina" flexure and "Salwan" fault. These faulting structures act as impervious barriers, but they are not continuous barriers because of their complicated structures. In the western highland, the groundwater flows from the west to the east intersecting the "Arja - Uweina" flexure which is composed of a group of discontinuous faults. In the northwestern part of the Jafr basin, the "Arja - Uweina" flexure acts as impervious barrier to intersect the flow to the east, then the groundwater flows turn to the northwest direction passing through the watershed boundary between Jafr and upper Hasa. In the north of the Salwan fault, the groundwater flows to the northeast and east, and flows out through the "Karak - Wadi Al Fiha" fault which is not a continuous faulting system and acts as a semi-pervious barrier with hydraulic continuity in the B2/A7.

The potential wellfields in the B2/A7 are regionally confined in and along the two major flow passes such as "Wadi Wuheida - Wadi Uqeiqa" and "Tell Burma - Qa al Jinz". The experimental wellfield of "East Ma'an" is located in the lower reaches of the wadi Wuheida 10 to 15 Km east of Ma'an. In the upper Hasa basin, the experimental wellfield of "South Hasa" is located 5 to 10 Km northeast of the Tell Burma and/or 2 to 7 Km northeast of the JT-1. (Fig.5.24)

5.5.4 Rijam (B4) aquifer

The sustained yield of the Rijam (B4) aquifer is evaluated to be as small as less than 2 MCM/y per annum, due to the limited groundwater recharge through the wadi beds during the occasional floods. No extensive exploitation will be recommended.

5.6 Model Simulation Study

5.6.1 Model construction

Regional groundwater flows in the aquifers of both B2/A7 and A1-6 are confined by three major faulting structures, "Karak - Wadi Al Fiha" fault, "Salwan" fault and "Arja - Uweina" flexure. These faults are complicated in their structures with irregular boundaries. The finite element method (FEM) is used to interpret the complicate boundary conditions in the simulation models. Aquifer hydraulics are also complicated by inclusion of both unconfined and confined conditions in the single aquifer unit. The UNISSF groundwater model takes account of the following hydrogeological data;

- Elevation contour of ground surface
- Geological structure; Elevation contour of the bottom of the aquifer
- Geological structure; Elevation contour of the top of the aquifer
- Regional permeability and storage coefficient / specific yield
- Initial (static) piezometric surface
- Groundwater hydrograph
- Pumping record and program

The simulation model is based on partial equations of the time dependent diffusion type which includes non-linear time dependent parameters. Potential analysis was carried out by using the FEM simulation models including the following;

- Steady state calibration of B2/A7 and A1-6 aquifer models.
- Non-steady calibration and prediction of B2/A7 aquifer model.

5.6.2 Mathematical models

Groundwater flow in the aquifer of the Jafr Basin are assumed to be governed by a two dimensional non-steady equation, which is based on a diffusion type of the partial differential equation with non-linear parameters of hydraulic conductivity and specific strativity.

The governing equation of the two dimensional groundwater flow is described below.

$$S(h) \frac{\partial h}{\partial t} + \frac{\partial}{\partial x} \{ Tx(h) \frac{\partial h}{\partial x} \} + \frac{\partial}{\partial y} \{ Ty(h) \frac{\partial h}{\partial y} \} = q$$

where S : coefficient of storage

T_x, T_y : coefficients of transmissivity in x, y directions

q : discharge/recharge per unit time

t : time

h : head

The equation above can be applied to a multi-layered aquifer by considering T and S as functions of the groundwater head.

confined aquifer

$$T = \sum_{i=0}^{n} K_i \ b_i$$

$$S = \sum_{i=0}^{n} Ss_i \ b_i$$

unconfined aquifer

$$T = \sum_{i=0}^{n} K_{i-1} \ b_{i-1} + K_i(h - h_{i-1}) \quad (h_{i-1} < h < h_i)$$

$$S = Sy_i + \sum_{i=0}^{n} Ss_{i-1} b_{i-1}$$

where K_i : coefficient of infiltration capacity of i-layer

Ss_i : coefficient of specific storage i-layer

Sy_i : specific yield of i-layer

b_i : thickness of i-layer

The numerical analysis of the simulation model was performed by finite element method (FEM), which is now widely used to solve regional aquifer problems.

The partial differential equation is formulated by the Galerkin finite element procedure, which is basically a rule for reducing the governing partial differential equations to a matrix statement involving a matrix of the unknown state variables.

The numerical solution of the matrix statement is accomplished by the band matrix method, which is mainly used for matrix calculations by the computer to save the computational time and memory.

5.6.3 Steady state calibration of A1-6

The finite-element grid mesh of A1-6, which is composed of tri-angular and/or quadrilateral elements, includes 223 elements with 231 nodes. The mesh map was designed to delineate the finer geological structures of "Karak - Wadi Al Fiha" fault, "Salwan" fault and "Arja - Uweina" flexure. These faulting structures require finer mesh grids as shown in Fig.5.25.

The boundary conditions are either of the specified-flow or specified-head type. Nodes along the western basin boundary, where average annual rainfall exceeds 150 mm in the outcrop area , are of specified-head type of the boundary condition. The specified-flow of the outflow type is given to the node along the eastern boundary of the model, where groundwater flows out to the further east-northeast areas. There is neither springs nor pumping wells from the A1-6 aquifer.

The steady state model was calibrated by comparing the difference between the piezometric surface in the monitoring well (JT-3; EL=877 m) and the computed head on the corresponding node (No.89; El=870 m). Fig.5.26 shows the calibrated piezometric surface and the computed regional flow vector.

5.6.4 Steady state calibration of B2/A7

The finite-element grid mesh of the B2/A7, which is composed of triangular and/or quadrilateral elements, includes 372 elements with 361 nodes. The mesh map is designed to delineate the complicated linearment with discontinuous faulting structures including "Karak - Wadi Al Fiha" fault, "Salwan" fault and "Arja - Uweina" flexure. These discontinuous faulting structures require finer mesh grids as indicated in Fig.5.27.

The boundary conditions are either of the specified-flow or specified-head type. Nodes along the western basin boundary, where average annual rainfall exceeds 150 mm in the outcrop area, are of specified-head type of the boundary condition. The specified-flow of the outflow type is given to the node along the eastern boundary of the model, where groundwater flows out to further east to northeast. Water balance of the simulated model through the boundaries is estimated at approximately +/- 16 MCM per annum. Spring waters from B2/A7 aquifer are located in the Western Highlands of the Jafr basin, which are estimated to yield approximately 0.75 MCM per annum. From the surface runoff simulation analysis using the tank model method, groundwater recharge through the wadi beds on the outcrops of B2/A7 in the Jafr basins estimated at approximately 6.7 MCM per annum.(see Section 3.2 of this chapter)

The steady state is based on the simple assumption that there are no artificial abstractions from the target aquifer. A semi-steady state condition is assumed to calibrate the simulation model, which is based on assumptions that artificial abstractions does not exceed the annual average groundwater recharge without any influences on the regional piezometric surface. It is assumed that the piezometric surface in the study area was in a steady state and/or semi-steady state before 1970.

The steady state model was calibrated by comparing the difference between the piezometric surface in the monitoring wells (JO-5; EL=724m, JT-4; EL=785m, S-121;988m, JT-1; EL=880m, JO-3; EL=790m, JT-2; EL=794m, S-111; EL=1,179m, S-65; EL=1,193m, S-118; EL=1,271m) and the computed head on corresponding mesh nodes (No.50; EL=728m, No.87; EL=741m, NO.94; EL=990m, No.114; EL=884m, No.128; EL=772m, No.160; EL=804m, No.185; EL=1,177m, No.197; EL=1,202m, No.214; EL=1,277m). Fig.5.28 shows the calibrated piezometric surface and the computed regional flow vector.

5.6.5 Non-steady calibration and predictions of B2/A7

Successive decreases in the piezometric head have been monitored in the WAJ monitoring well at S-121 (Palestine grid; E=228.70, N=002.08) since 1973. The non-steady state model assumes that the regional piezometric surface was in a steady state and/or semi-steady state before 1973. Fifteen years of monitoring records (1973-1988) at S-121 are used to calibrate the computed piezometric head. The calibrated storage coefficient in and around the S-121 is in the range between 1.4×10^{-4} and 5.2×10^{-5}, while the coefficient of permeability is in the range between 1 and 0.1 m/day. The computed drawdown from 1973 to 1988 is estimated at 8.4 m, which is 98 % of the measured drawdown of 8.3 m in the monitoring well S-121. Calibrated non-steady piezometric surface by the year 1988 is shown in Fig.5.29.

The simulation model predicts the influences of the future groundwater exploitation such as at "South Hasa" and "East Ma'an" on the regional groundwater flows. Each experimental wellfield assumes production wells of 10 to 20 in number with a unit pumping rate at 0.5 to 1 MCM/y located at a distance from each other 1 to 2 km. From the model analysis, which assumes the abstraction of 10 MCM/y from each proposed wellfield, the piezometric surface is estimated to be lowered by 40 to 55 m in the "South Hasa" wellfield and 25 to 30 m in the "East Ma'an" wellfield by the year 2010 and 2040. The estimated piezometric surface after 20 and 50 years pumping respectively is shown in Figs.5.30 and 5.31. The estimated drawdown at representative mesh nodes in each wellfield are shown on Fig.5.32.

The model prediction also includes the alternative studies on the groundwater recharge dam. The conjunctive development study is also carried out by using the simulation model. The model is based on groundwater exploitation by coupling with the two groups of recharge dams such as A1-2-3 and B1-2-3 which assume the commencement of the impounding in 1993 with net infiltration capacity of 5.2 MCM and 3.2 MCM per annum respectively. The piezometric level is estimated to be raised by 5 to 10 m after 20 to 50 years pumping by adding the groundwater recharge dams as shown on Figs.5.33 and 5.34. The estimated changes in the piezometric surface which is raised by the infiltration through the recharge dams are shown in the groundwater profiles on Fig.5.35.

The regional effect of the groundwater recharge dam in the Shoubak area is evaluated by using the simulation model. From priority ranking study for the proposed recharge dams, the A-2 recharge dam is selected to evaluate the effects of infiltration on the unconfined aquifer in the Shoubak area, where the piezometric surface is being lowered by the intensive groundwater irrigation.

The pumping rate for the irrigation is assumed at 3.27 MCM/y in the simulation model. In addition, the double pumping rate of 6.54 MCM/y is also assumed to estimate the upper limit of pumping in the complicated Shoubak wellfield. The alternative simulation study includes the following four cases;

Case 1) 3.27 MCM/y of abstraction without recharge dam

Case 2) 3.27 MCM/y of abstraction with 1.81 MCM/y of A-2 recharge dam

Case 3) 6.54 MCM/y of abstraction without recharge dam

Case 4) 6.54 MCM/y of abstraction with 1.81 MCM/y of A-2 recharge dam

The impounding and/or infiltration of the recharge dam is assumed to start after 5 years which consider the time for the construction of dam.

From the cases 1)-2) and cases 3)-4), the area effected by the A-2 dam is found at the northern part of the Shoubak area as seen in the drawdown map of Fig. 5.36.

Groundwater profiles in and around the Shoubak wellfield in the cases 1) through 4) are shown in Fig.5.37 and 5.38. The piezometric levels in a part of Shoubak wellfield will be raised some 5 m to 10 m after 20 to 50 years by adding the A-2 recharge dam.

Figs. 5.39 to 5.41 show the groundwater hydrographs at selected simulation mesh nodes in the Shoubak wellfield. From the case 1) and 3) the drawdowns are estimated to be 10 to 50 m after 20 to 50 years pumping, which includes a critical water table condition in some part of the Shoubak wellfield. From the case 2) and 4), minor or negligible influences are seen in the southern Shoubak wellfield such as at mesh node "180", "181", "182", "183", "193", "194" and "195", while obvious influences of rising the piezometric surface in the northern Shoubak wellfield such as at mesh node "152", "173", "174", "175" and "176" are estimated as seen in the predicted hydrographs.

All the data and computer output files, which have been used in the model simulation studies, are installed in the 3.5 inch size mini-floppy diskette. Those input data are transferred to WAJ's VAX-8200 by means of RS-232C data communication system. The version (3.0) of the UNISSF simulation manual, which is the final version of the simulation models with input and output files, is transferred to WAJ at the end of the 3rd computer simulation seminar.

5.7 Proposed Groundwater Development

5.7.1 Design of proposed wellfields

From the model simulation study, the potential yields of the two proposed wellfields such as "South Hasa" and "East Ma'an" are estimated at 20 MCM/y in total. The proposed two wellfields are located in parallel the National Water conveyer route (Mudawwara-Ma'an-Amman) within a distance at 1 to 15 km.

The "South Hasa" wellfield comprises a group of 20 deep wells which are installed at a distant of 1 to 2 Km as shown in Fig.5.36. Following is the feature of the water source facilities;

<u>Wells</u>

Nos. of well	;20 wells
Diameter of well	;17-1/2 inches
Well depth	;350 m
Diameter of pump chamber pipe (0-200m)	;13-3/8 inches
Diameter of screen pipe	;9-5/8 inches

<u>Pump</u>

Nos. of pump	;20 units
Type of pump	;Submersible pump
Design head	;150 - 175 m
Motor capacity	;45 - 75 KW
Design discharge	;70 - 90 m^3/hr

The "East Ma'an" wellfield is composed of a group of 20 deep wells which are drilled at a distant of 1 to 2 km as shown in Fig.5.40. Following is the feature of the water source facilities;

Wells

Nos. of well	;20 wells
Diameter of well	;17-1/2 inches
Well depth	;250 m
Diameter of pump chamber pipe (0-175m)	;13-3/8 inches
Diameter of screen pipe	;9-5/8 inches

Pump

Nos. of pump	;20 units
Type of pump	;Submersible pump
Design head	;125 - 150 m
Motor capacity	;40 - 70 KW
Design discharge	;70 - 90 m^3/hr

5.7.2 Preliminary cost estimates

The national water carrier of Disi-Mudawwara-Amman route, which pass through the Study area within a distant 1 to 15 km from the proposed two wellfields, is proposed by WAJ, and the project cost is preliminarily estimated at US$200 (=J.D.140) millions. To compare with the huge amount of the project cost for the pipeline construction, the investment cost of the well construction is, however, as small as J.D.1.75 million for "South Hasa" wellfield and J.D.1.25 million for "East Ma'an" wellfield by assuming the unit rate of drilling at J.D.250 per linear meter lump-sum. While the other cost of the electric facilities such as transformers, control panels, remote control panels and flow meters, transmission line and collecting pipes will be in the range between 100 and 200 % of the cost of the well construction.

REFERENCES

5.1 Abu Ajamieh,M.M., 1967, "A Quantative Assessment of the Groundwater Potential of the Rijam Formation Aquifer in the Jafr Basin", UN Special Fund - FAO, Sandstone Aquifers of East Jordan Project Report, Amman

5.2 United Nation (FAO), 1970, "Investigation of the Sandstone Aquifers of East Jordan, Main Report and Annex I"

5.3 German Agency for Technical Cooperation Ltd., Federal Republic of Germany, 1977, "National Water Master Plan", Vol.I,II,III,IV,V,VI and VII

5.4 Howard Humphreys, 1986, "Groundwater Resources Study in the Shidiya Area"

TABLES

Table 5.1 List of Well Inventory (1/6)

No. of	Coordinate		Surface	Geological Group: Plateau	Belqa			Ajlun		Kurnub	Khreim	Disi	S.W.L	Name of	Test Yield	Spec. Cap.	Drawdown	EC	Remark
Well	East	North	El (m)	R	B4	B3	B1-2	A7	A1-6	K1-2	Kh	D	(EL)	Aquifer	(m3/h)	(m3/h/m)	(m)	(micromho/cm)	
S-1	225.42	954.57	1,049.200			154	304	405	550	704	934	1,393	919.20	AB				1200	NOV 1967
													747.20	A					JUN 1965
													749.20	Ku				1080	OCT 1967
													609.20	D				1120	OCT 1965
S-15	260.7	967.25	875.300	18	60	305	341		647	846	1,383		798.60	AB	36	0.8	45	1750	APR 1966
													500.30	Ku					
													545.30	Kh					
S-29	246.65	30.85	879.500	18			141	201					799.50	AB				800	OCT 1966
S-30	236.39	16.18	909.250				150						828.85	AB	39	16.5	2.4	775	
S-32	213.72	971.77	1,175.370			85	120						1,195.37	AB	60	3	20	710	OCT 1966
S-34	214.77	982.16	1,168.130			242	280						1,180.13	AB	128	4.92	26		NOV 1966
S-37	202.75	958.77	1,318.100			34	93	150					1,286.50	AB	12			950	DEC 1966
S-39	222.46	967	1,079.700		66	415	434						814.70	AB	1.9	0.11	17.3	950	OCT 1967
S-40	204.62	950.97	1,318.180			25	96						1,284.33	AB	50	94.3	0.5	1170	DEC 1966
S-41	198.28	942	1,429.900			37	190	197					1,437.10	AB	7	0.97	7.2	720	JAN 1967
S-45	224.64	983.24	1,063.130	7	134	495	600						974.87	AB	7.2	0.03	24	750	MAY 1968
S-52	265.5	956.5	867.000		16	70							846.50	B3					MAY 1967
S-53	239.4	924	982.900	3			87		220				916.33	AB					
S-54	258.35	957.05	870.000		16	30							861.00	B4					
S-55	251.2	980	908.000		34								883.00	B4					
S-56	214.71	992.08	1,199.340	39	244	657	702			64	Basalt		1,079.82	AB					
S-57	286	943	877.890	23			56		338	497	1,300		739.29	Ku					
													720.89	Ku				4400	
													643.89	Kh				3000	
S-58	230.33	14.81	1,025.780	38			149	200					852.65	AB	11.87	1.7	7	880	APR 1968
S-59	205.16	950.4	1,317.800			161	208	250					1,283.30	AB	180	2.1	4.8	880	JUL 1967
S-60	204.1	950.5	1,330.800			5	78	103					1,284.34	AB	104	133	0.8	1120	SEP 1967
S-61A	204.63	951.38	1,322.430	7			78	95					1,284.57	AB	111	59.55	1.9	1210	DEC 1967
S-62	222.07	930.2	1,188.850			108	155						1,048.35	AB				1050	AUG 1967

Table 5. 2 List of Well Inventory (2/6)

No. of	Coordinate		Surface	Geological Group									S.W.L	Name	Test	Spec.	Drawdown	EC	Remark
				Plateau	Belqa			Ajlun		Kurnub	Khreim	Disi		of	Yield	Cap.			
Well	East	North	El (m)	R	B4	B3	B1-2	A7	A1-6	K1-2	Kh	D	(EL)	Aquifer	(m3/h)	(m3/h/m)	(m)	(micromho/cm)	
S-63	214.24	989.69	1,198.910	286	307	756	782												
S-65	210.14	977.52	1,275.820			136	207						1,192.82	AB	63.5	4.29	14.8	700	OCT 1967
S-67	197.19	947.6	1,450.080			119	225	290					1,400.08	AB					NOV 1967
S-68	235.26	945.24	993.900			58	151	180	240				914.90	AB					DEC 1957
S-74	226.46	0.64	1,070.170			66	145						988.69	AB	82	390	0.4	530	MAY 1968
S-79	228.48	2.9	1,044.640			88	155						987.78	AB	155	77.5	2	620	FEB 1969
S-80	229.29	1.13	1,045.310	23		120	159						987.82	AB	10				JUL 1968
S-86	228.88	1.31	1,047.030			121	201						987.85	AB	157	131.9	1		FEB 1969
S-88	291.9	963.5	860.000	27		122	150		427	522	803		777.00	AB				4000	
S-94	196.23	941.14	1,483.250				104						1,463.46	AB	111	21.3	5.2	1100	APR 1969
S-100	196.13	941.72	1,494.250			78	163						1,463.35	AB	67	20.67	3.2	1000	JUN 1969
S-101	207.78	977.13	1,298.830	11		147	159						1,298.83	AB	8	0.1	80	570	MAR 1969
S-102	211.875	979.44	1,218.360	5		168	245	363					1,181.27	AB	42	1.3	32	695	MAY 1969
S-103	206.73	979.835	1,316.190	5		36	37						1,303.99	AB				700	MAR 1969
S-104	206.55	976.935	1,320.050				48						1,303.33	AB	120	445.5	0.3	570	MAY 1969
S-105	215.53	981.225	1,208.880		39	310	333						1,171.68	AB					APR 1969
S-106	209.27	979.79	1,270.530			169	203						1,202.60	AB				625	MAY 1969
S-107	213.435	982.155	1,190.830	10		224	282						1,175.15	AB	57	1.29	44.2	640	JUN 1969
S-108	204.77	976.63	1,358.310	5			62						1,308.86	AB					JUL 1969
S-109	214.85	980.93	1,172.050			226	306						1,173.05	AB	153	3.32	46.1	670	JUN 1969
S-110	209.7	982.34	1,259.190			196	210						1,184.55	AB					JUL 1969
S-111	211.65	981.41	1,220.950	9		200	213						1,179.29	AB	1.5	0.024	62.5	710	JUL 1969
S-112	214.13	982.01	1,184.610	17		261	266						1,169.89	AB					JUN 1969
S-113	212.69	978.14	1,227.790	25		193	210						1,182.81	AB					JUL 1969
S-115	215.39	970.56	1,160.250	4		174	200						1,176.25	AB	19.2	1.2	16	690	JUN 1969
S-116	207.76	970.03	1,286.990	5		160	170						1,252.51	AB					JUL 1969
S-117	207.71	977.7	1,432.410				62						1,428.44	AB				670	JUN 1969
S-118	206.79	969.76	1,301.960	4		166	259						1,270.67	AB	43			1210	OCT 1969
S-121	228.7	2.08	1,046.670			81	171						988.49	AB	44.26	92.2	0.5	660	OCT 1969
S-136	195.23	947.54	1,516.380	13				105					1,516.38	AB	93.5	4.92	19	740	AUG 1969
S-137	199.94	958.24	1,462.500	13				92					1,462.50	AB	29	0.53	54.7	740	AUG 1969

Table 5.3 List of Well Inventory (3/6)

No. of	Coordinate		Surface	Geological Group: Plateau	Belqa			Ajlun		Kurnub	Khreim	Disi	S.W.L	Name of	Test Yield	Spec. Cap.	Drawdown	EC	Remark
Well	East	North	El (m)	R	B4	B3	B1-2	A7	A1-6	K1-2	Kh	D	(EL)	Aquifer	(m3/h)	(m3/h/m)	(m)	(micromho/cm)	
PP-8	255	976.8	899.000		49	304	398		515				856.00	B4	49	2.5	19.6		MAR 1962
													796.00	AB					OCT 1963
PP-15	263	969	870.630	11.5	54	85							857.86	B4	177	196	0.9	879	
PP-16	243	969	860.000			95													
PP-17	263.109	969.533	872.160	6	55								858.02	B4	179.5	320	0.6	1120	
PP-18	277.3	969.9	845.000	26	39	96							816.60	B4				1780	
PP-19	289.7	966.7	850.500	14		80							Dry						
PP-20	268.6	968	860.450	19	47	70							843.69	B4	20	0.52	38.5	1120	
PP-21	266.3	960.5	860.140		8	50							847.14	B3				1000	
PP-22	274.6	962	862.600	1	40	96							833.60	B4				1290	
PP-23	262.9	976.2	879.330	8	46	63							858.29	B4	48	1.6	25	800	
PP-24	271	976	860.190	5	40								842.24	B4					
PP-25	264	976	870.290		47	60							858.29	B4	42.3	2.2	19.2	820	
PP-26	257.7	969	868.150	11	32	53							844.74	B4					
PP-27	259.8	973.2	881.920	5	61								858.03	B4	140.9	21	6.7	860	
PP-28	261.5	974.9	877.940		34	50							858.79	B4	218	419	0.5	800	
PP-29	261.9	981.06	882.190		28	70							839.89	B3					
PP-30	263.109	969.553	878.230	6	39	50							863.19	B4	139	104	1.3	909	
PP-37	245.4	24.5	812.089	10			120						789.40	AB	26	0.85	30.2		
PP-38	252.6	20	832.270			44	103						800.87	AB	113.6	847	0.1	810	
PP-40	269	5	913.240	51		102	191						799.64	AB				1120	
PP-41	251.21	20.43	830.500			19	148						800.68	AB	203	8.18	25.1	840	APR 1966
PP-42	250	21	828.290			37	150						800.29	AB	210	1312	0.2		NOV 1966
PP-43	251.2	25	852.370			23	132	185					797.09	AB	160	11.8	13.6		
PP-44	248.23	27.14	903.760				104	212					802.76	AB	90	6	15	680	FEB 1967
PP-50	230.63	8.14	1,002.260			113	172						958.36	AB	41	6.2	6.6	700	SEP 1966
PP-51	215.32	22.91	1,240.000					162		200	Shueib Formation		1,181.00	AB	8	0.095	84.2	756	
PP-52	218.78	22.24	1,185.000					151		203	Shueib Formation		1,131.00	AB	56	1.4	40	520	MAR 1966
PP-55	223.5	0.3	1,116.900			122	229						988.90	AB	87	114	0.8	550	SEP 1966
PP-56	200.38	992	1,435.000				66.5						1,400.85	AB	107				
PP-57	200.74	991.31	1,420.000				91						1,398.50	AB	119	57.7	2.1	550	

Table 5.4 List of Well Inventory (4/6)

No. of Well	Coordinate East	Coordinate North	Surface El (m)	Plateau R	Belqa B4	Belqa B3	Belqa B1-2	Ajlun A7	Ajlun A1-6	Kurnub K1-2	Khreim Kh	Disi D	S.W.L (EL)	Name of Aquifer	Test Yield (m3/h)	Spec. Cap. (m3/h/m)	Drawdown (m)	EC (micromho/cm)	Remark
				Geological Group															
PP-58	200.46	989.67	1,437.000					123					1,397.80	AB	113.6	55.1	2.1	500	JAN 1968
PP-59	200.4	988.53	1,455.000					120					1,402.20	AB	81.5	40.75	2	620	SEP 1967
PP-60	200.81	989.58	1,353.000					105					1,310.00	AB	99	660	0.2	525	SEP 1967
PP-61	204.07	983.25	1,423.290				148	232					1,329.79	AB	70	2.18	32.1	555	SEP 1967
PP-62	198.78	980.82	1,550.000					109					1,503.00	AB	Very Low				
PP-63	206.94	973.14	1,319.090			48	72						1,303.59	AB	58	2	29	600	JUL 1965
PP-64	203.5	967	1,380.000			34	94						1,338.00	AB	106	35	3	520	
PP-65	211.85	961.39	1,205.650				98	144					1,117.15	AB	115	38.3	3	850	MAY 1966
PP-66	195.95	947.18	1,482.650			150	259						1,471.15	AB	100	1.33	75.2	1050	
PP-67	197.7	935.6	1,517.000					102					1,465.00	AB				740	
PP-90	219.33	26.2	1,130.000										1,050.03	AB	11.58	0.13	89.1	1060	APR 1968
PP-457	248.4	27.06	900.800	3			119	230					785.20	AB	31	1.39	22.3		SEP 1968
PP-470	261.6	969.55	865.000	8	50								848.50	B4	106.7	45	2.4	975	APR 1969
PP-471	261.32	969.46	865.000		51								846.72	B4	118	7	16.9	810	SEP 1969
PHO-1	221.76	941.17	1,110.710			76	122	170	389	500			Dry						
PHO-2	232.7	920.73	1,119.500				16		152	280	500		Dry						
PHO-3	249.24	909.38	999.750				32	38	84	297	350		851.75	Ku				2220	
													693.75	Kh				2940	
PHO-4	255.11	935.2	905.200			22	46	108	227	304			743.00	AB				980	
PHO-5	278.29	956.58	860.190	16		69	102	164	400				789.05	AB				2775	
PHO-6	250.15	923.37	948.220			14	50	86	198	200			Dry						
PHO-7	293.7	927.61	893.000				23	32	101	282	300		Dry						
PHO-8	278.55	919.89	899.940	4			24	30	91	274	330		Dry						
PHO-9	259.08	955.94	870.550		34	190	218	300	402				836.70	B4				1980	
													788.96	AB				1680	
PHO-10	266.69	941.41	877.420	14			28	108	120				788.90	A				1005	
PHO-11	247.81	951.86	905.460		18	127	157	205	322				789.30	AB				2175	
PHO-12	311.4	967.45	869.490			64	112	166	200				744.50	AB				5100	
PHO-13	300.98	940.29	871.830				42	89	175				734.97	A				2700	
PHO-14	250	962.9	889.210		6	170	209	284					789.00	AB				1300	
PHO-15	233.08	960.11	979.330			194	258	310	365				791.70	AB				1000	

Table 5.5 List of Well Inventory (5/6)

No. of Well	Coordinate East	Coordinate North	Surface El (m)	Plateau R	Belqa B4	Belqa B3	Belqa B1-2	Ajlun A7	Ajlun A1-6	Kurnub K1-2	Khreim Kh	Disi D	S.W.L (EL)	Name of Aquifer	Test Yield (m3/h)	Spec. Cap. (m3/h/m)	Drawdown (m)	EC (micromho/cm)	Remark
PHO-16	292.01	963.29	856.900			58	102	150	200				760.50	AB				6300	
PHO-17	272.47	949.11	861.180	12		28	92	161	338	380			788.85	AB				2100	
PHO-18	233.96	947.71	985.490			98	150	196	307	310			796.59	AB				1050	
PHT-5	278.3	956.6	859.790	16		69	102	164	335				788.26	AB				1800	
PHT-9	259.07	955.91	870.630		34	190	218	290					788.79	AB				1500	
PHT-11	247.79	951.86	905.180		18	127	157	205	340				788.90	AB				1200	
PHT-14	250.07	962.91	888.290		6	170	209	284	295				788.90	AB				1320	
PHT-15	233.09	960.12	978.620			194	258	300					789.52	AB				1056	
PHT-16	292.03	963.28	857.060			58	102	150	165				760.26	AB				6300	
PHT-17	272.49	949.12	861.000	12		28	92	161					788.80	AB				1300	
PHT-19	280.2	975.93	849.640			75	116	182	210				782.00	AB				4600	
PP-449	255.1	14.2	837.370			60	97						795.37	AB					1962
W-22	205.48	987.28	1,351.000				99						1,310.00	B2	122	2	61	560	FEB 1972
W-23	205.85	986.26	1,346.000				101						1,301.00	B2	190	3.2	63.3	540	NOV 1973
W-24	207.45	977.95	1,300.000				195						1,293.00	B2	94	1.6	58.8	575	JAN 1973
W-25	206.02	985.62	1,358.000				162						1,307.00	B2	250	5.7	43.9	560	APR 1975
W-26	200.18	987.7	1,471.000				244						1,398.00	B2	150	9.4	10.6	525	OCT 1975
W-27	200.4	989.86	1,437.000				122						1,397.00	B2	200	1.7	117.6	520	MAR 1974
W-28	200.2	992.8	1,455.000										1,404.00	B2	25	1	25		SEP 1974
W-30	260.35	970.5	875.000	19	59								856.00	B4	105	1.2	87.5	676	JUN 1975
W-31	260.1	970.45	876.000	22	52								854.00	B4	76	5	15.2	512	AUG 1975
W-32	206.89	968.86	1,299.000				114						1,265.00	AB	78	3.7	21.1	790	MAR 1970
W-34	235.93	0.86	1,080.000				102						978.00	AB	100	6.9	14.5	348	DEC 1975
W-35	219.34	26.3	1,131.000				83						1,048.00	AB	5	0.1	50	1080	JAN 1974
W-36	220.7	27.9	1,100.000				85						1,046.00	AB	140	4.1	34.1	500	MAY 1974
W-37	221.1	27.5					48	161						AB	250	7.7	32.5	500	NOV 1974
W-38	224.5	22.4	1,150.000				188	250					995.00	AB	20	6.1	3.3		AUG 1974
W-39	224.5	20.7	1,120.000				101	199					1,022.00	AB	36	4.5	8	510	SEP 1973
W-40	221	20.8	1,180.000				105	185					1,075.00	AB	20	9.2	2.2	543	APR 1973

Table 5.6 List of Well Inventory (6/6)

No. of Well	Coordinate East	Coordinate North	Surface El (m)	Plateau R	Belqa B4	Belqa B3	Belqa B1-2	Ajlun A7	Ajlun A1-6	Kurnub K1-2	Khreim Kh	Disi D	S.W.L (EL)	Name of Aquifer	Test Yield (m3/h)	Spec. Cap. (m3/h/m)	Drawdown (m)	EC (micromho/cm)	Remark
W-41	248.23	27.2	904.000				111						793.00	AB	24	5.2	4.6	650	SEP 1968
W-42	248.05	27.61	899.000				105						794.00	AB	31	1.2	25.8	740	FEB 1972
W-43	248.82	26.12					60							AB	80	3.1	25.8	740	JAN 1973
W-44	249.13	26	848.000				64						785.00	AB	200	3.1	64.5	750	NOV 1974
W-45	249.4	26.8	880.000				88						794.00	AB	155	3.6	43.1		MAR 1975

FIGURES

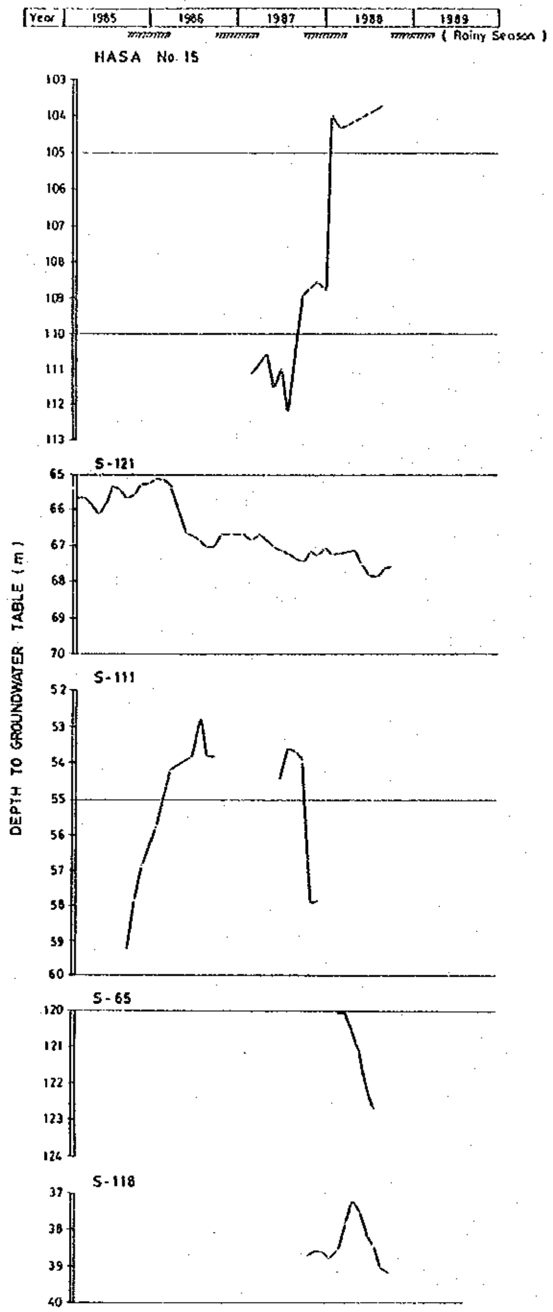

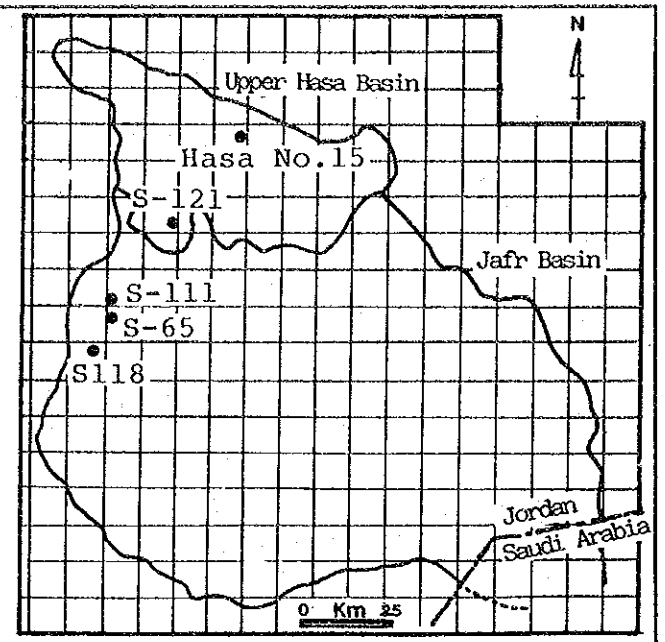

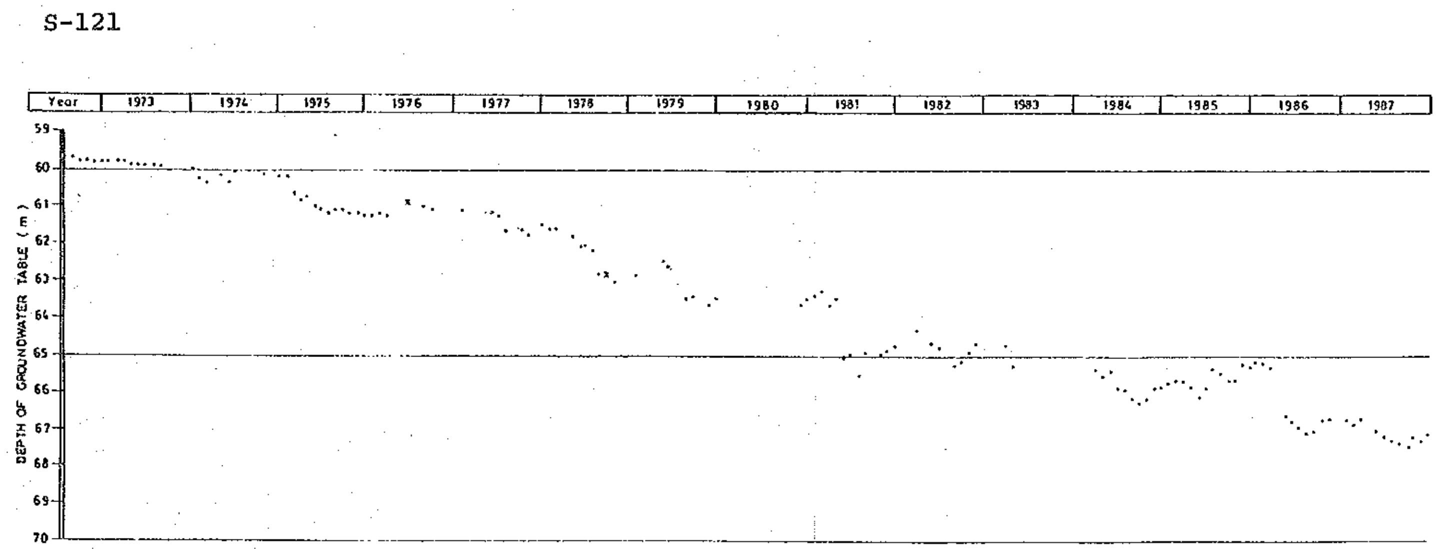

Fig.5.1

Groundwater Hydrograph of

Monitoring Wells

THE HASHEMITE KINGDOM OF JORDAN

WATER RESOURCES STUDY OF THE JAFR BASIN

JAPAN INTERNATIONAL COOPERATION AGENCY

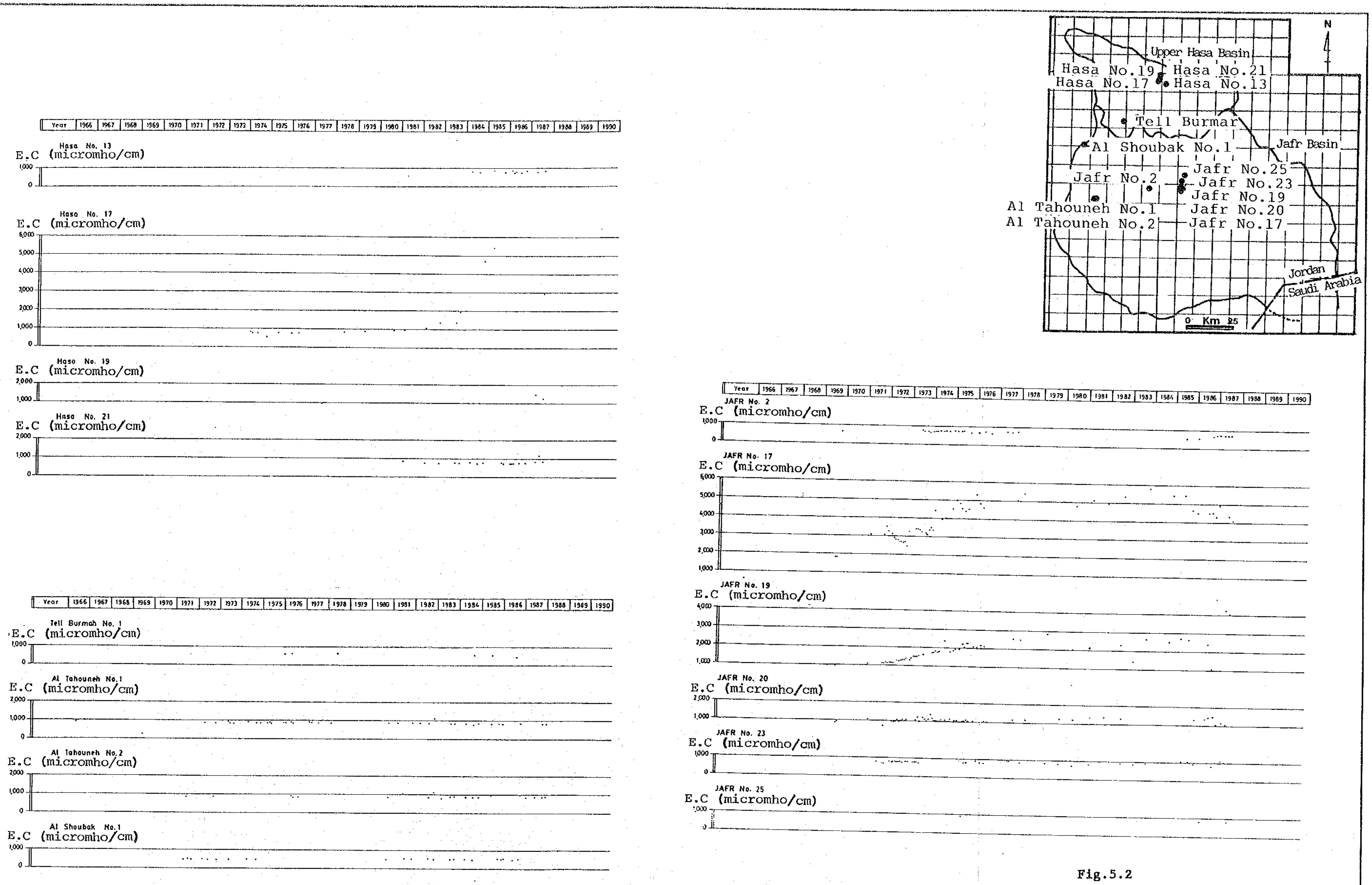

Fig.5.2
Change in Water Salinity (E.C) of Monitoring Wells

THE HASHEMITE KINGDOM OF JORDAN

WATER RESOURCES STUDY OF THE JAFR BASIN

JAPAN INTERNATIONAL COOPERATION AGENCY

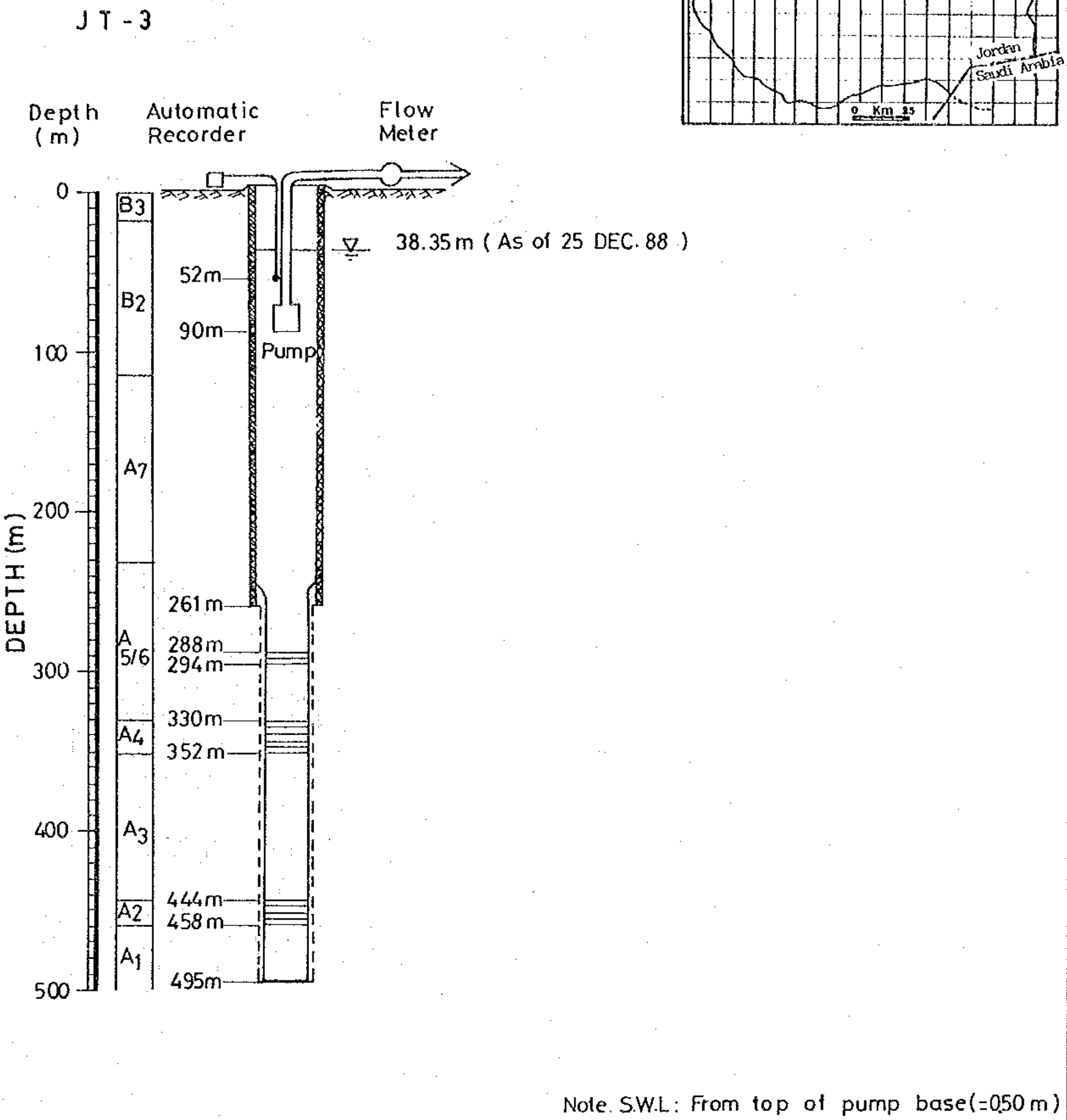

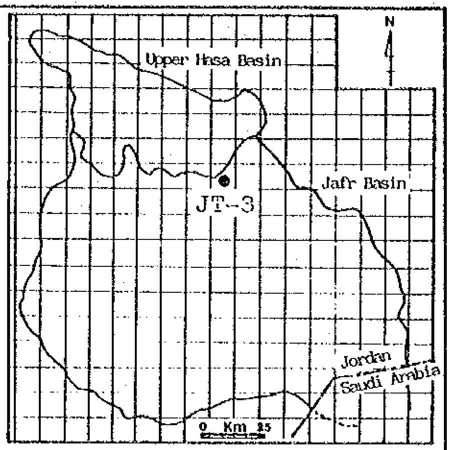

Fig.5.3

Schematics of JT-3 Test Well

THE HASHEMITE KINGDOM OF JORDAN

WATER RESOURCES STUDY OF THE JAFR BASIN

JAPAN INTERNATIONAL COOPERATION AGENCY

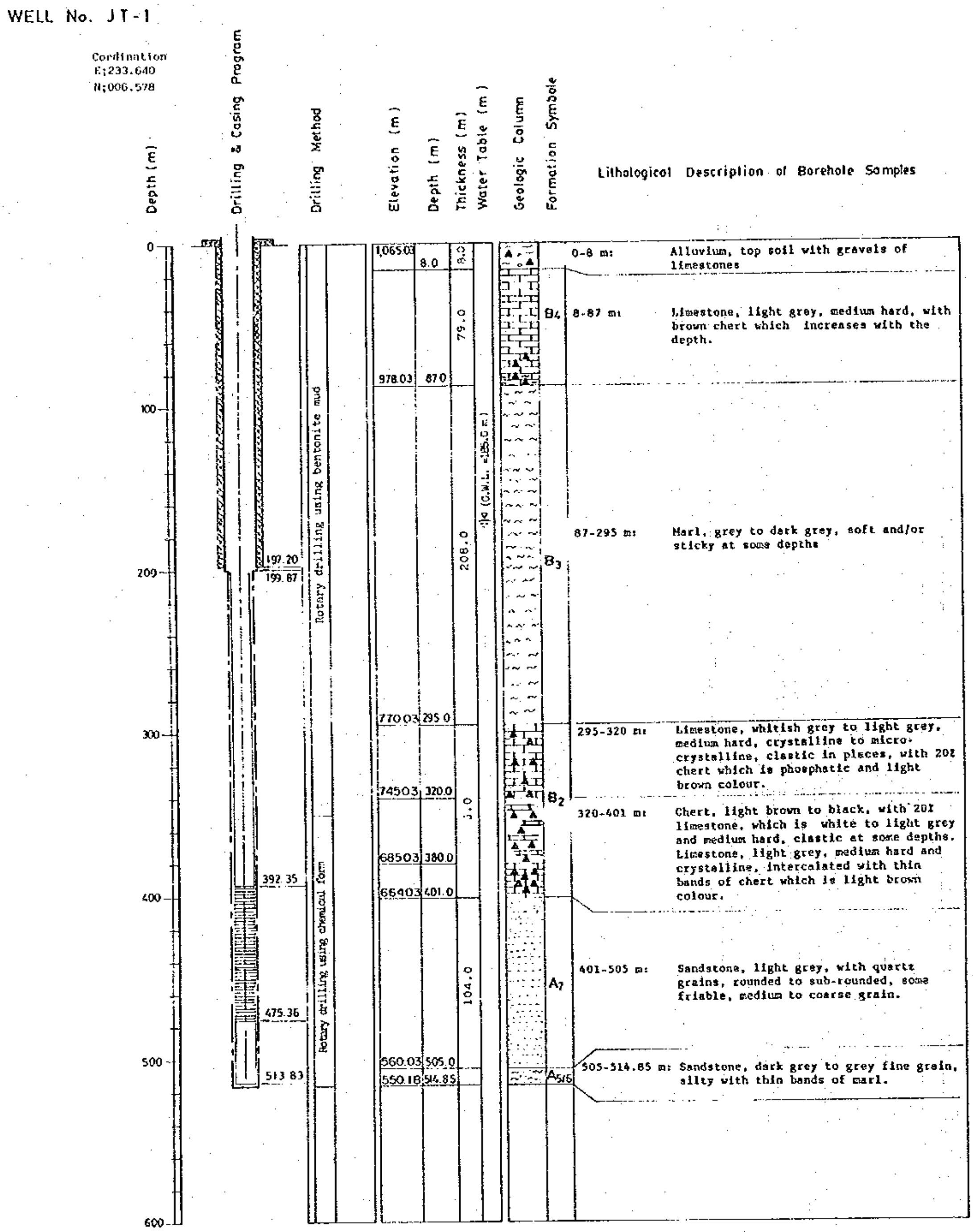

Fig.5.4

Well Log of JT-1

THE HASHEMITE KINGDOM OF JORDAN

WATER RESOURCES STUDY OF THE JAFR BASIN

JAPAN INTERNATIONAL COOPERATION AGENCY

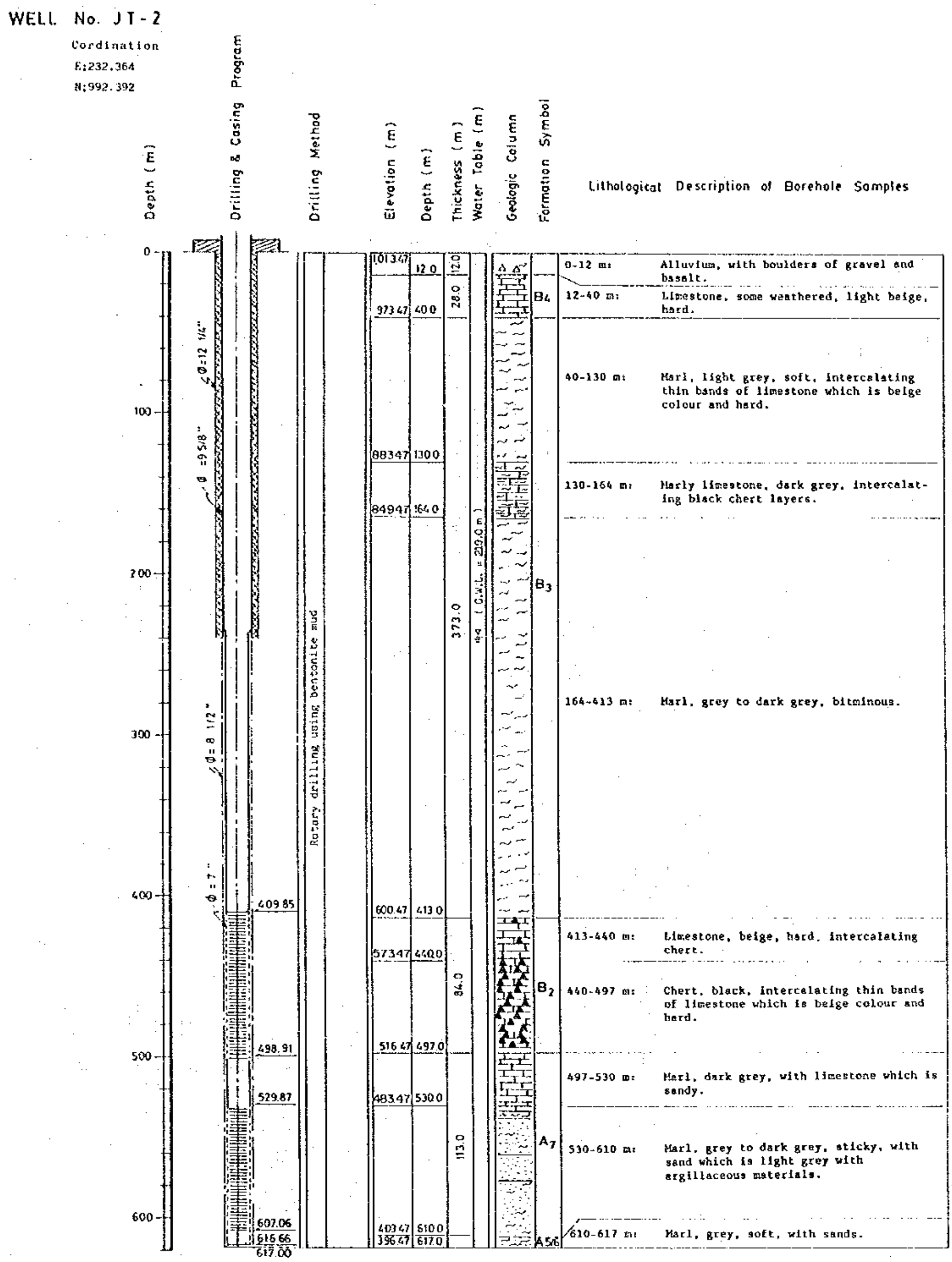

Fig.5.5

Well Log of JT-2

THE HASHEMITE KINGDOM OF JORDAN

WATER RESOURCES STUDY OF THE JAFR BASIN

JAPAN INTERNATIONAL COOPERATION AGENCY

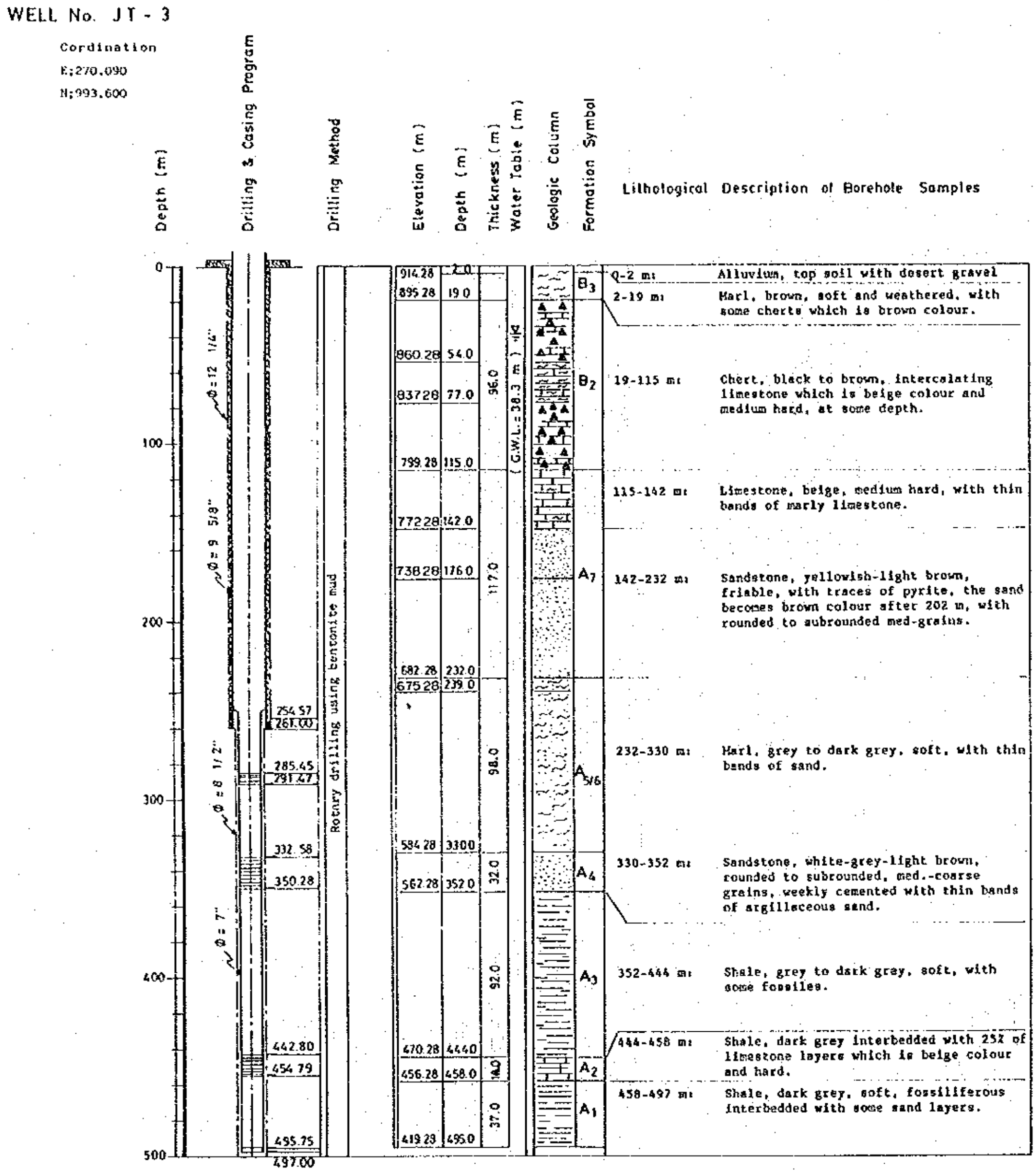

Fig.5.6

Well Log of JT-3

THE HASHEMITE KINGDOM OF JORDAN

WATER RESOURCES STUDY OF THE JAFR BASIN

JAPAN INTERNATIONAL COOPERATION AGENCY

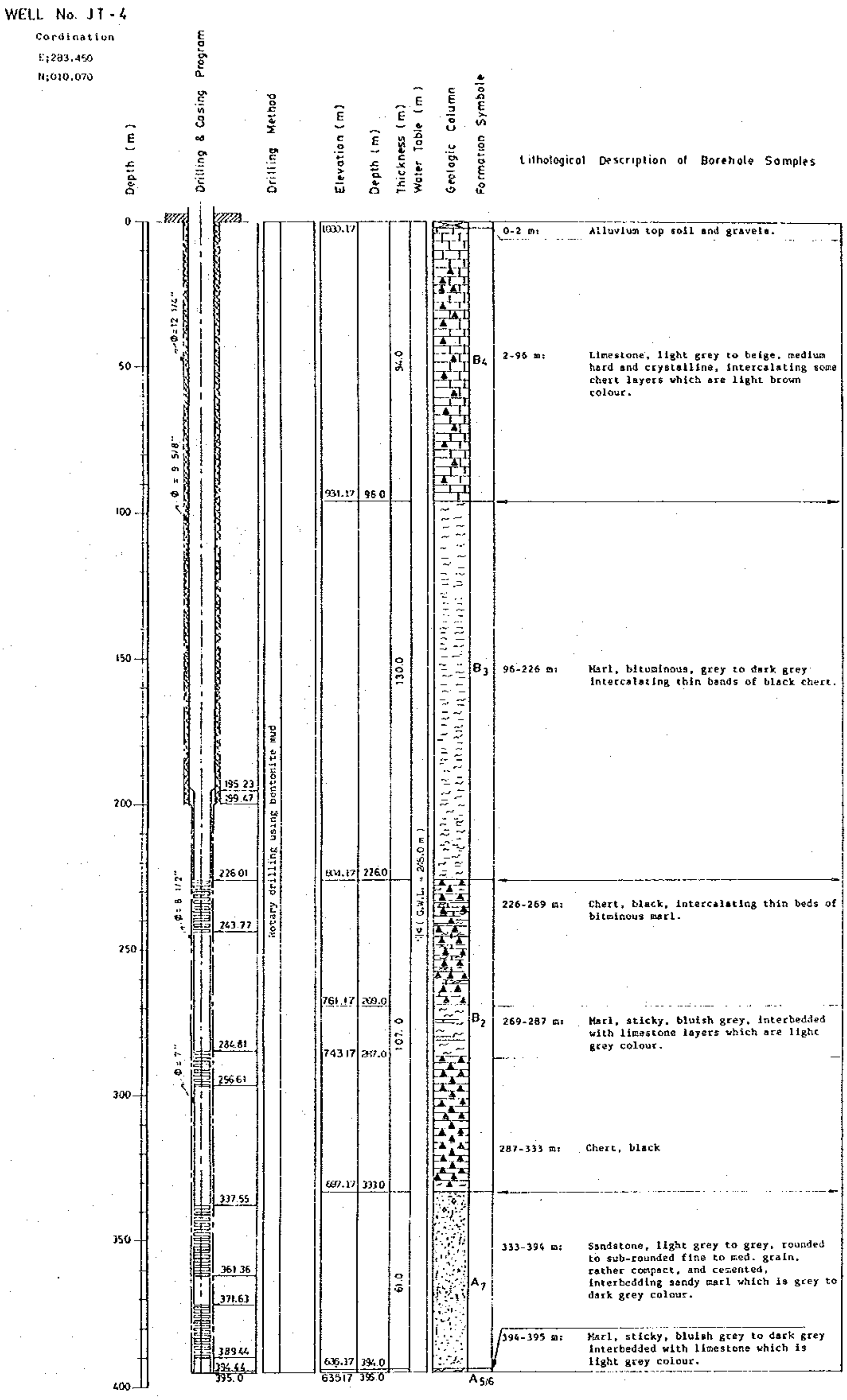

Fig.5.7
Well Log of JT-4

THE HASHEMITE KINGDOM OF JORDAN

WATER RESOURCES STUDY OF THE JAFR BASIN

JAPAN INTERNATIONAL COOPERATION AGENCY

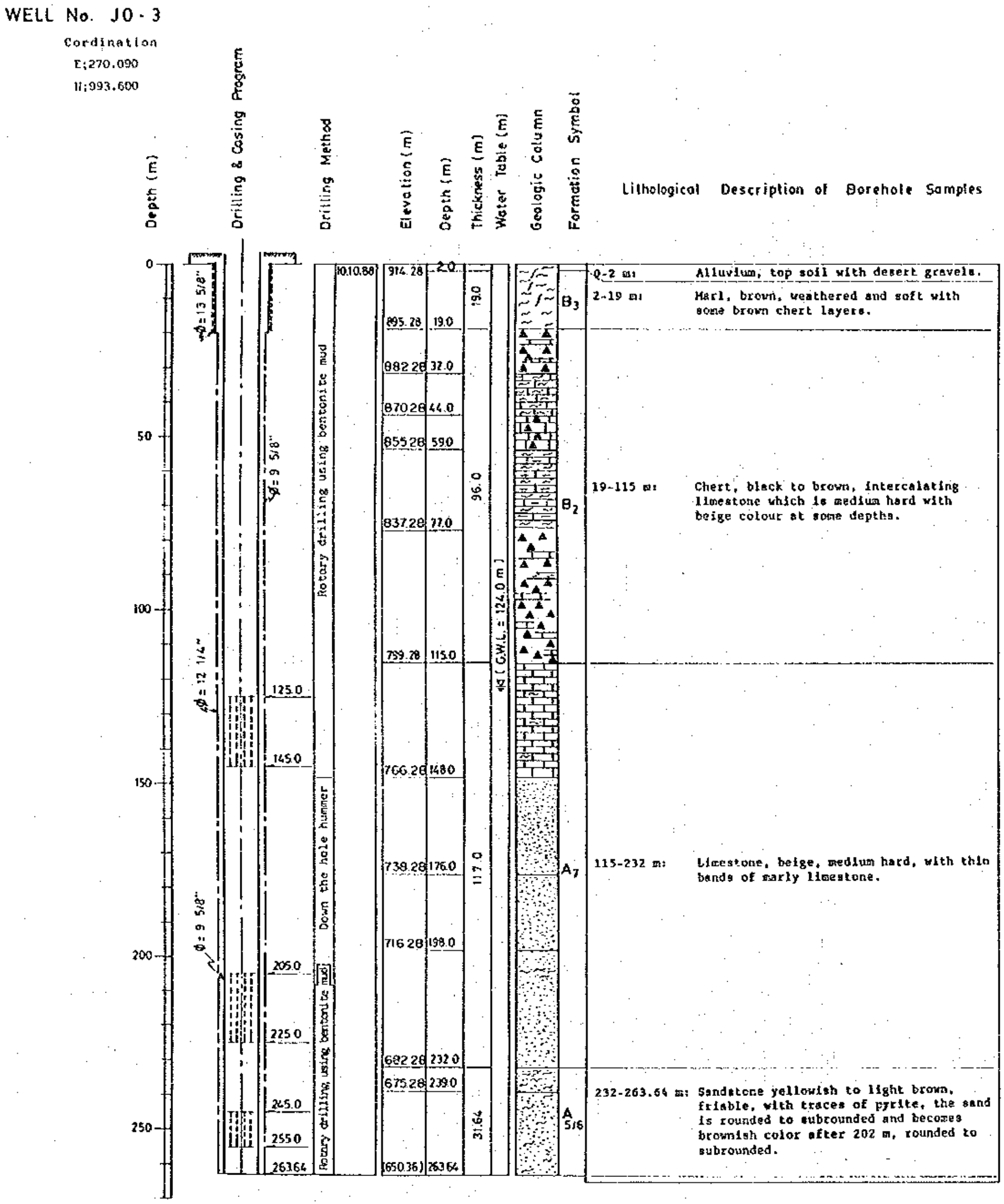

Fig.5.8

Well Log of JO-3

THE HASHEMITE KINGDOM OF JORDAN

WATER RESOURCES STUDY OF THE JAFR BASIN

JAPAN INTERNATIONAL COOPERATION AGENCY

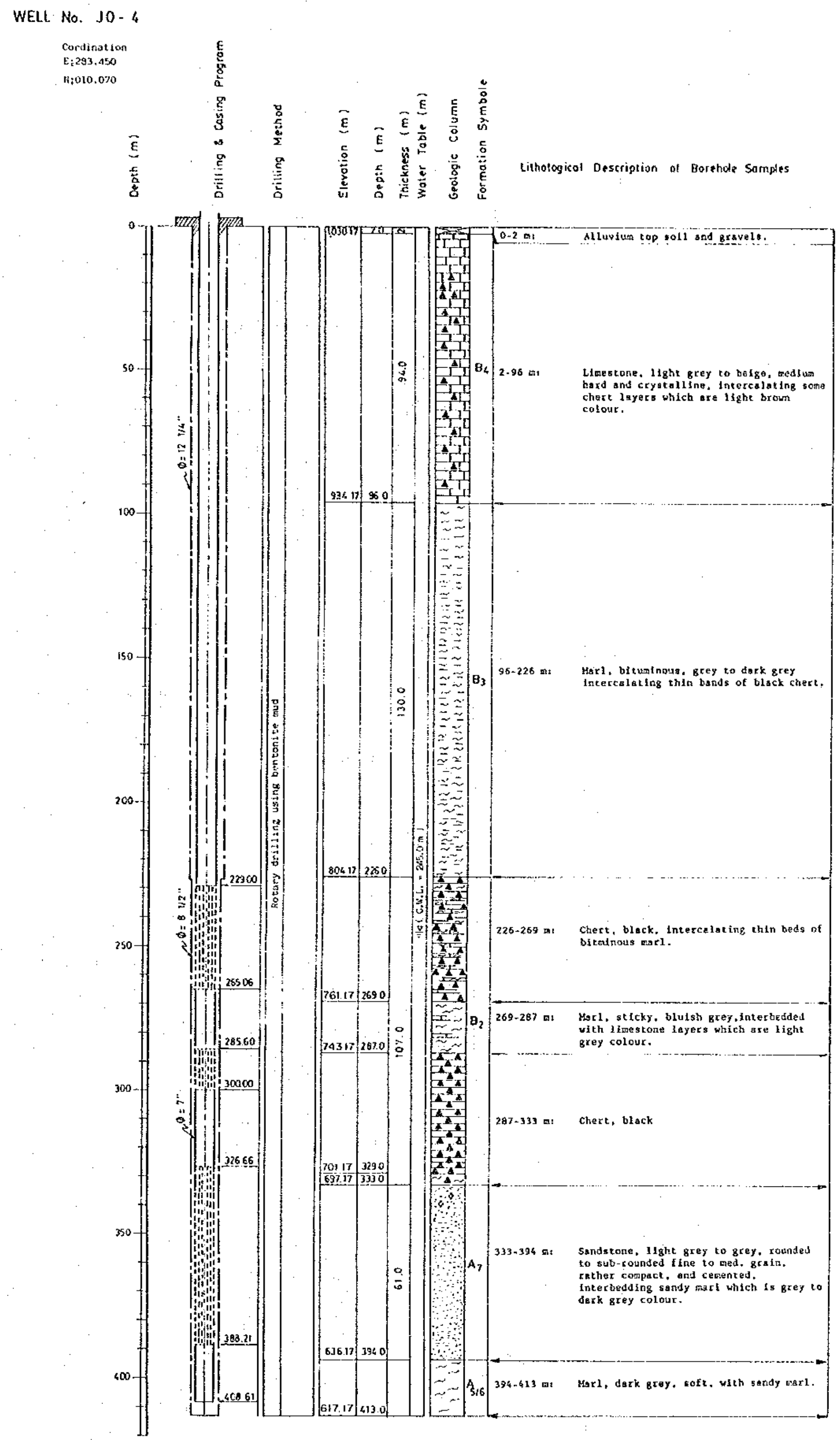

Fig.5.9

Well Log of JO-4

THE HASHEMITE KINGDOM OF JORDAN

WATER RESOURCES STUDY OF THE JAFR BASIN

JAPAN INTERNATIONAL COOPERATION AGENCY

WELL No. JO-5

Cordination
E;276.350
N;022.300

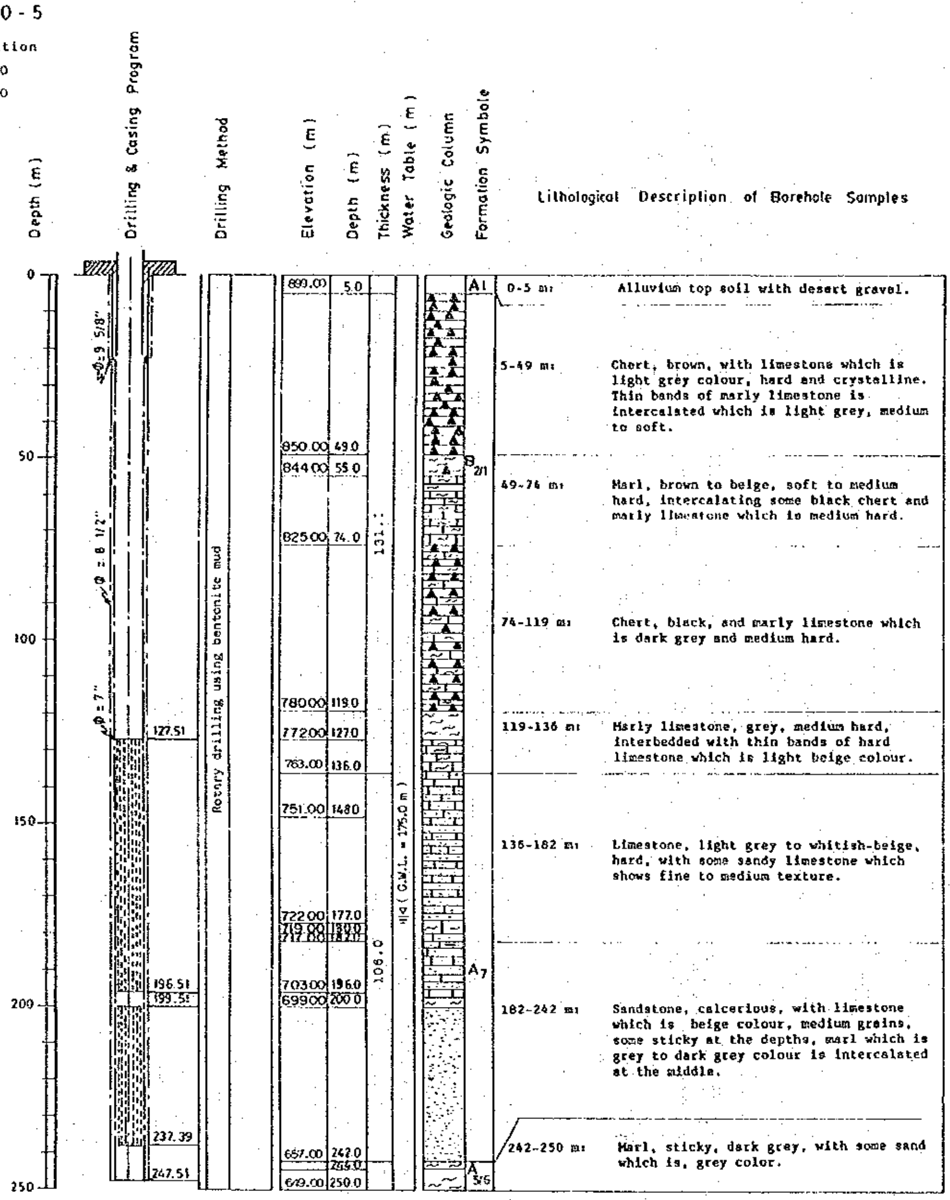

Fig.5.10

Well Log of JO-5

THE HASHEMITE KINGDOM OF JORDAN

WATER RESOURCES STUDY OF THE JAFR BASIN

JAPAN INTERNATIONAL COOPERATION AGENCY

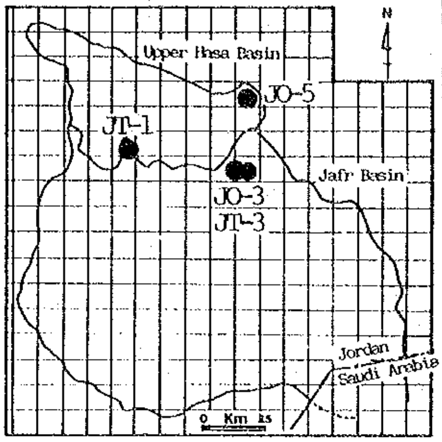

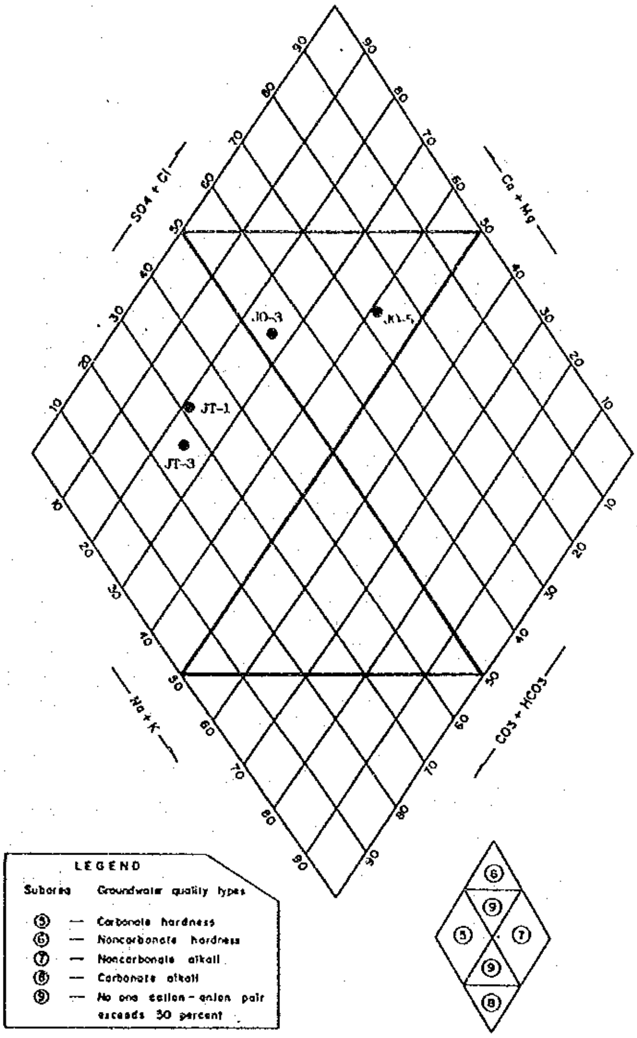

Piper's Trilinear Diagram

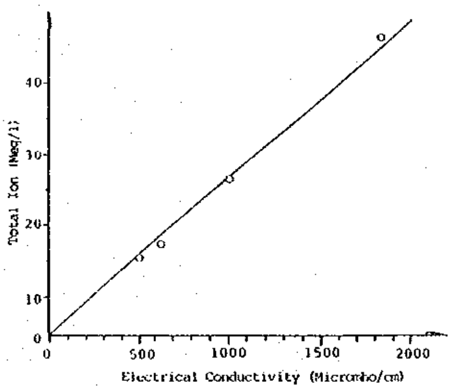

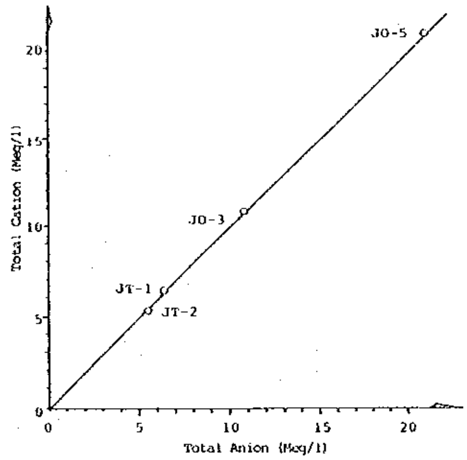

Fig.5.11
Piper's Tri-linear Diagram
(JT-1, JT-3, JO-3 and JO-5)

THE HASHEMITE KINGDOM OF JORDAN
WATER RESOURCES STUDY OF THE JAFR BASIN
JAPAN INTERNATIONAL COOPERATION AGENCY

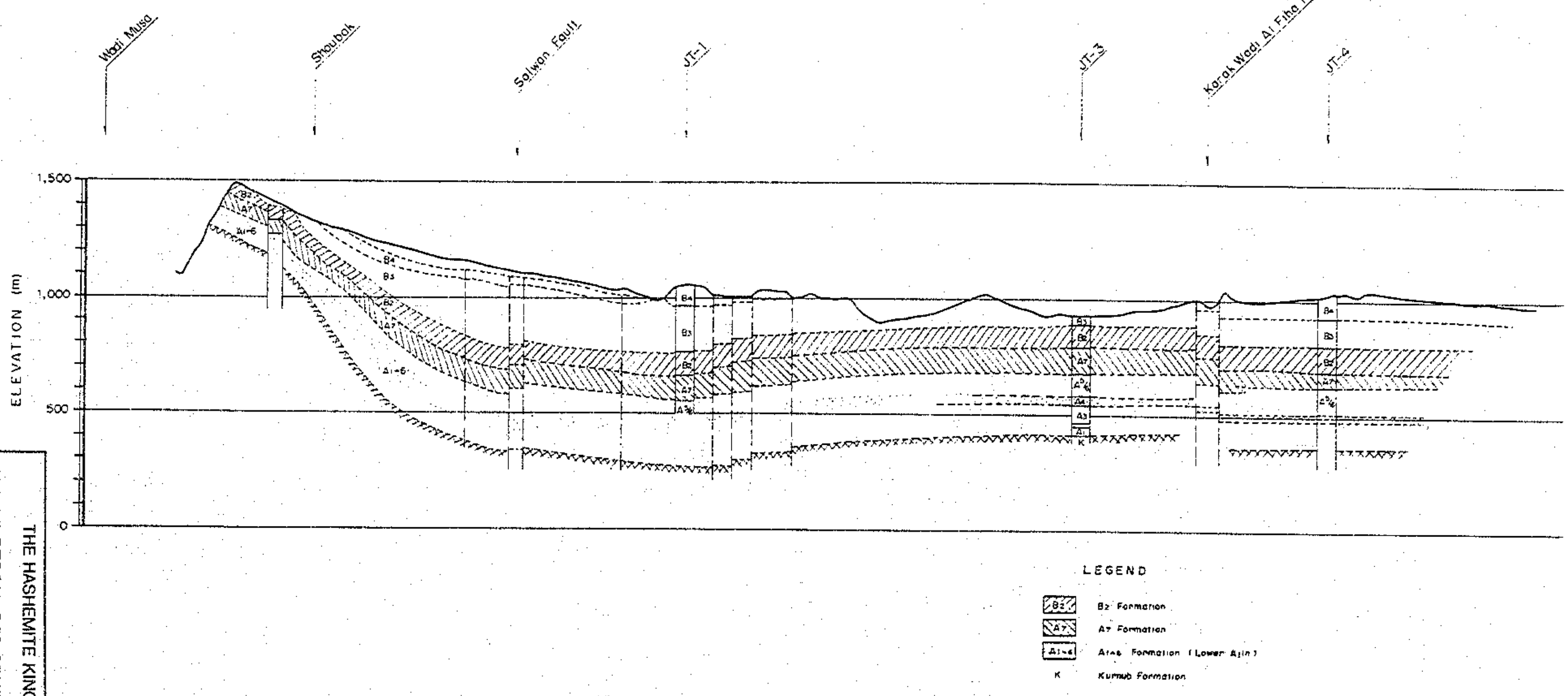

Fig.5.12 Geological Profile along Boundary Between Upper Hasa and Jafr Basin

THE HASHEMITE KINGDOM OF JORDAN

WATER RESOURCES STUDY OF THE JAFR BASIN

JAPAN INTERNATIONAL COOPERATION AGENCY

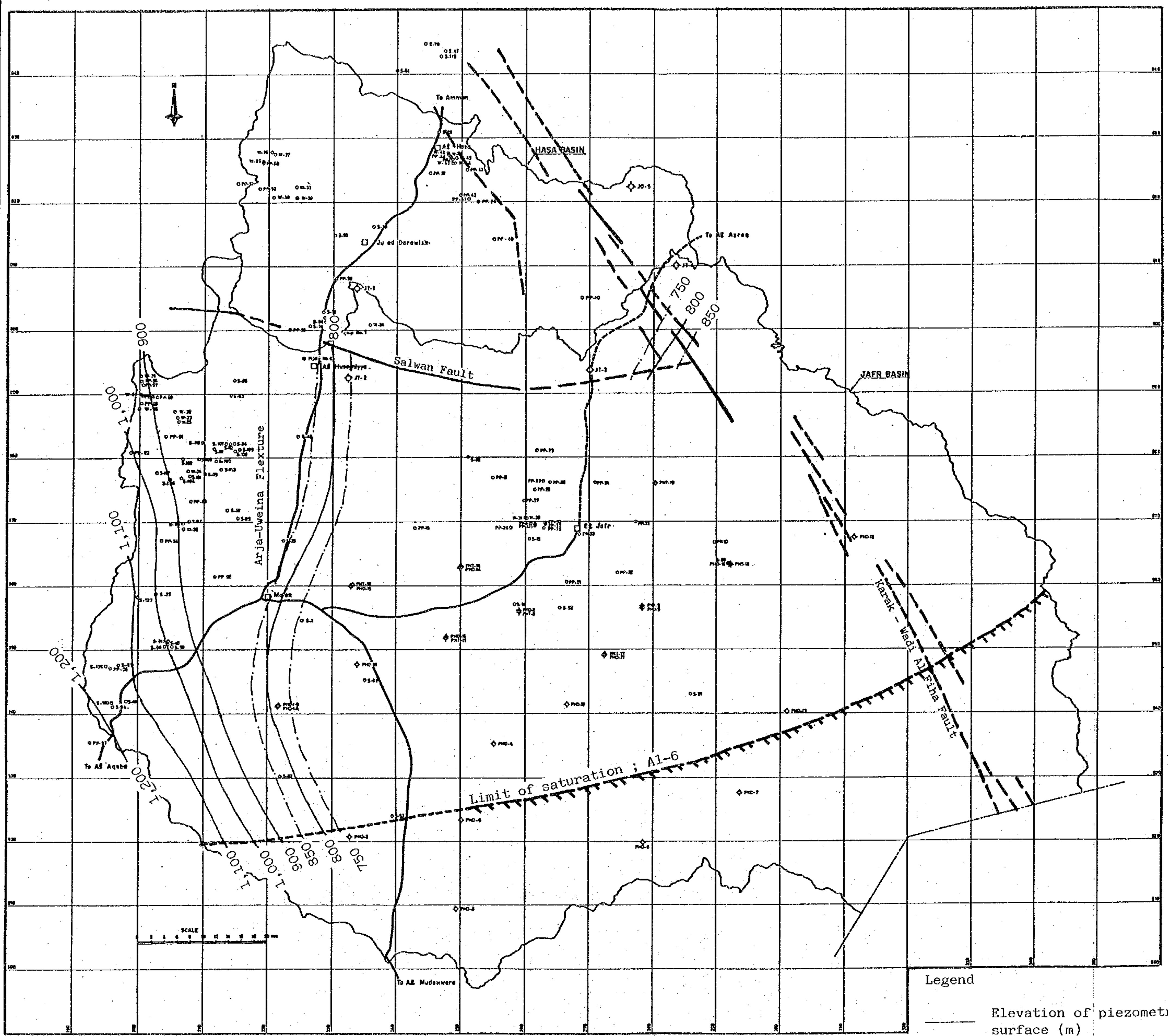

Legend

Elevation of piezometric surface (m)

Fig 5.13

Groundwater Level Map of A1-6

THE HASHEMITE KINGDOM OF JORDAN

WATER RESOURCES STUDY OF THE JAFR BASIN

JAPAN INTERNATIONAL COOPERATION AGENCY

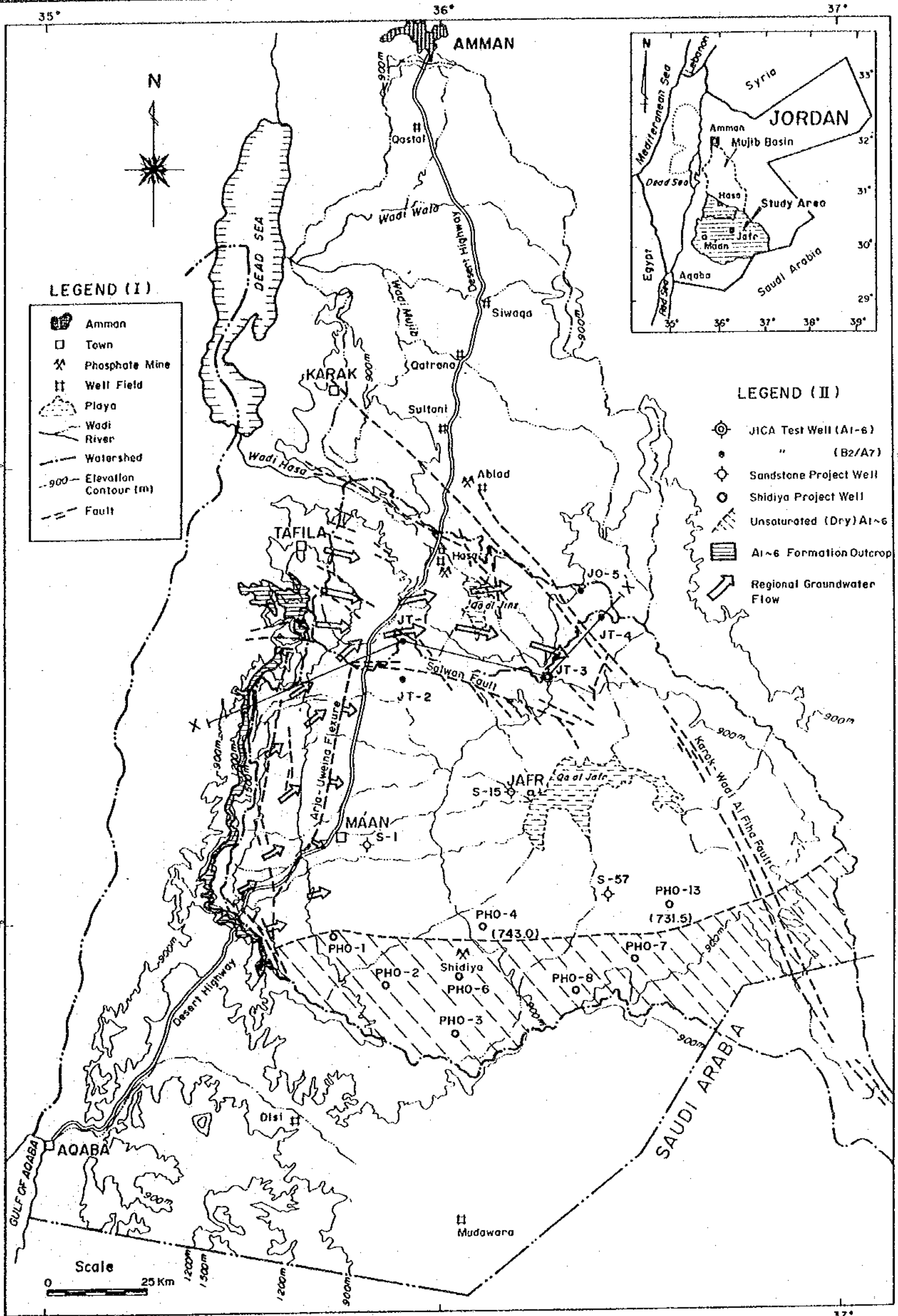

Fig.5.14 Hydrogeological Map of Lower Ajlun (A1-6) Formation

THE HASHEMITE KINGDOM OF JORDAN

WATER RESOURCES STUDY OF THE JAFR BASIN

JAPAN INTERNATIONAL COOPERATION AGENCY

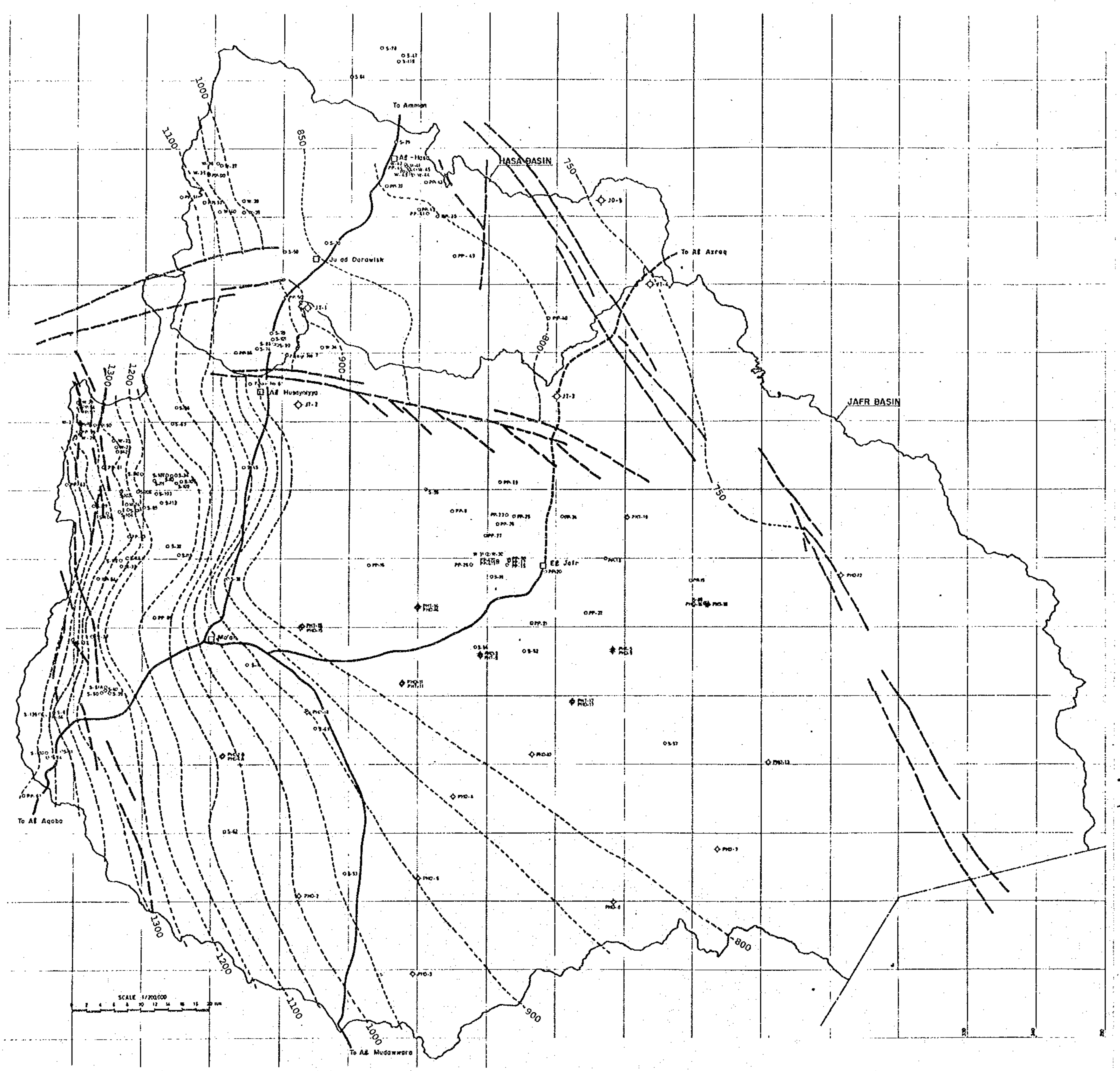

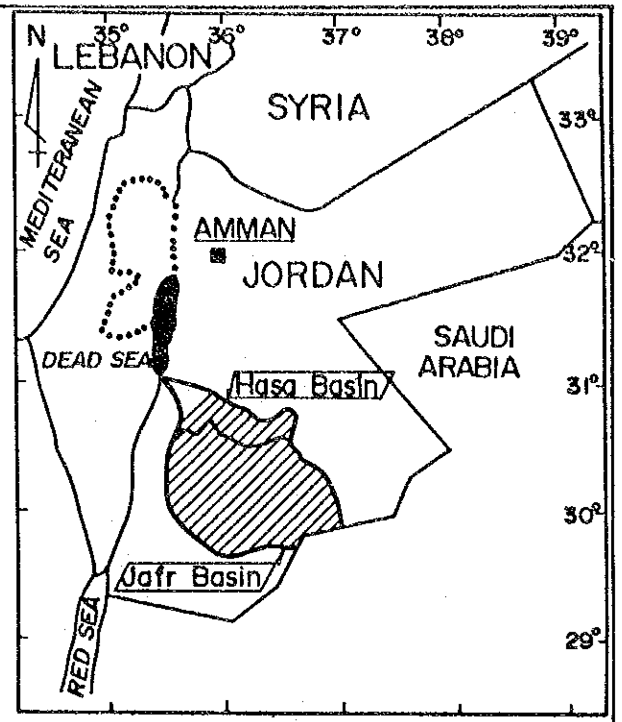

Legend

— — —:Mejor fault

------:Contour line of static water level (m)

Fig.5.15

Groundwater Level Map of B2/A7

THE HASHEMITE KINGDOM OF JORDAN

WATER RESOURCES STUDY OF THE JAFR BASIN

JAPAN INTERNATIONAL COOPERATION AGENCY

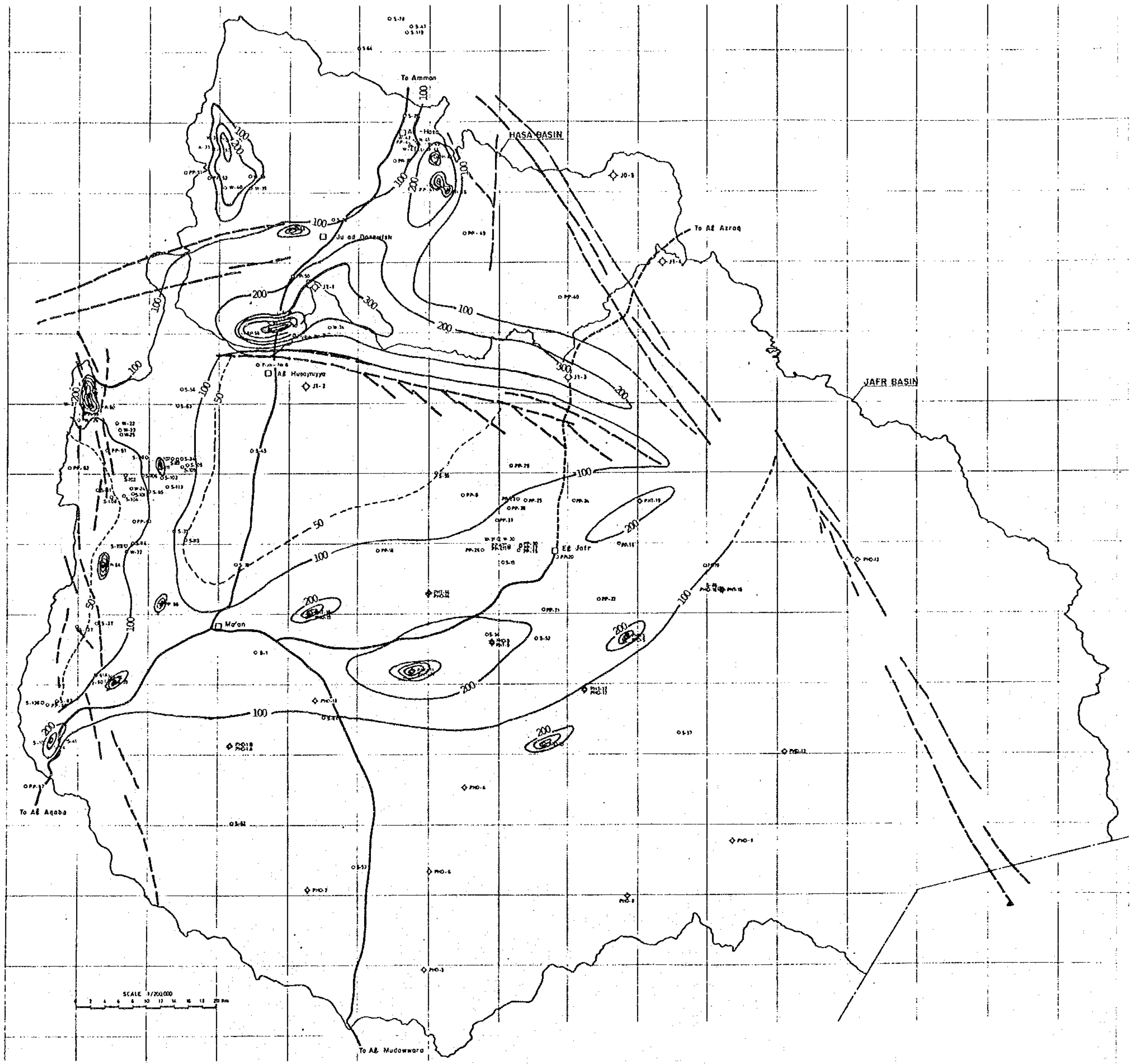

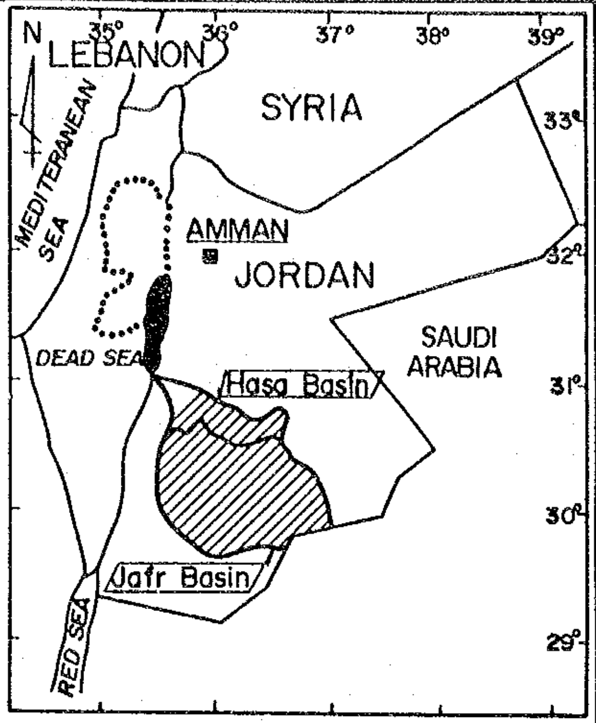

Legend

━ ━ ━ : Mejor fault

------ : Contour line of transmissivity (m^2/day)

Fig.5.16

Transmissivity Map of B2/A7

THE HASHEMITE KINGDOM OF JORDAN

WATER RESOURCES STUDY OF THE JAFR BASIN

JAPAN INTERNATIONAL COOPERATION AGENCY

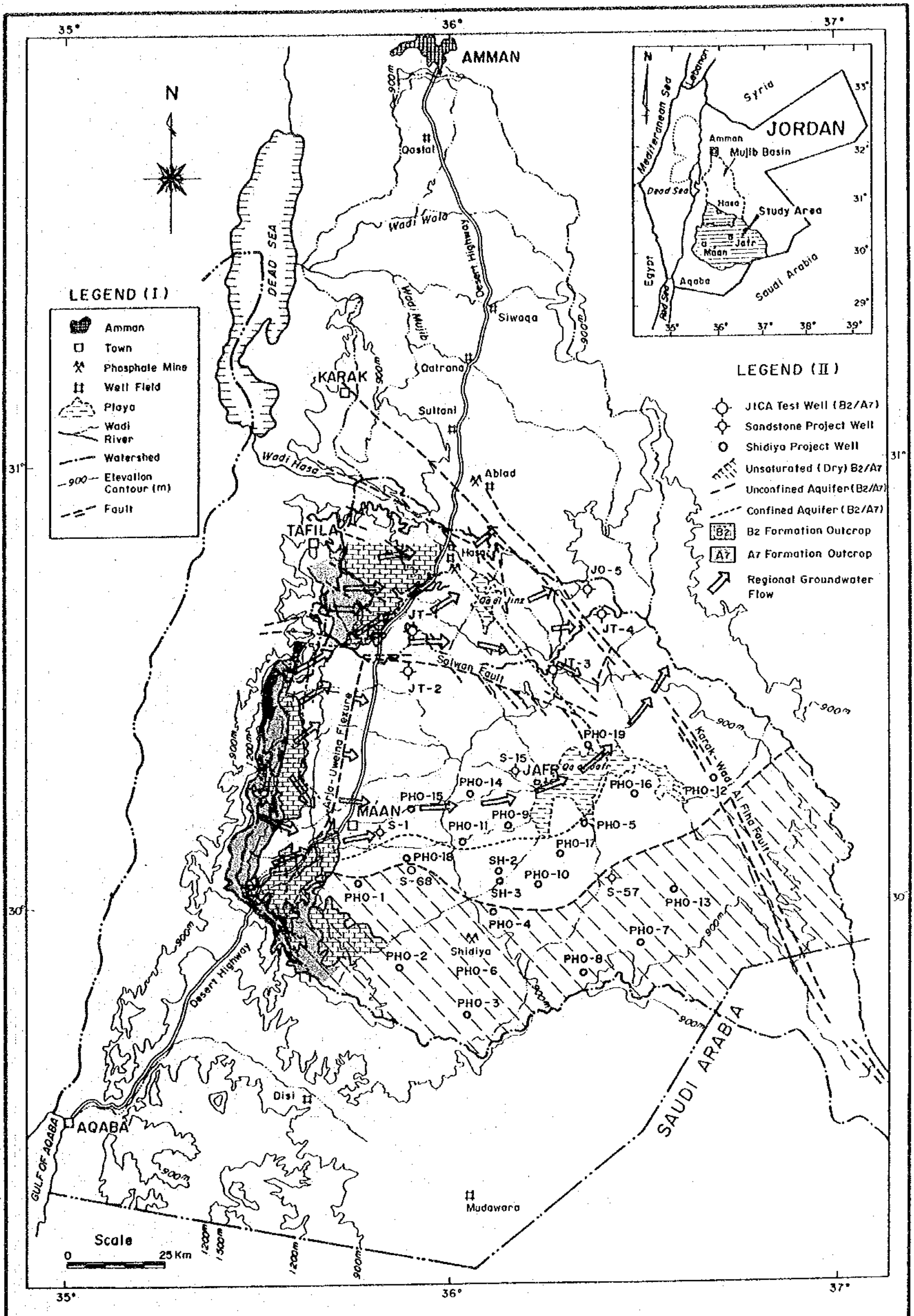

Fig.5.17 Hydrogeological Map of Amman - Wadi Sir (B2/A7) Formation

THE HASHEMITE KINGDOM OF JORDAN

WATER RESOURCES STUDY OF THE JAFR BASIN

JAPAN INTERNATIONAL COOPERATION AGENCY

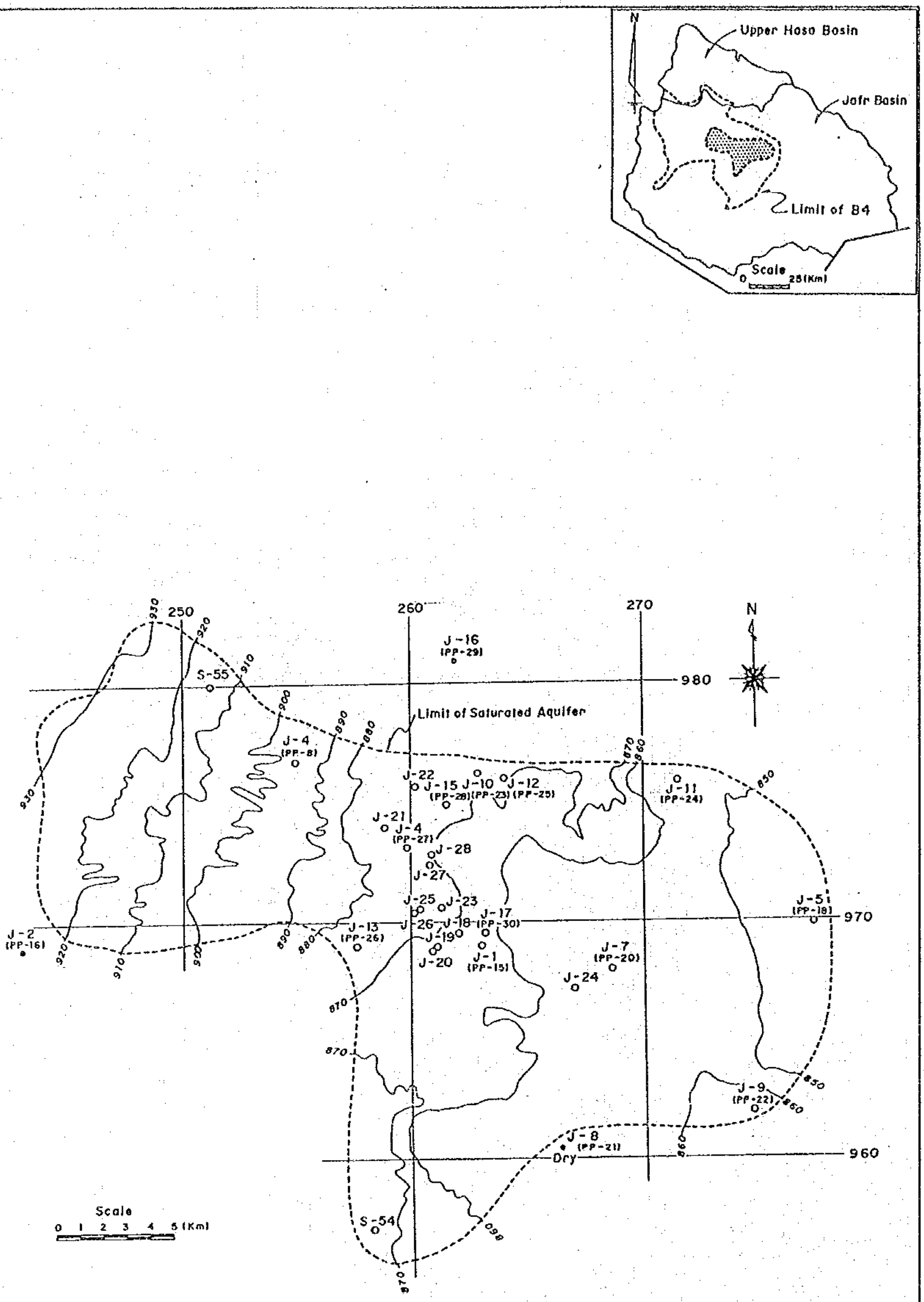

Fig.5.18

Location Map of Rijam (B4) Aquifer

THE HASHEMITE KINGDOM OF JORDAN

WATER RESOURCES STUDY OF THE JAFR BASIN

JAPAN INTERNATIONAL COOPERATION AGENCY

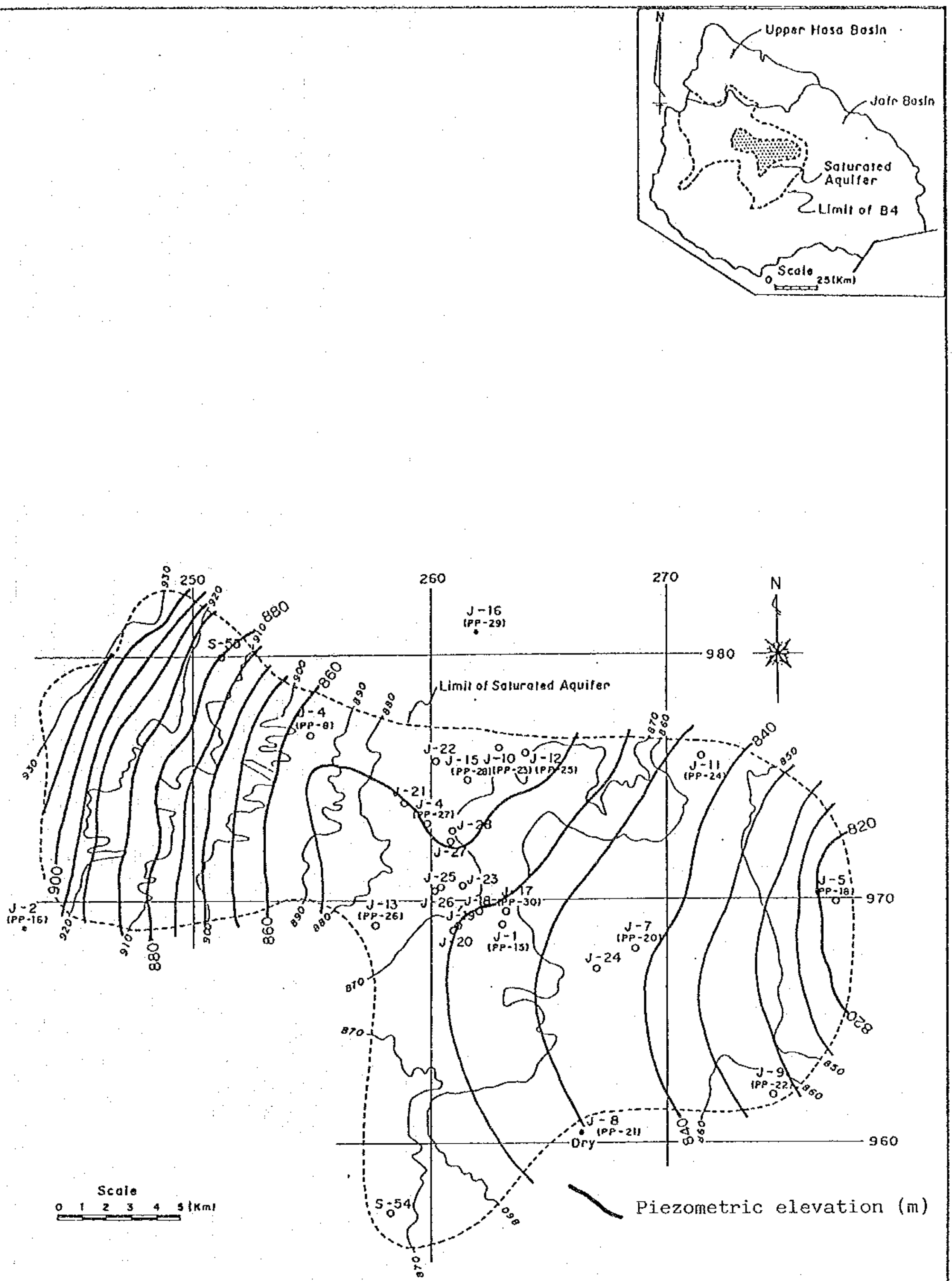

Fig.5.19

Groundwater Level Map of B4

THE HASHEMITE KINGDOM OF JORDAN

WATER RESOURCES STUDY OF THE JAFR BASIN

JAPAN INTERNATIONAL COOPERATION AGENCY

List of well No. in Jafr area

JAFR-1	(PP-15)	JAFR-16	(PP-29)
JAFR-2	(PP-16)	JAFR-17	(PP-30)
JAFR-3	(PP-17)	JAFR-18	
JAFR-4	(PP- 8)	JAFR-19	(PP-470)
JAFR-5	(PP-18)	JAFR-20	(PP-471)
JAFR-6	(PP-19)	JAFR-21	
JAFR-7	(PP-20)	JAFR-22	
JAFR-8	(PP-21)	JAFR-23	
JAFR-9A	(PP-22)	JAFR-24	
JAFR-10	(PP-23)	JAFR-25	(W-30)
JAFR-11	(PP-24)	JAFR-26	(W-31)
JAFR-12	(PP-25)		
JAFR-13	(PP-26)		
JAFR-14	(PP-27)		
JAFR-15	(PP-28)		

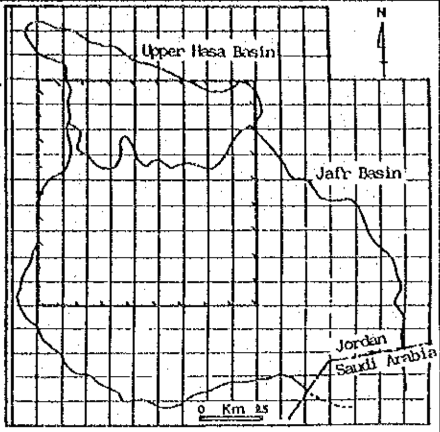

Legend

Isopach contour of B4

Contour line of Transmissivity (m^2/d)

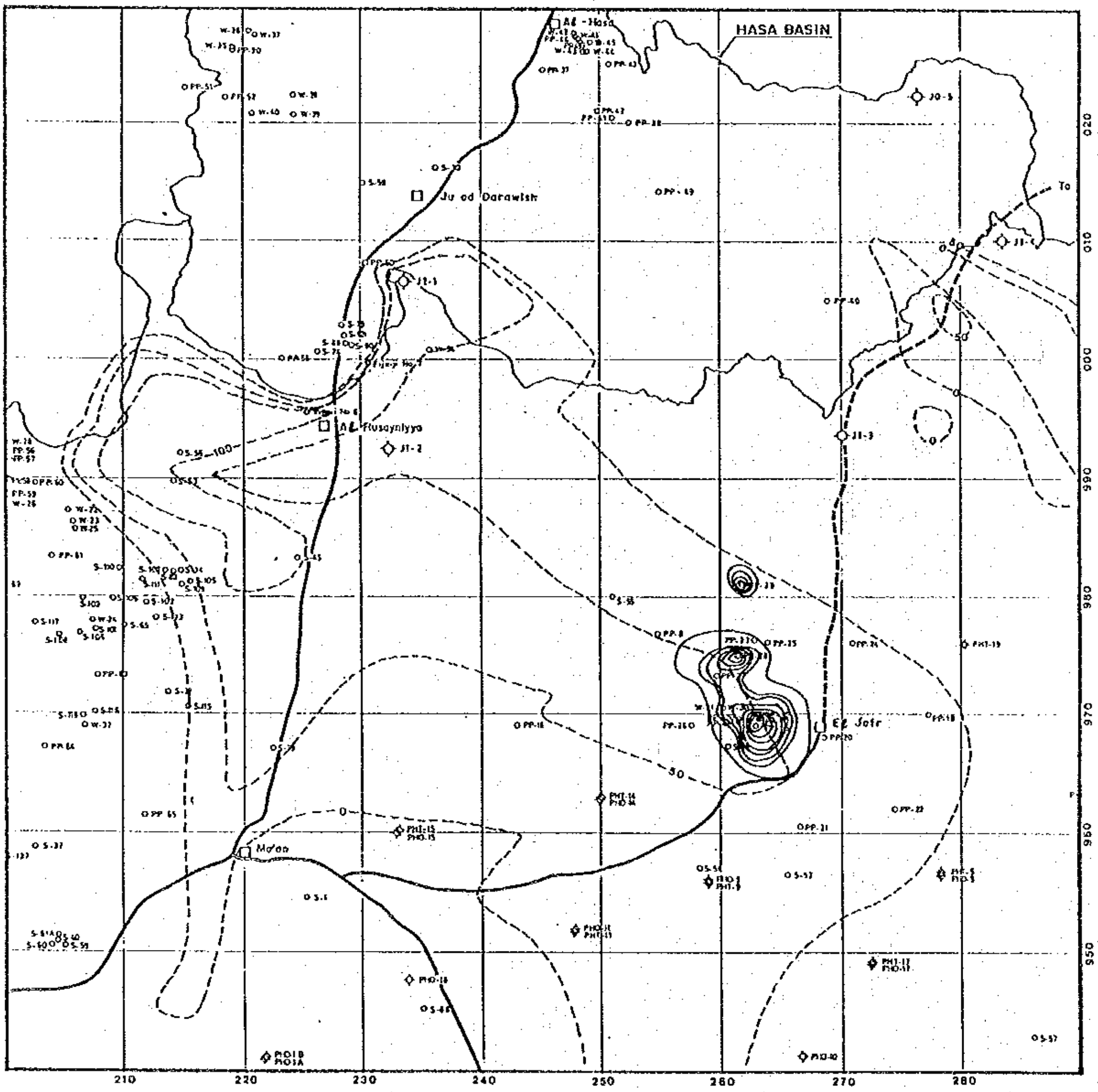

Fig.5.20

Transmissivity Map of B4

THE HASHEMITE KINGDOM OF JORDAN

WATER RESOURCES STUDY OF THE JAFR BASIN

JAPAN INTERNATIONAL COOPERATION AGENCY

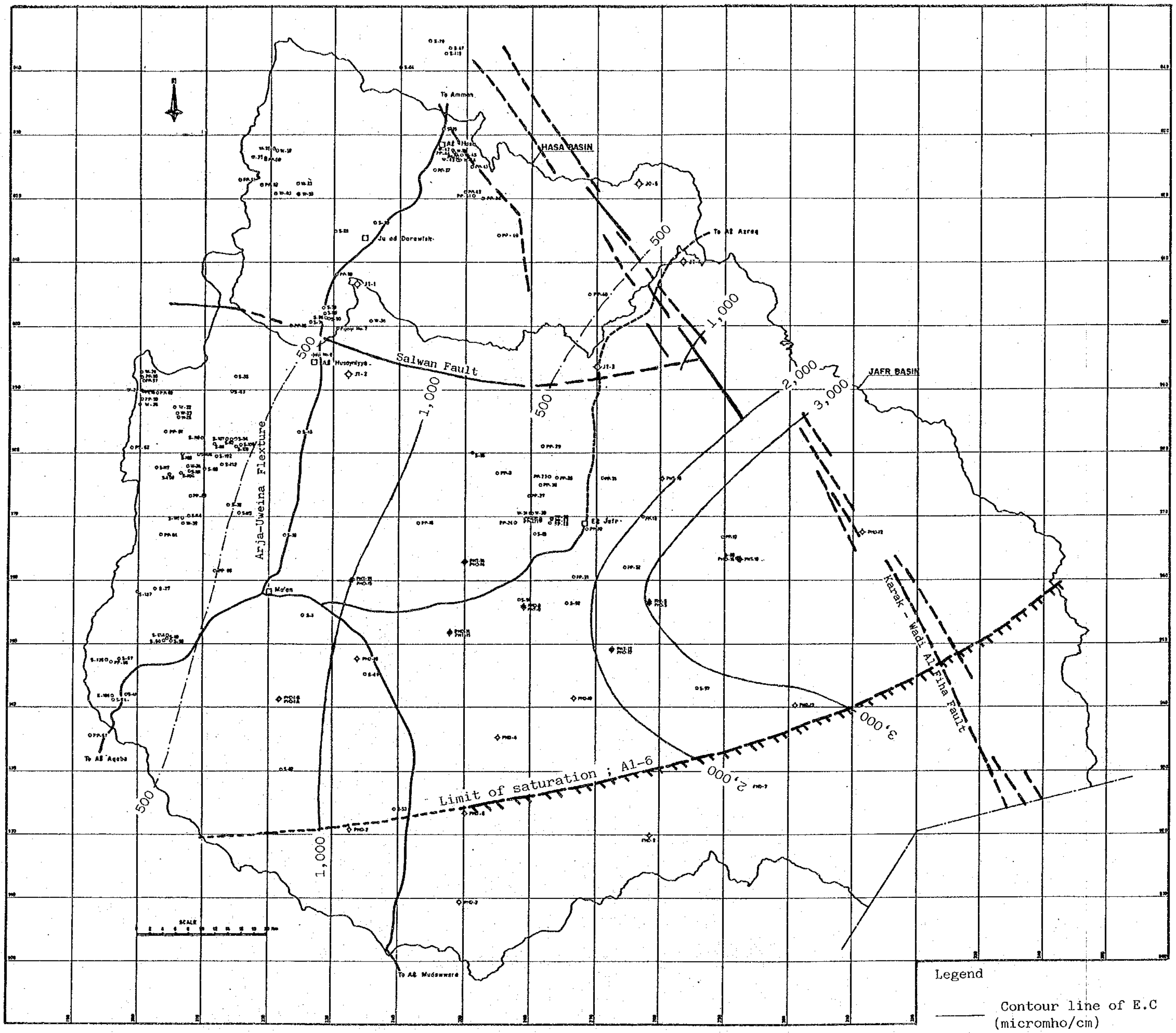

Fig.5.21

Water salinity (E.C) Map of A1-6

Legend

Contour line of E.C (micromho/cm)

THE HASHEMITE KINGDOM OF JORDAN

WATER RESOURCES STUDY OF THE JAFR BASIN

JAPAN INTERNATIONAL COOPERATION AGENCY

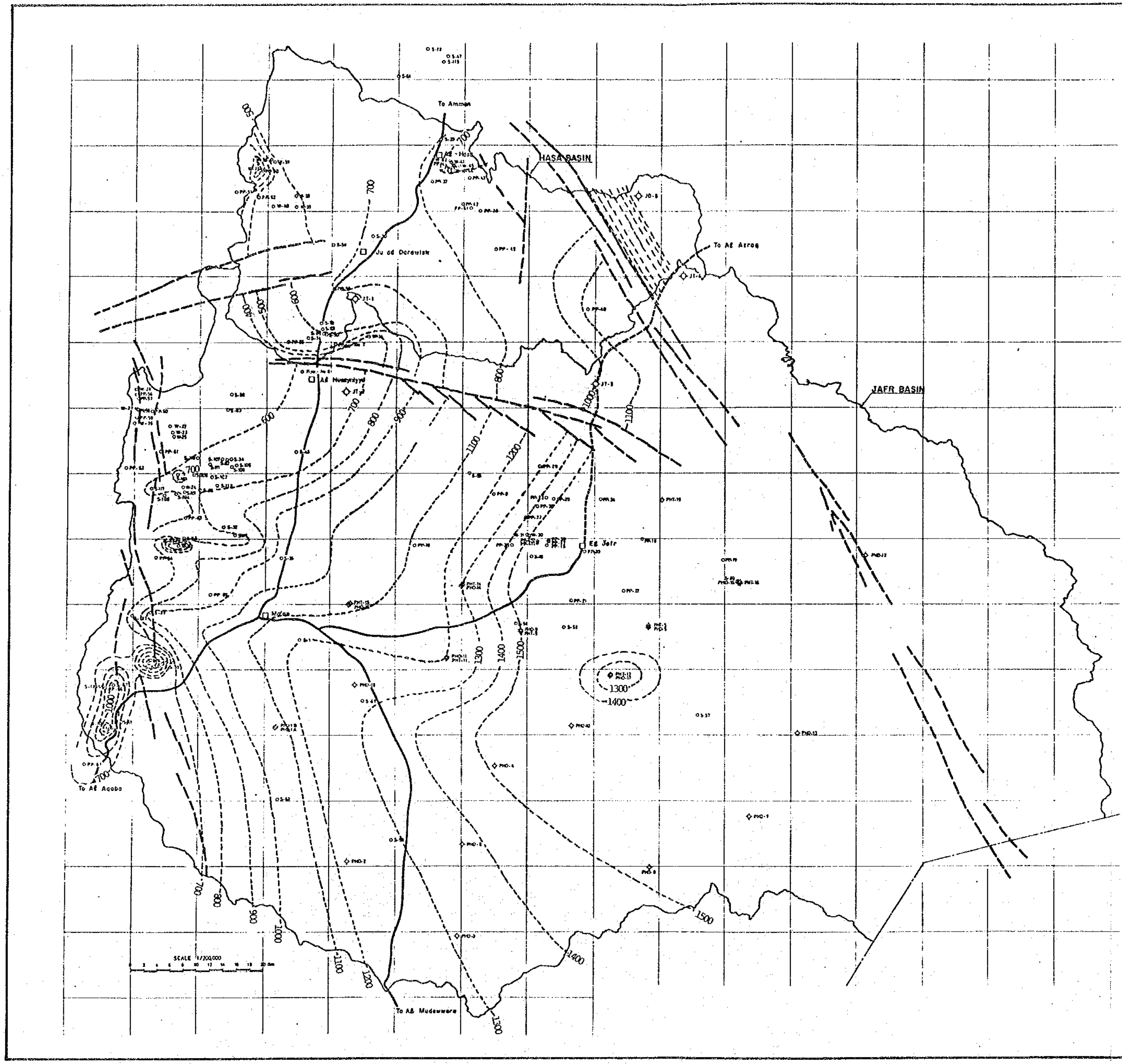

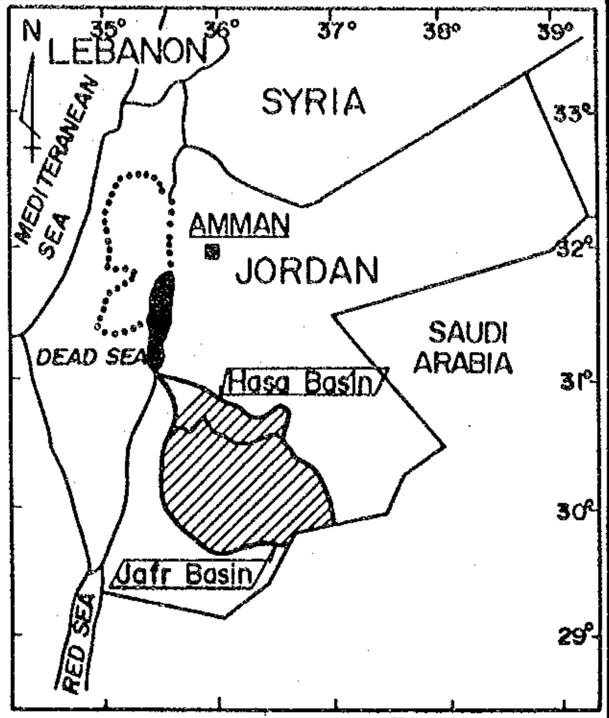

Legend

▬ ▬ ▬:Mejor fault

------:Contour line of electric conductivity (micro mho/cm)

Fig.5.22

Water Salinity (E.C) Map of B2/A7

THE HASHEMITE KINGDOM OF JORDAN

WATER RESOURCES STUDY OF THE JAFR BASIN

JAPAN INTERNATIONAL COOPERATION AGENCY

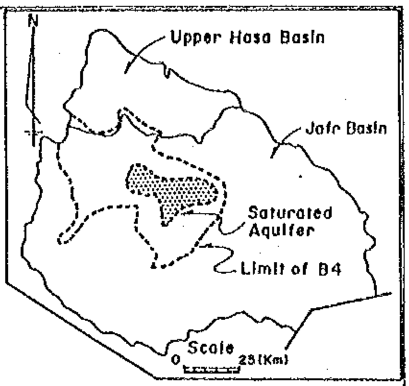

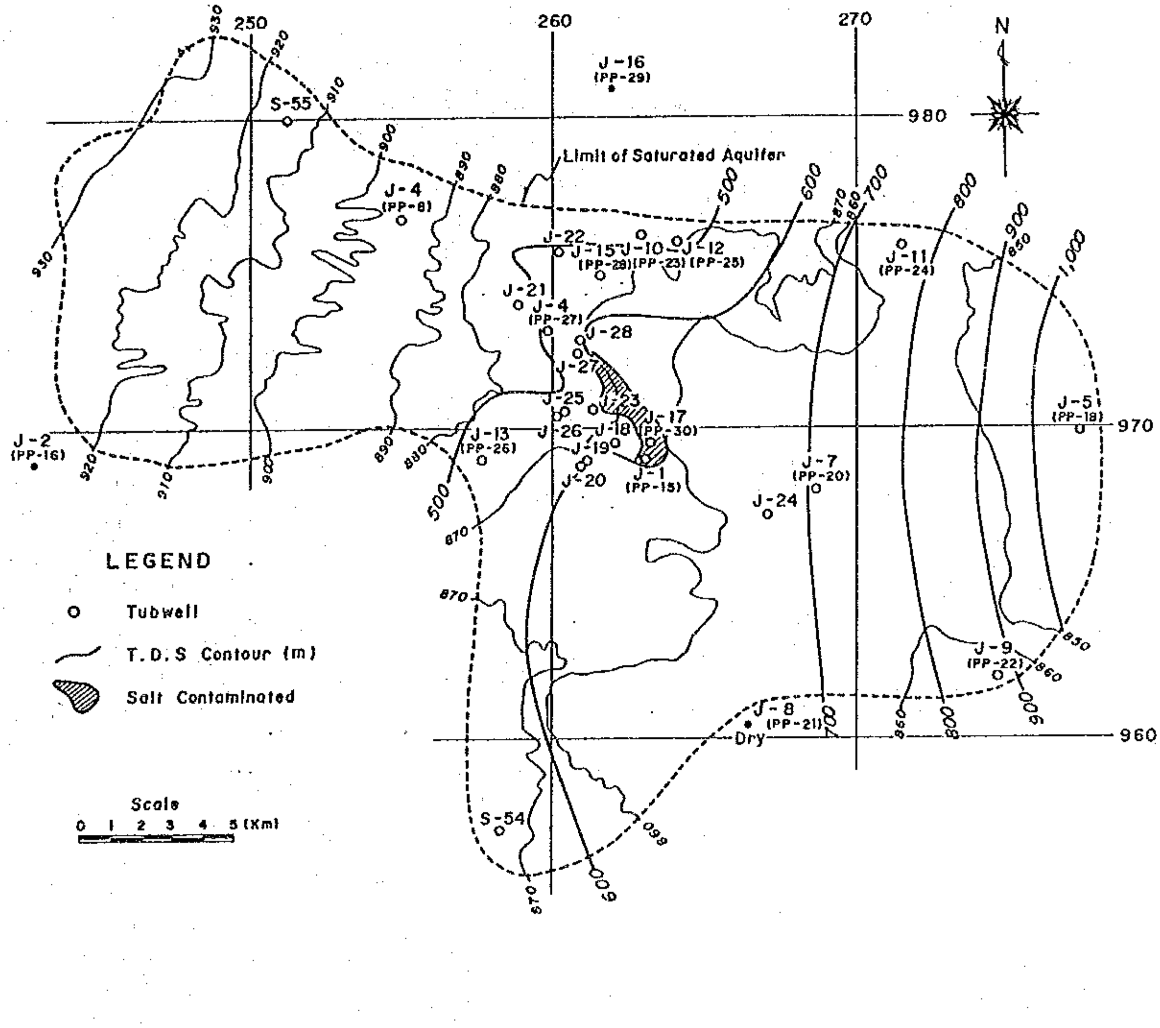

Fig.5.23

Water Salinity (E.C) Map of B4

THE HASHEMITE KINGDOM OF JORDAN

WATER RESOURCES STUDY OF THE JAFR BASIN

JAPAN INTERNATIONAL COOPERATION AGENCY

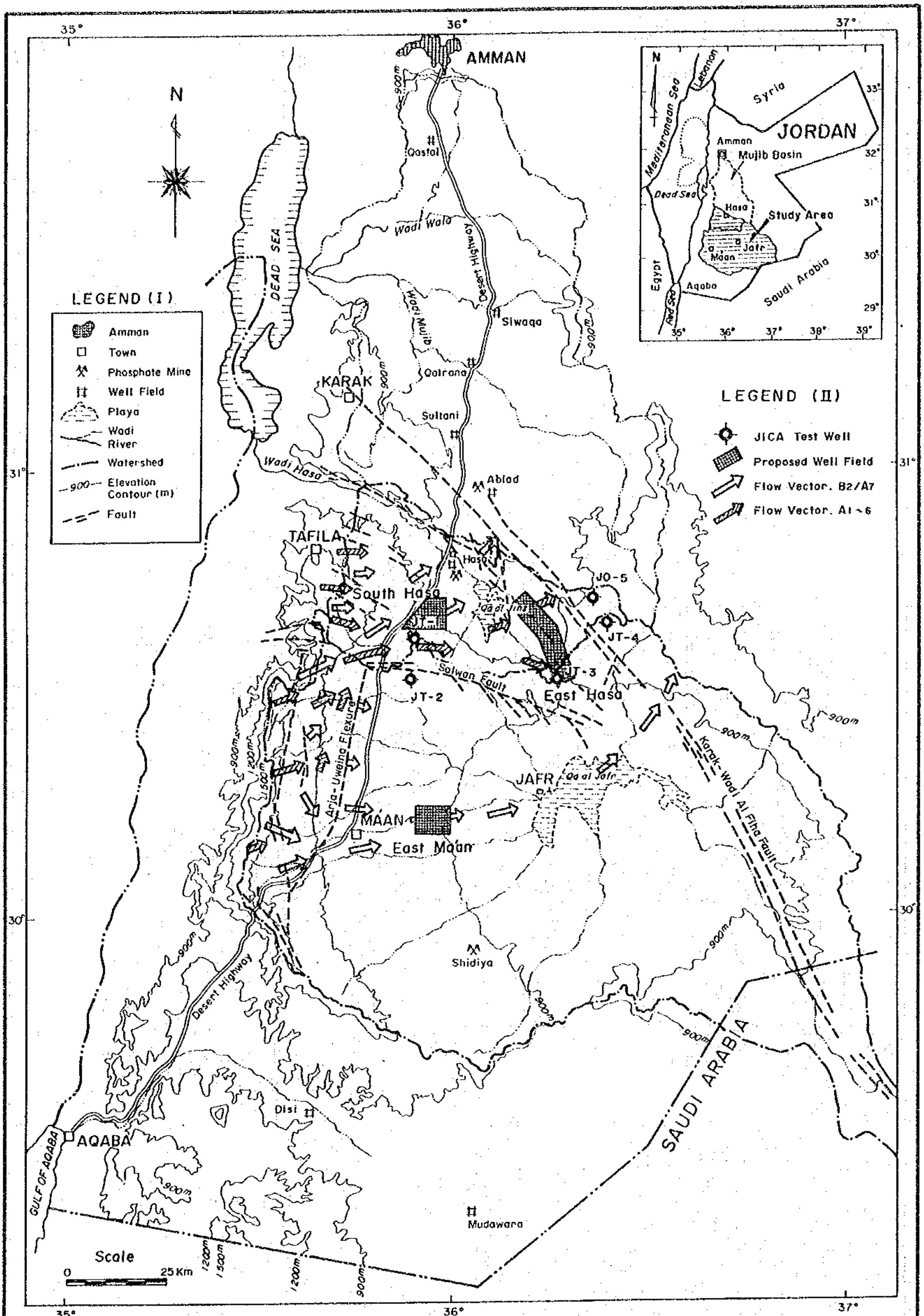

Fig.5.24 Proposed Well Field in the Simulation Model

THE HASHEMITE KINGDOM OF JORDAN

WATER RESOURCES STUDY OF THE JAFR BASIN

JAPAN INTERNATIONAL COOPERATION AGENCY

Boundary Condition

Specified Head: Node	Specified Head: Head (EL m)	Specified Flow: Node	Specified Flow: Flow (m3/day)
7	937.5	4	-600
13	950.0	5	-600
16	1000.0	6	-600
37	1030.0	12	-600
39	1000.0	29	-600
40	950.0	30	-600
102	950.0	32	-500
103	945.8	33	-500
121	965.0	34	-600
122	960.0	35	-600
124	975.0	56	-700
136	962.7	67	-700
142	1171.2	100	-2600
150	1202.5	101	-2600
151	1131.6	191	-880
155	1052.5	192	-880
168	1152.5	230	-550
169	1068.7		
193	1102.5		
199	1272.5		
200	1272.5		
202	1302.5		

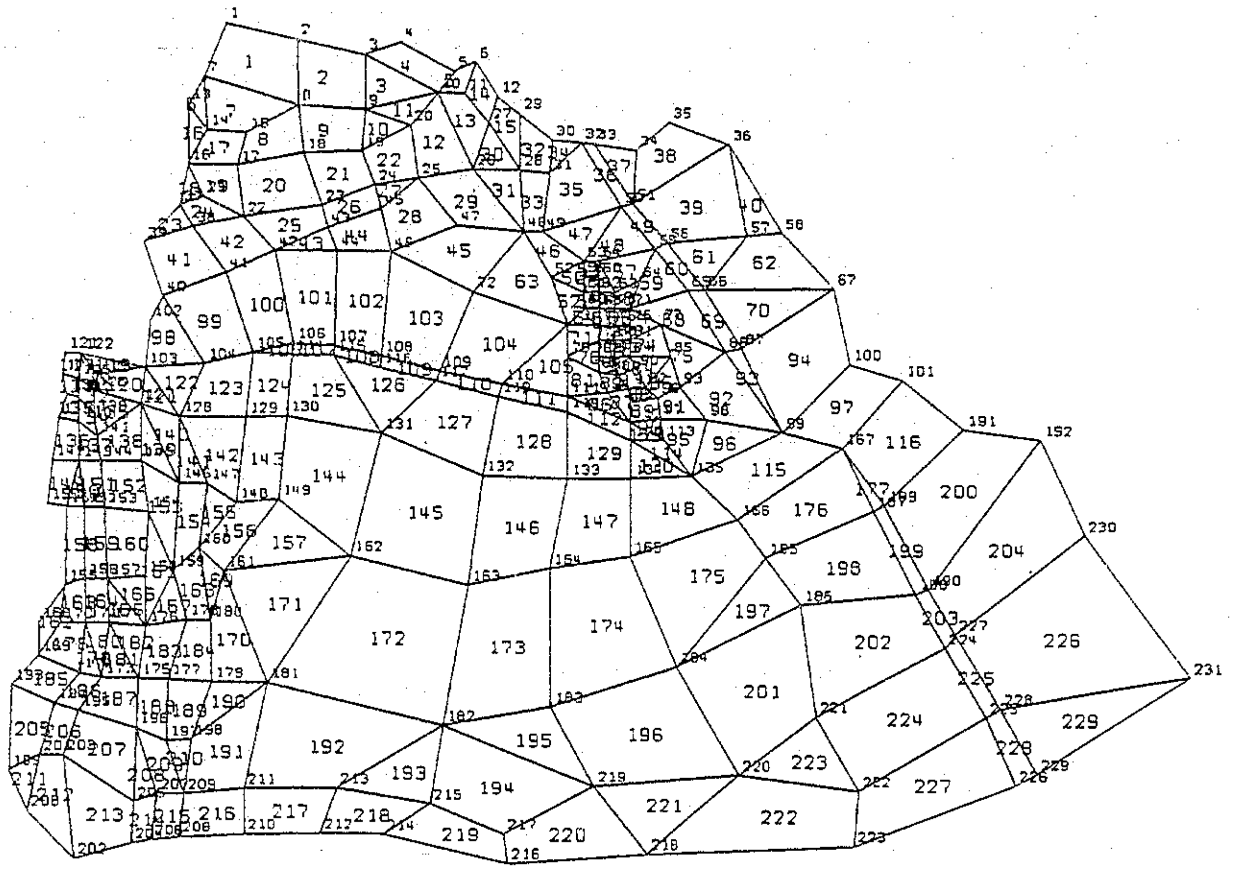

FEM PLOT SCALE 0.0 16637.4

FEM PLOT SCALE 0.0 16637.4

LOWER AJLUN (A1/6)
FEM MESH

Fig.5.25 FEM Simulation Mesh of Lower Ajlun (A1-6) Aquifer System

THE HASHEMITE KINGDOM OF JORDAN

WATER RESOURCES STUDY OF THE JAFR BASIN

JAPAN INTERNATIONAL COOPERATION AGENCY

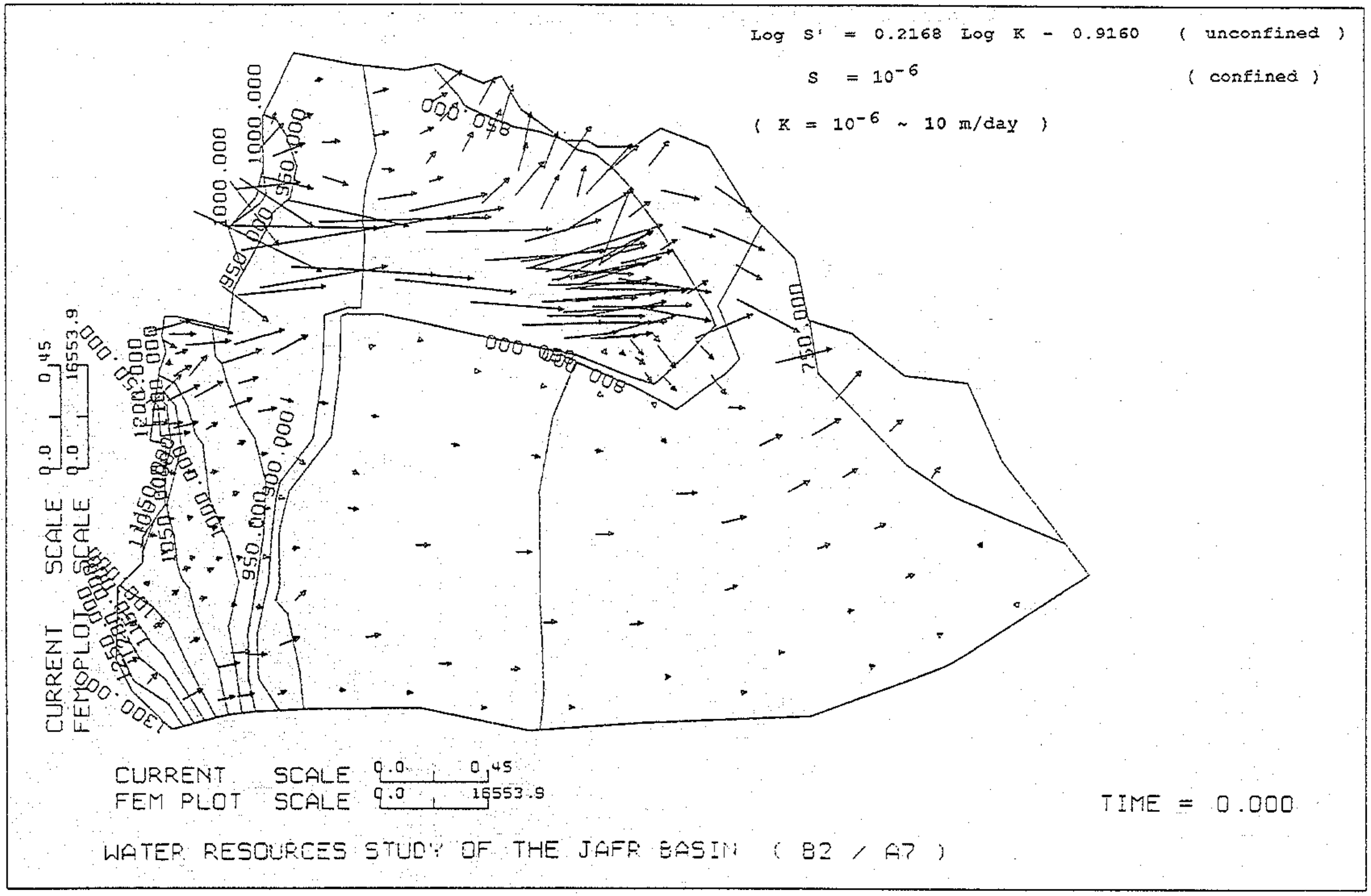

Fig.5.26 Calibrated Piezometric Surface and Computed Regional Flow Vector of Lower Ajlun (A1-6).

THE HASHEMITE KINGDOM OF JORDAN

WATER RESOURCES STUDY OF THE JAFR BASIN

JAPAN INTERNATIONAL COOPERATION AGENCY

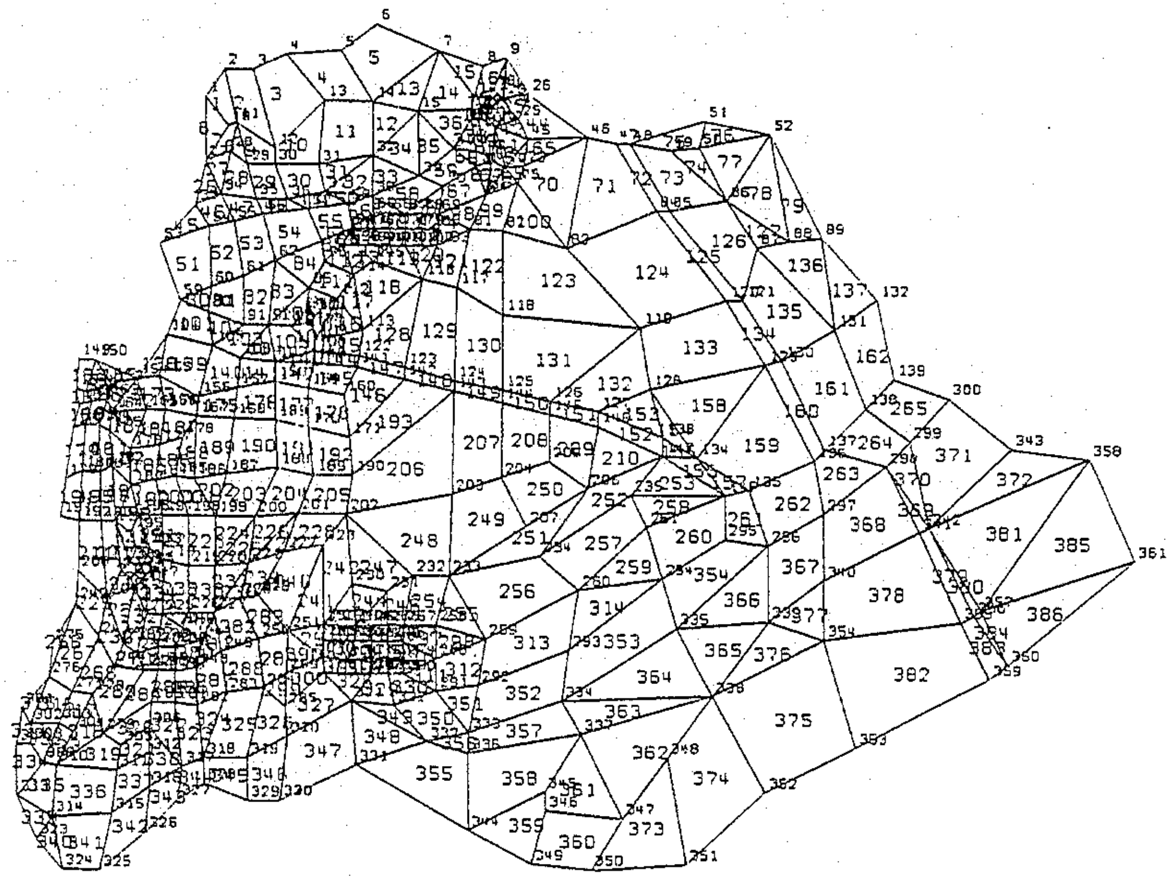

FEM PLOT SCALE 0.0 15897.4

FEM PLOT SCALE 0.0 15897.4

AMMAN / WADI SIR (B2/A7)
FEM MESH

Boundary Condition

Specified Head		Specified Flow	
Node	Head (EL m)	Node	Flow (m3/day)
1	1120.0	7	-1800
27	1120.0	8	-2400
33	1120.0	9	-2400
53	1140.0	26	-2400
59	1160.0	46	-2400
104	1190.0	47	-1200
149	1450.0	48	-1200
150	1420.0	49	-2200
151	1440.0	51	-2400
154	1310.0	52	-2400
161	1440.0	89	-4000
172	1440.0	132	-4800
179	1460.0	139	-5600
191	1500.0	300	-5600
192	1420.0	343	-4800
208	1480.0	358	-4800
242	1480.0		
275	1500.0		
276	1470.0		
301	1500.0		
307	1500.0		
313	1500.0		
323	1500.0		
324	1500.0		

Fig.5.27 FEM Simulation Mesh of Amman - Wadi Sir (B2/A7) Aquifer System

THE HASHEMITE KINGDOM OF JORDAN

WATER RESOURCES STUDY OF THE JAFR BASIN

JAPAN INTERNATIONAL COOPERATION AGENCY

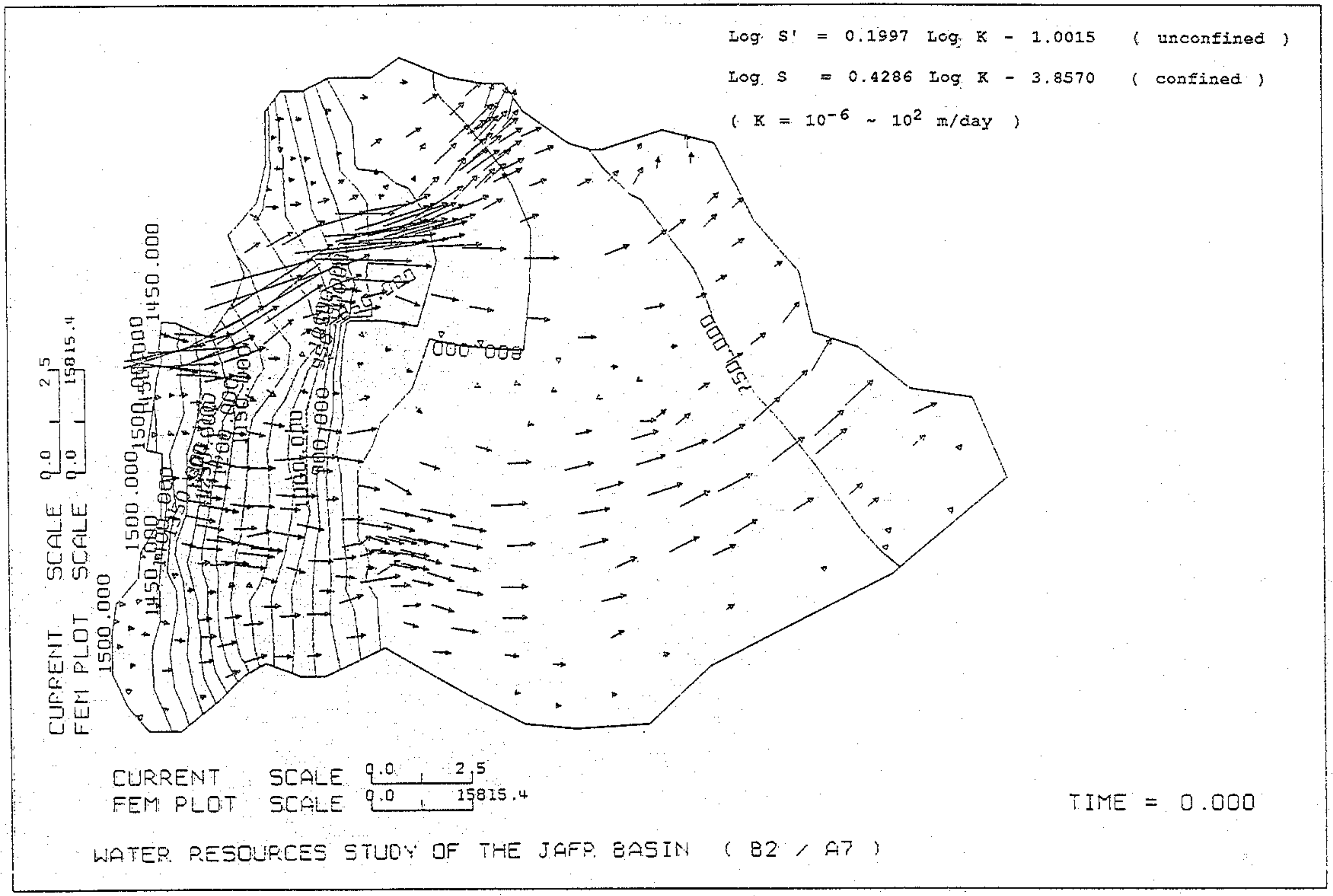

Fig. 5.28 Calibrated Piezometric Surface and Computed Regional Flow Vector of Amman - Wadi Sir (B2/A7)

THE HASHEMITE KINGDOM OF JORDAN

WATER RESOURCES STUDY OF THE JAFR BASIN

JAPAN INTERNATIONAL COOPERATION AGENCY

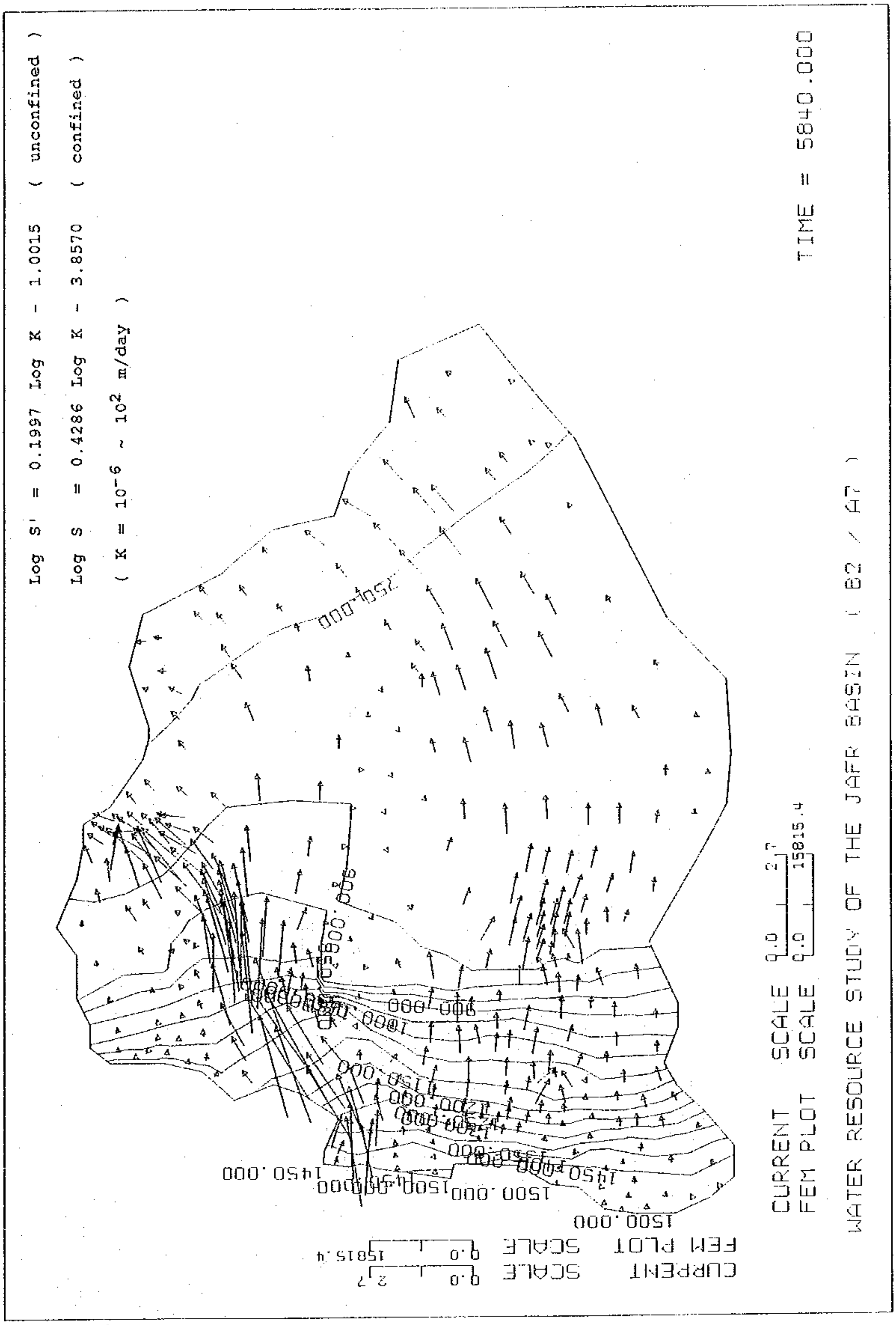

Fig.5.29 Calibrated Piezometric Surface of B2/A7 by the Year 1988

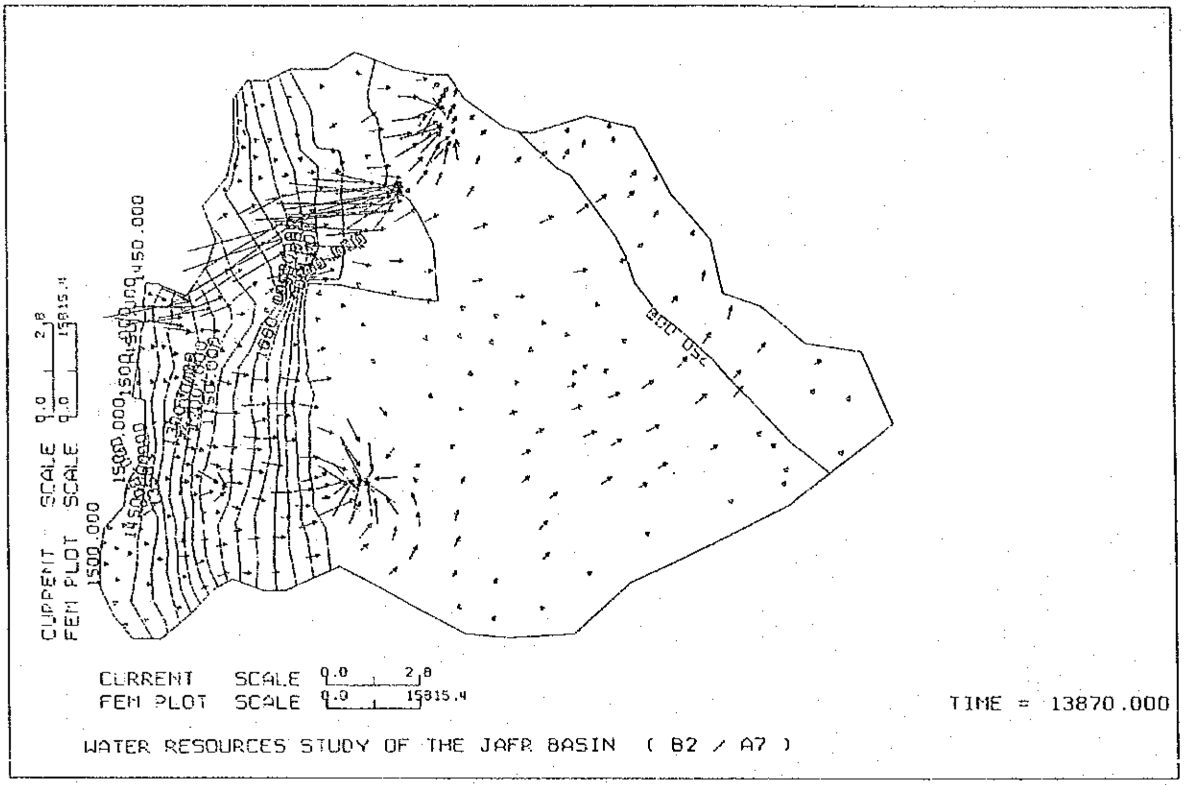

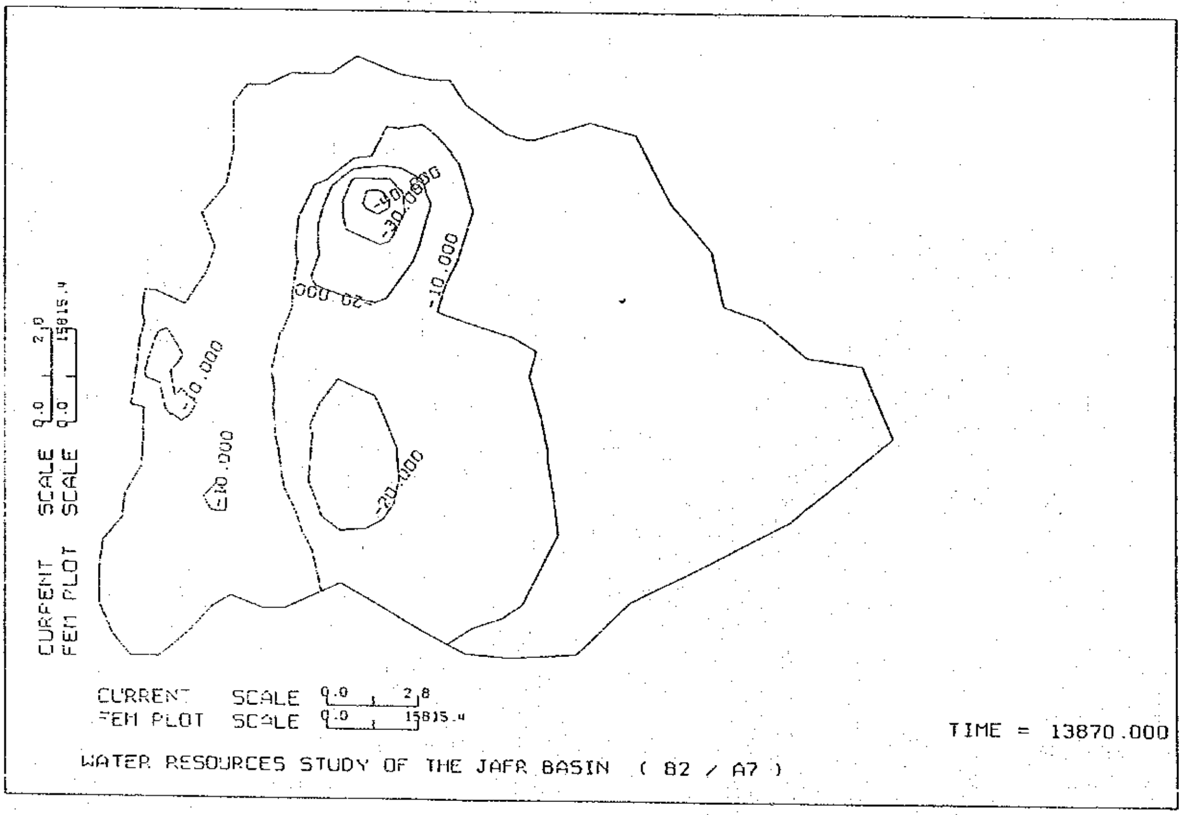

Fig. 5.39 Predicted Piezometric Surface of B2/A7 Aquifer; After 20 Years Pumping

THE HASHEMITE KINGDOM OF JORDAN

WATER RESOURCES STUDY OF THE JAFR BASIN

JAPAN INTERNATIONAL COOPERATION AGENCY

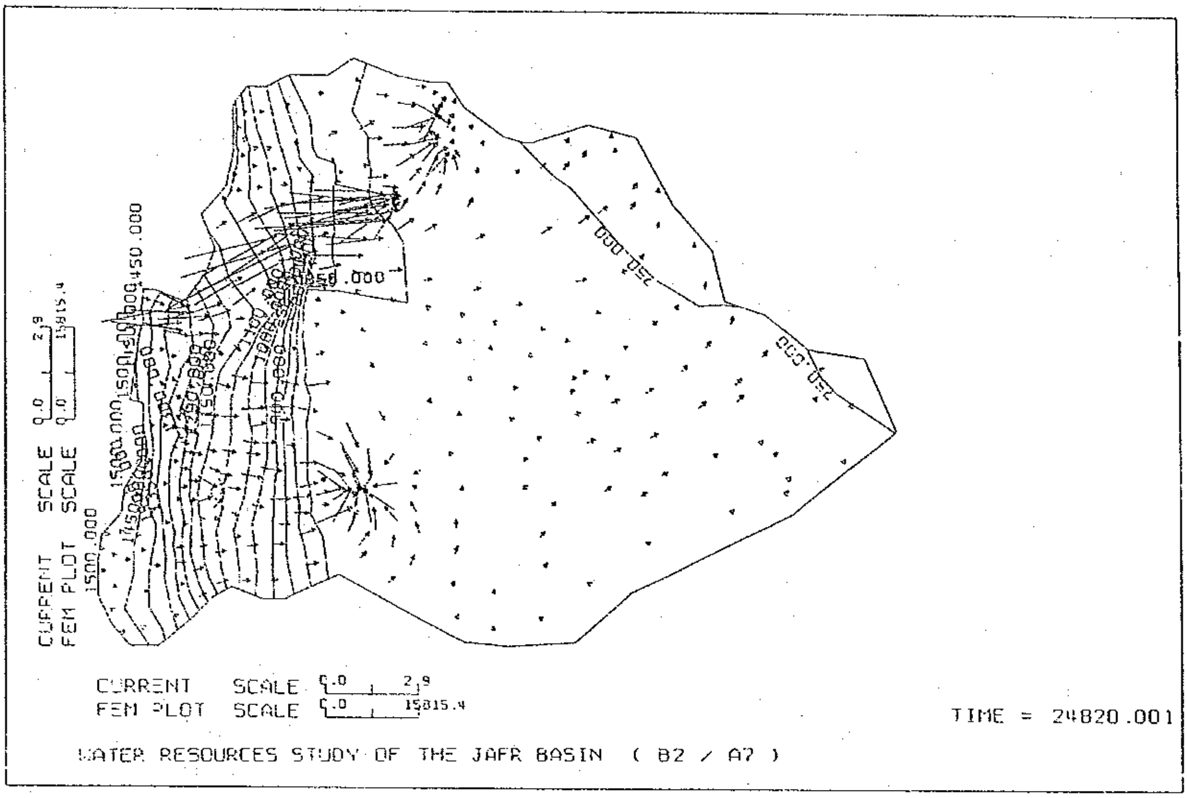

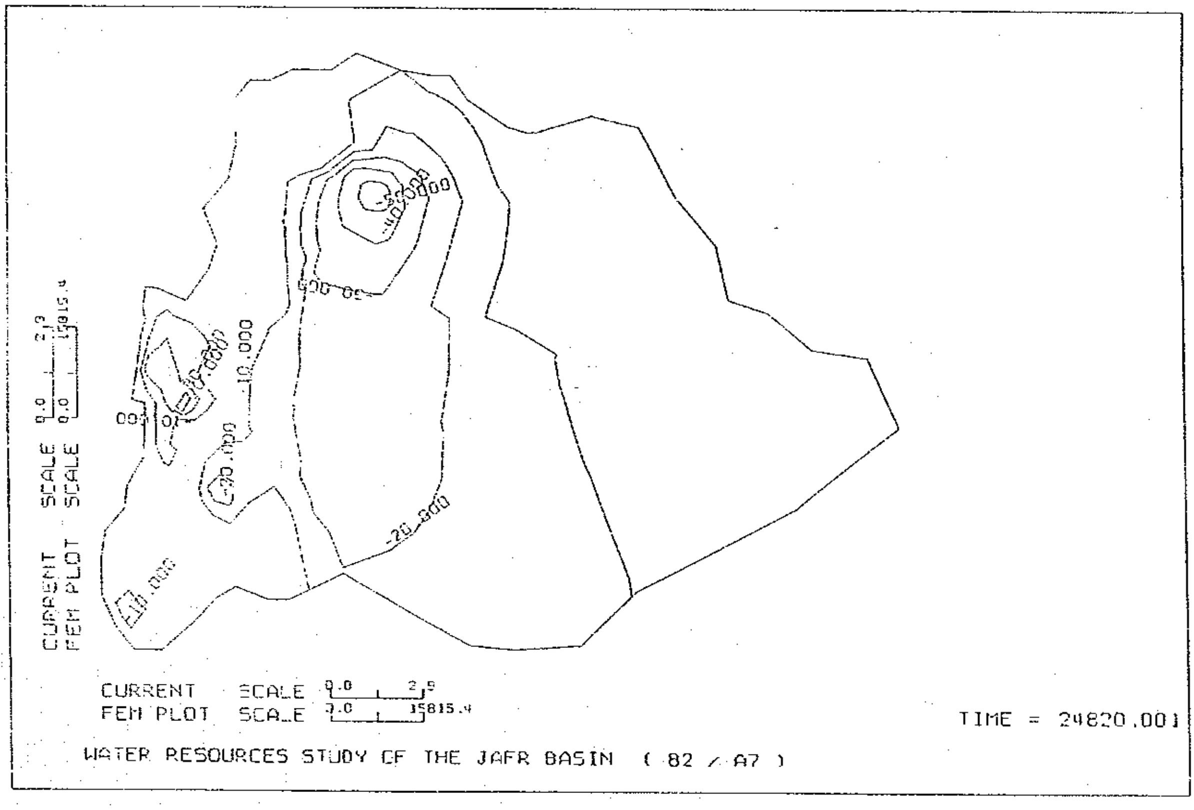

Fig. 5.31 Predicted Piezometric Surface of B2/A7 Aquifer; After 50 Years Pumping

THE HASHEMITE KINGDOM OF JORDAN

WATER RESOURCES STUDY OF THE JAFR BASIN

JAPAN INTERNATIONAL COOPERATION AGENCY

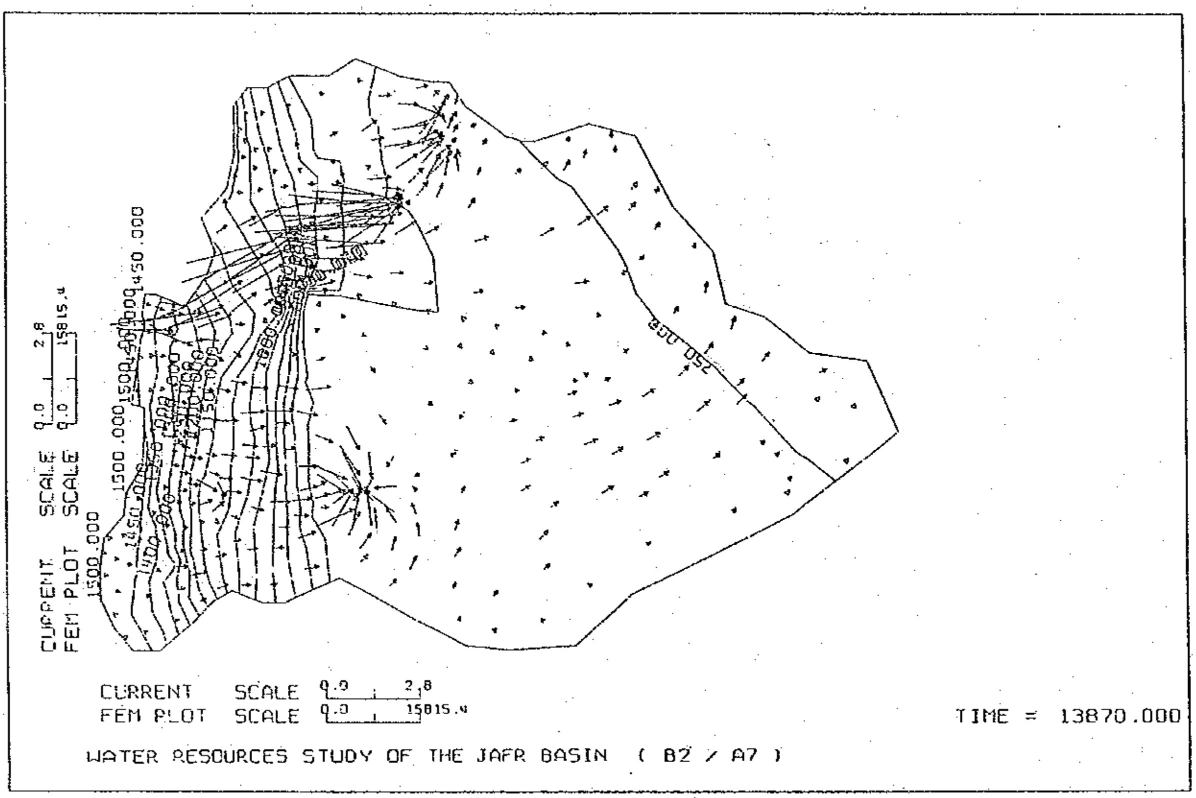

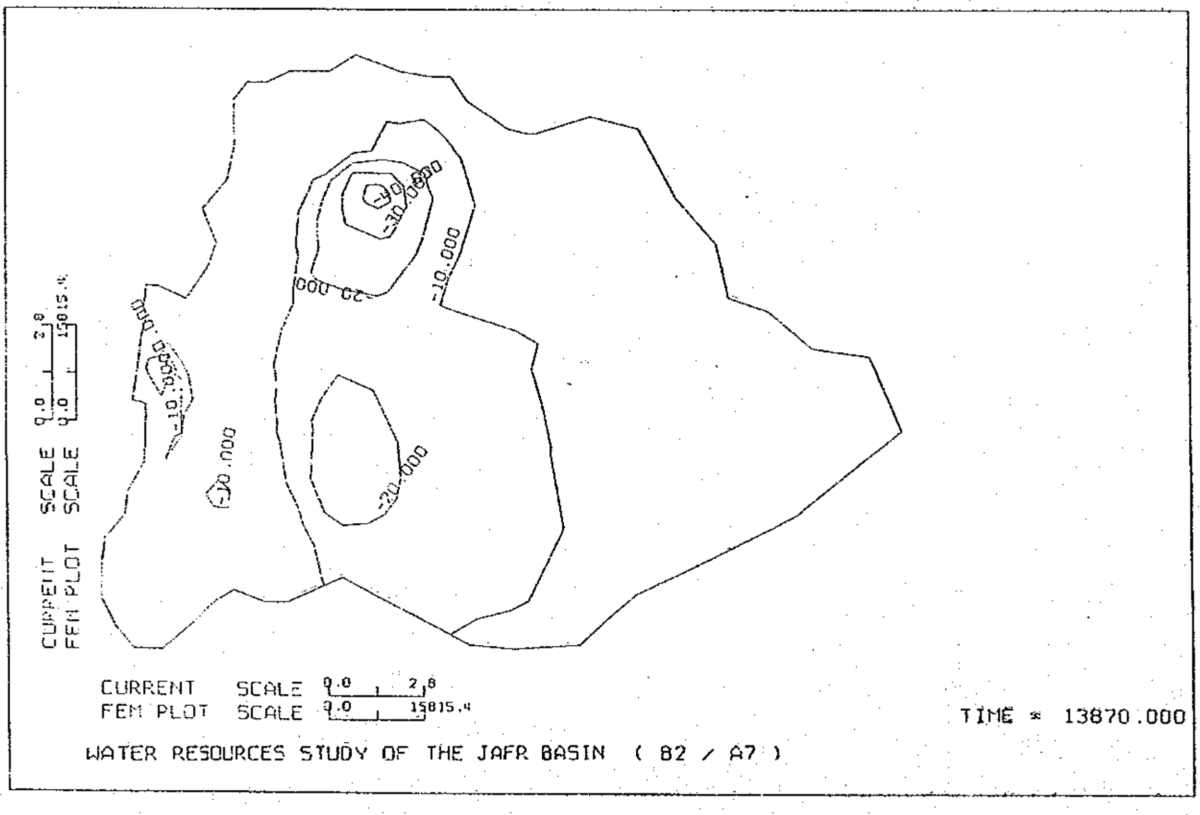

Fig. 5.32 Predicted Piezometric Surface of B2/A7 with Groundwater Recharge Dam; After 20 Years Pumping and Recharging

THE HASHEMITE KINGDOM OF JORDAN

WATER RESOURCES STUDY OF THE JAFR BASIN

JAPAN INTERNATIONAL COOPERATION AGENCY

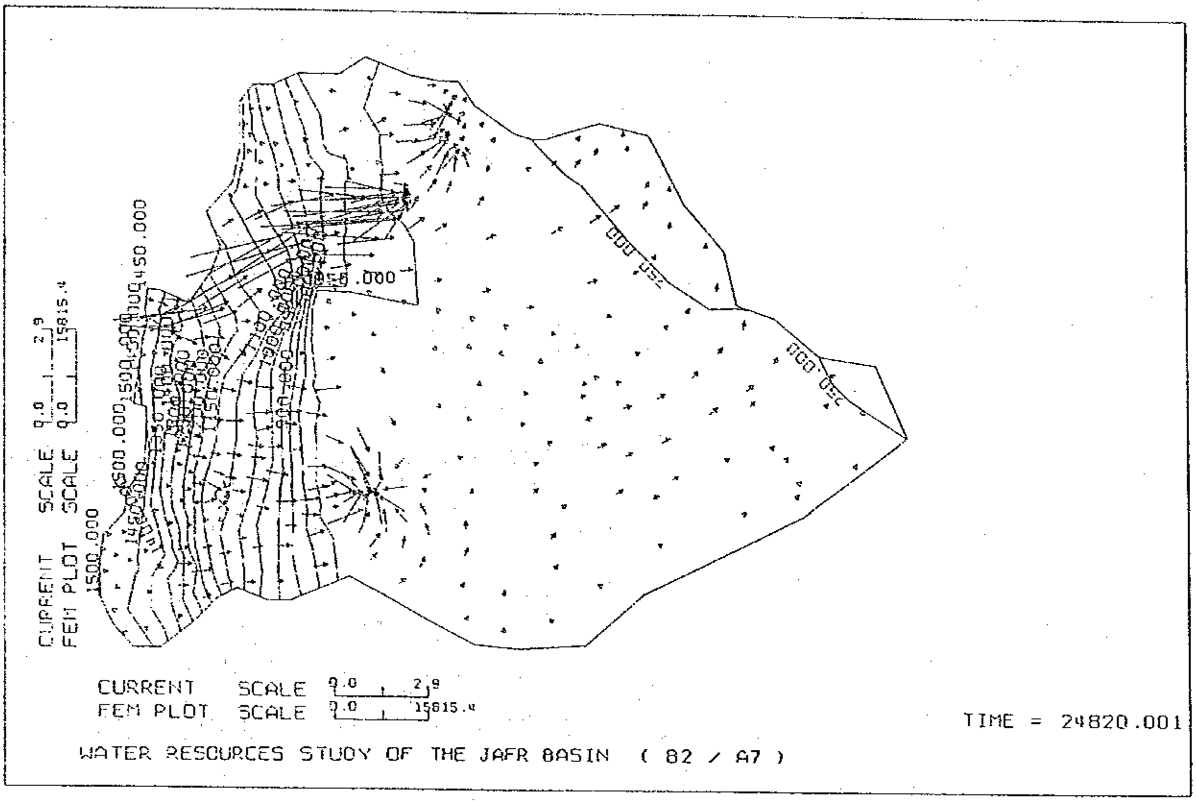

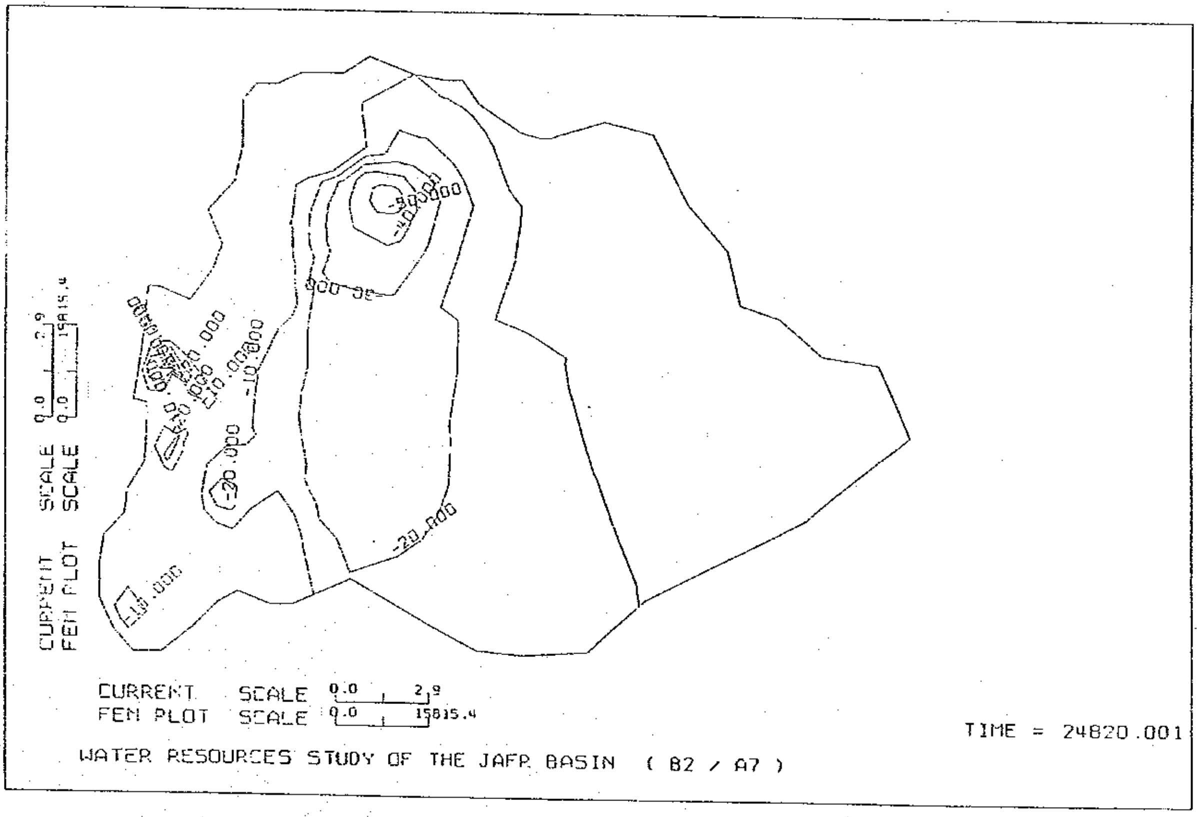

Fig. 5.33 Predicted Piezometric Surface of B2/A7 with Groundwater Recharge Dam; After 50 Years Pumping and Recharging

THE HASHEMITE KINGDOM OF JORDAN

WATER RESOURCES STUDY OF THE JAFR BASIN

JAPAN INTERNATIONAL COOPERATION AGENCY

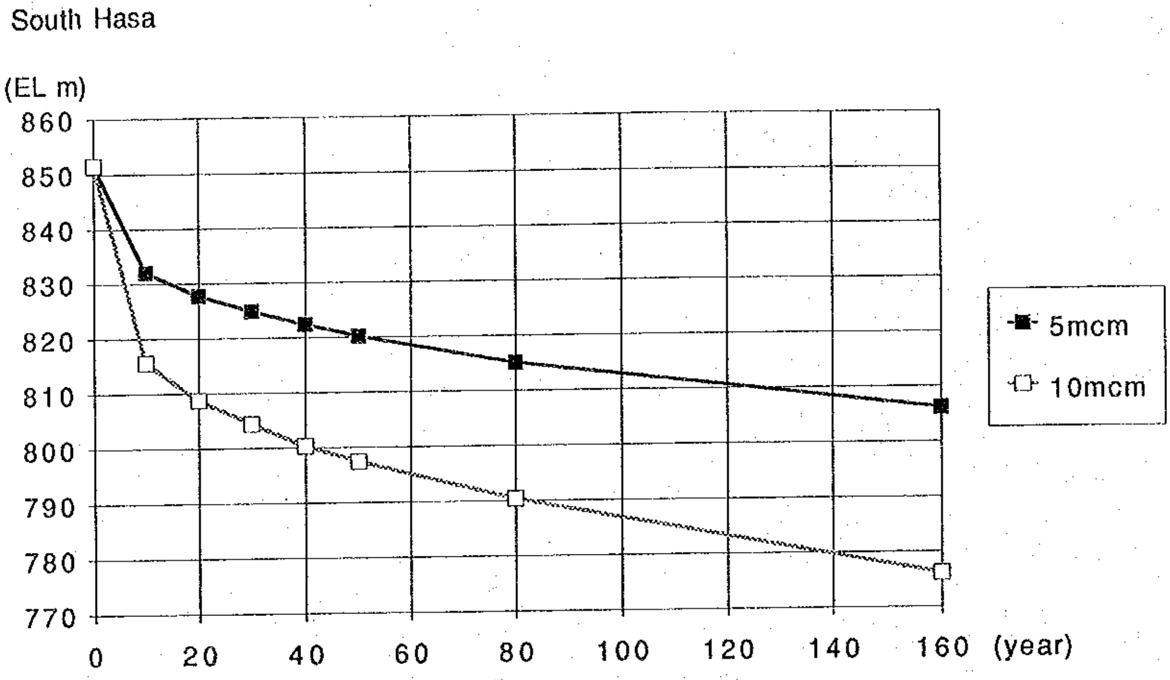

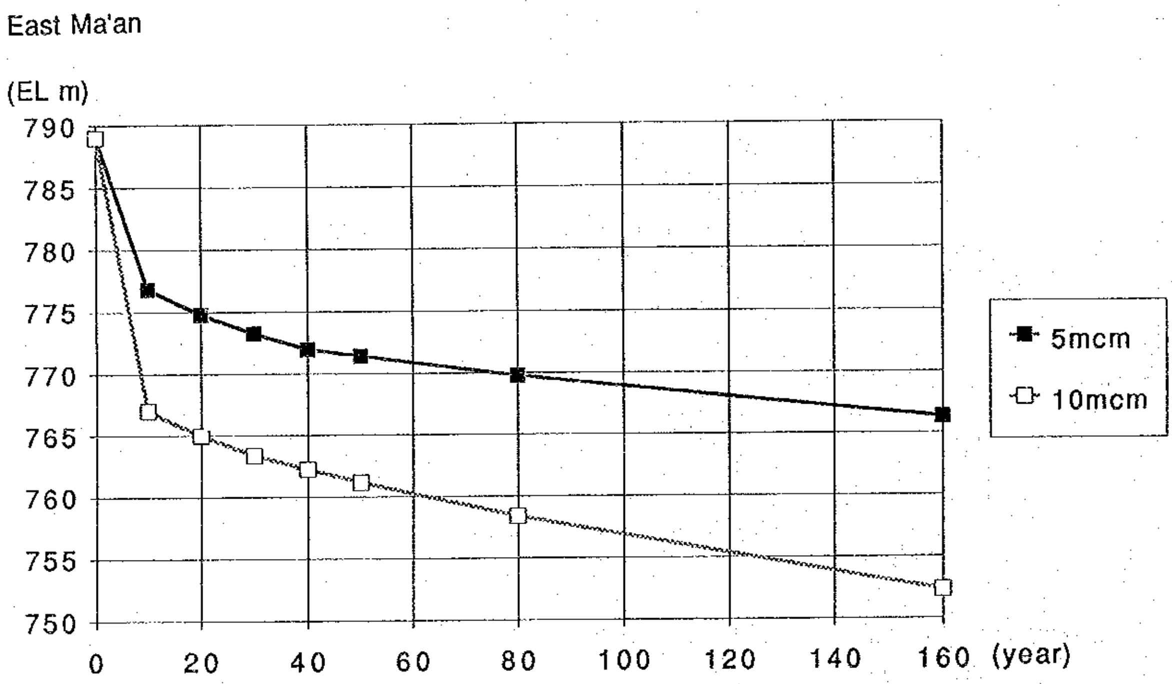

Fig.5.34 Estimated Drawdown in Representative Wellfields

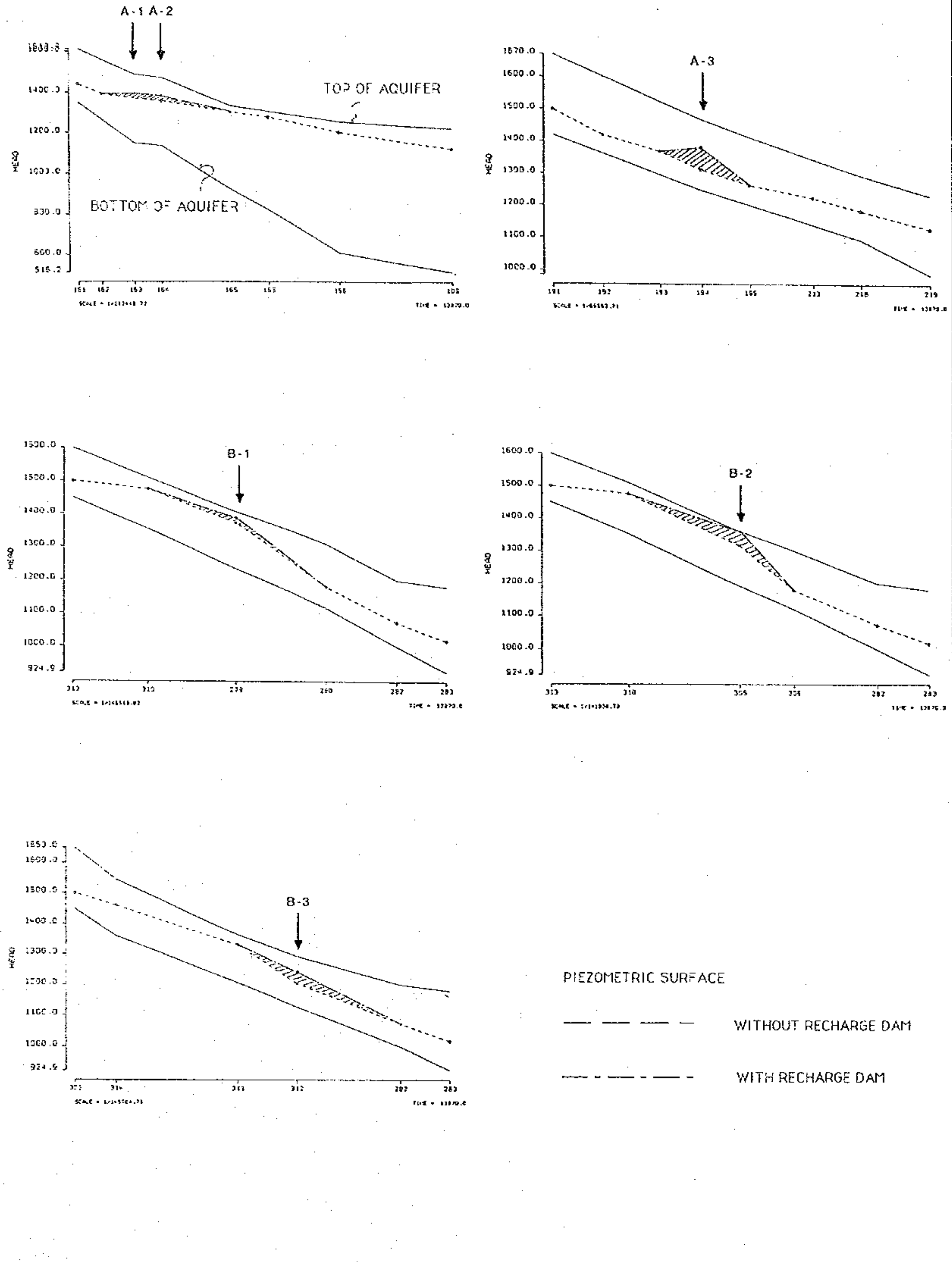

Fig.5.35 Estimated Change in Piezometric Surface by Recharge Dams

THE HASHEMITE KINGDOM OF JORDAN

WATER RESOURCES STUDY OF THE JAFR BASIN

JAPAN INTERNATIONAL COOPERATION AGENCY

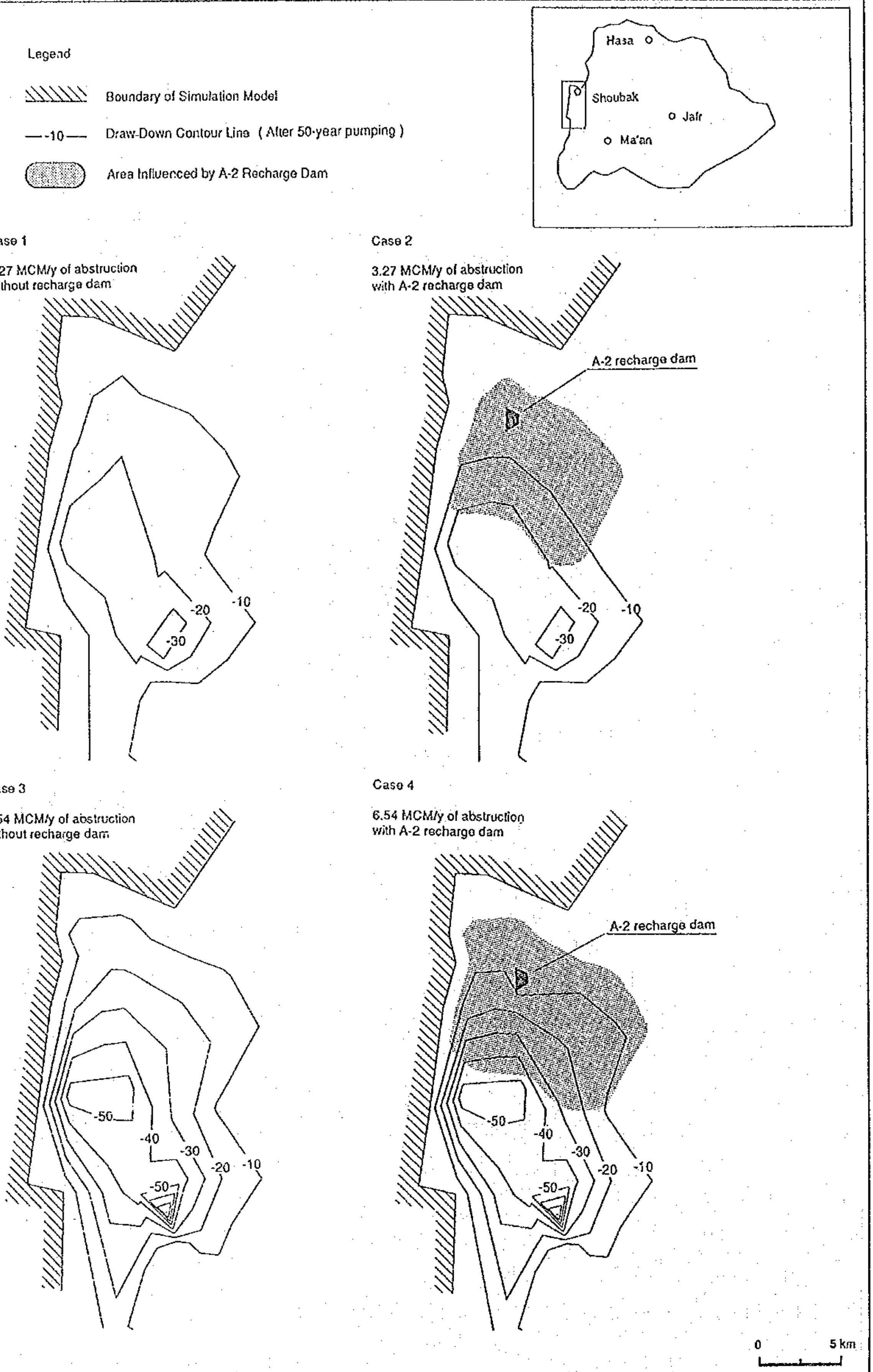

Fig.5.36 Area Affected by the A-2 Recharge Dam

THE HASHEMITE KINGDOM OF JORDAN

WATER RESOURCES STUDY OF THE JAFR BASIN

JAPAN INTERNATIONAL COOPERATION AGENCY

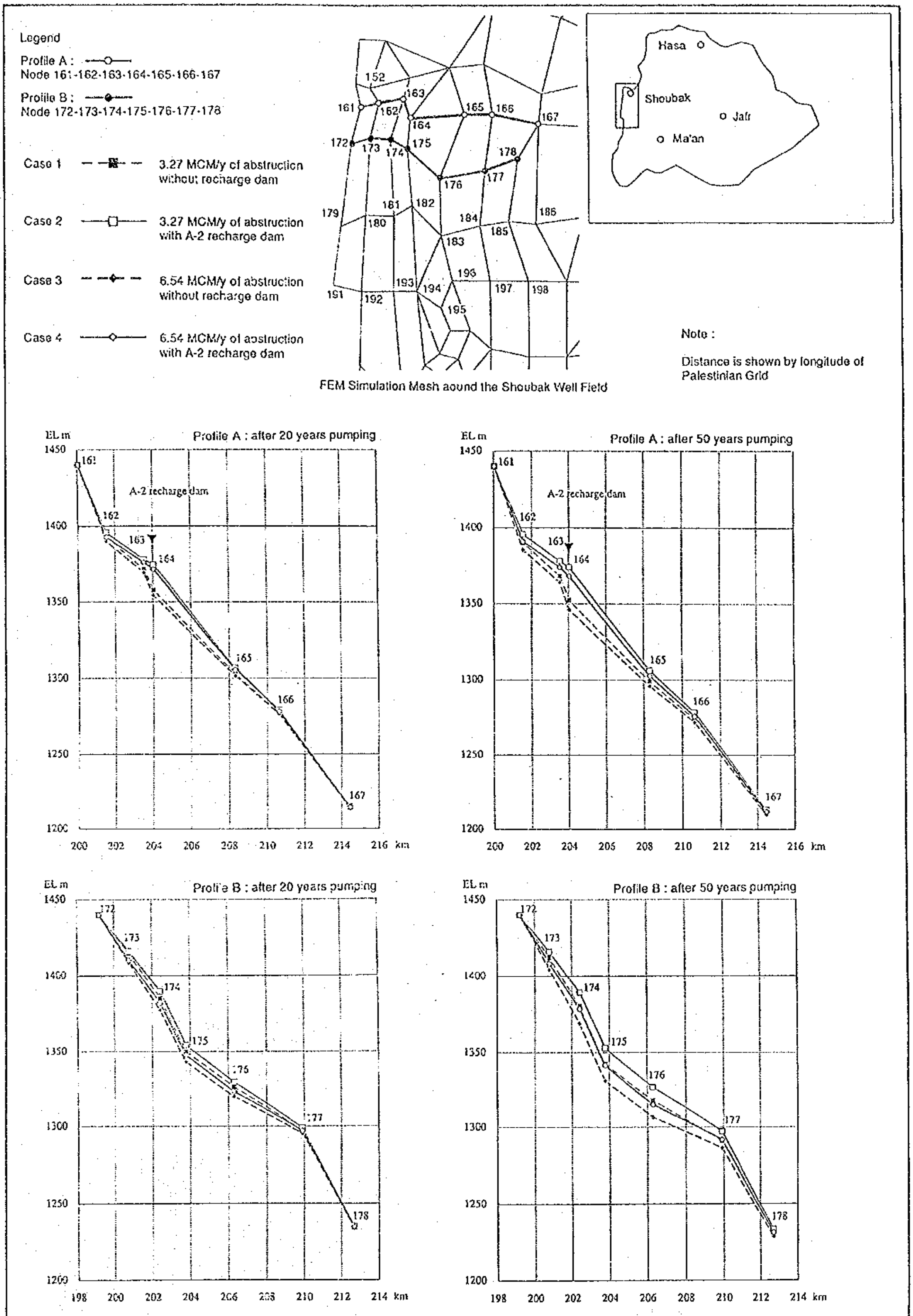

Fig.5.37

Profile of Piezometric Surface in the Shoubak Area (1/2)

THE HASHEMITE KINGDOM OF JORDAN

WATER RESOURCES STUDY OF THE JAFR BASIN

JAPAN INTERNATIONAL COOPERATION AGENCY

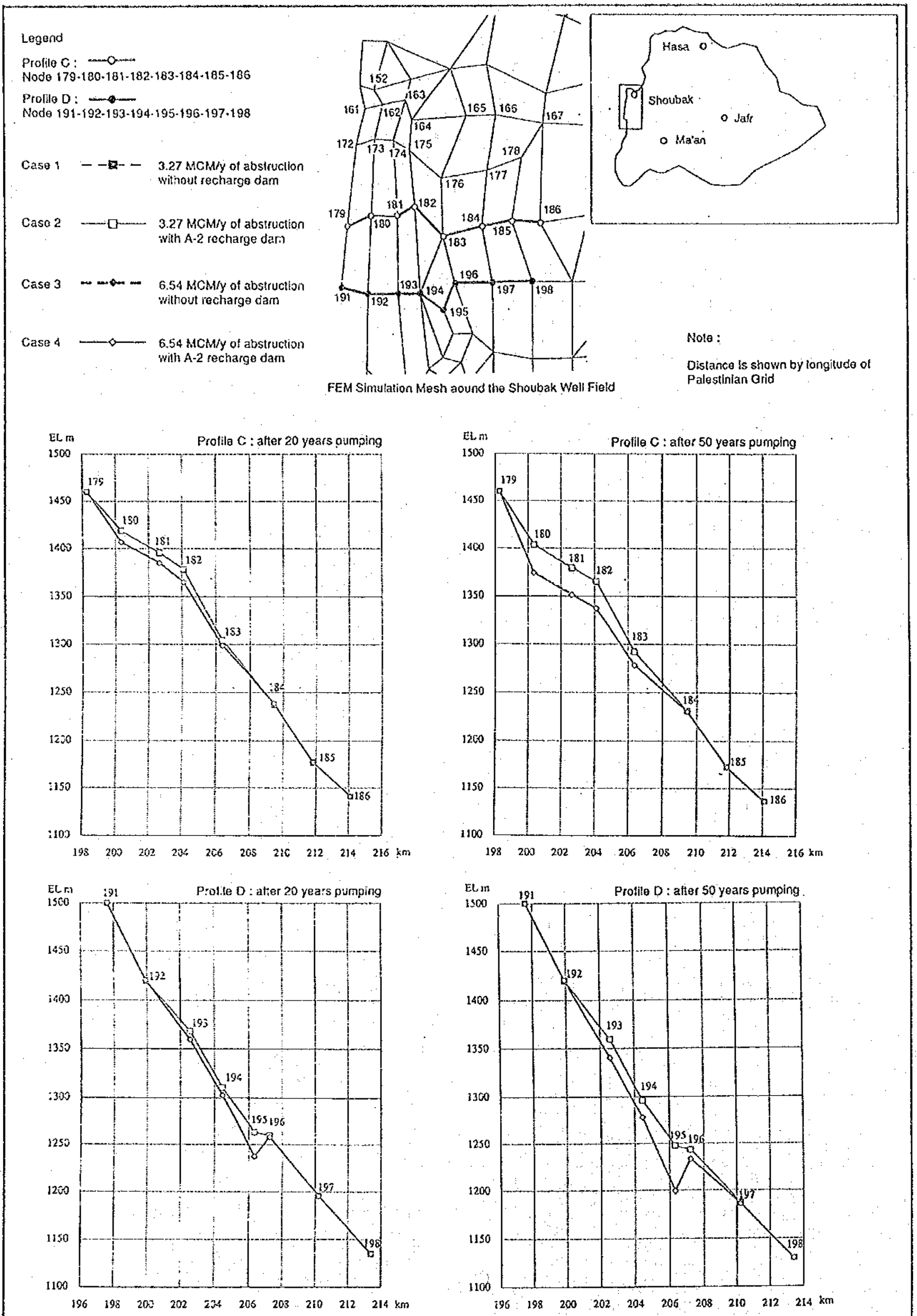

Fig.5.38

Profile of Piezometric Surface in the Shoubak Area (2/2)

THE HASHEMITE KINGDOM OF JORDAN

WATER RESOURCES STUDY OF THE JAFR BASIN

JAPAN INTERNATIONAL COOPERATION AGENCY

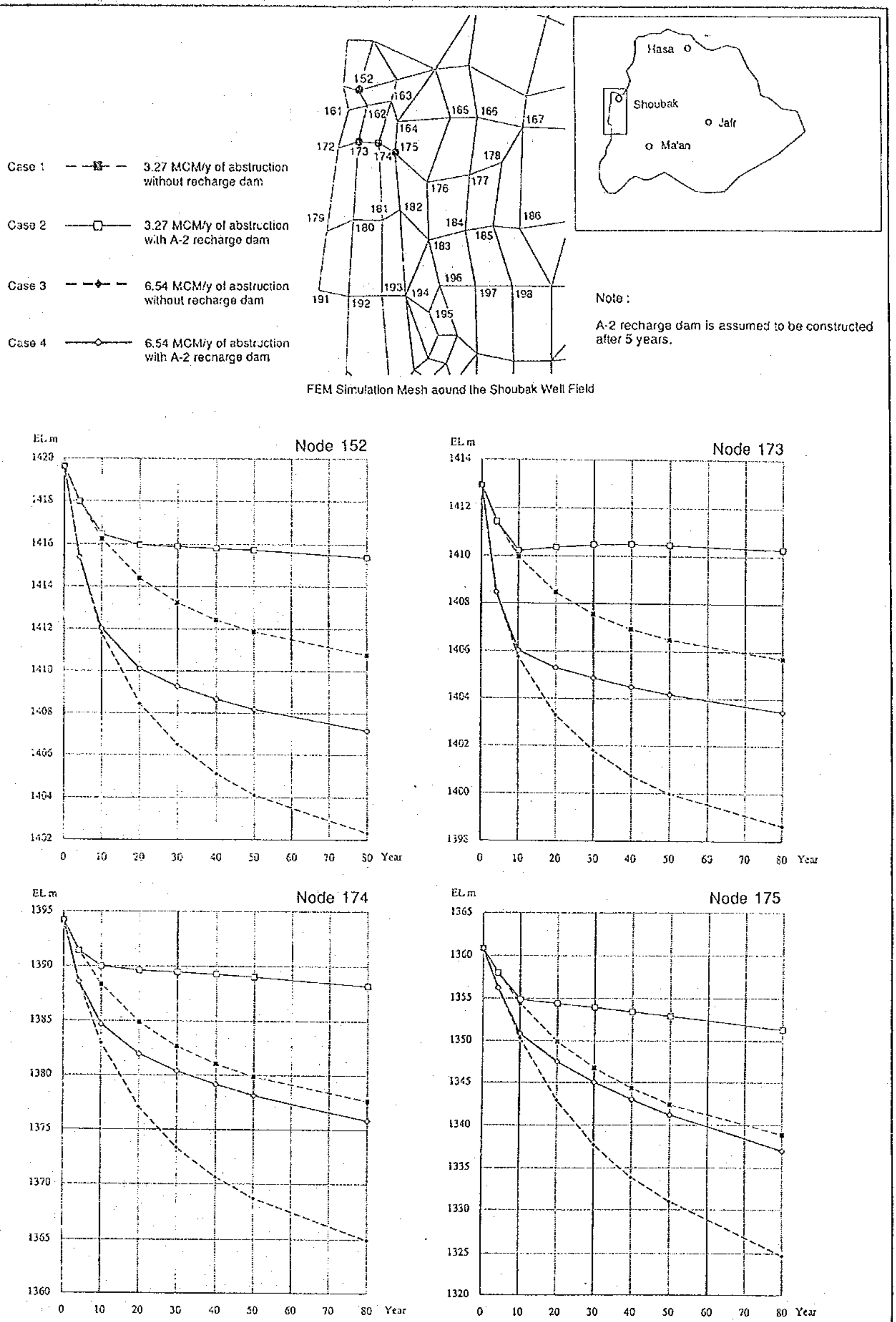

Fig.5.39

Predicted Piezometric Levels for the Mesh Nodes in the Shoubak Area (1/3)

THE HASHEMITE KINGDOM OF JORDAN

WATER RESOURCES STUDY OF THE JAFR BASIN

JAPAN INTERNATIONAL COOPERATION AGENCY

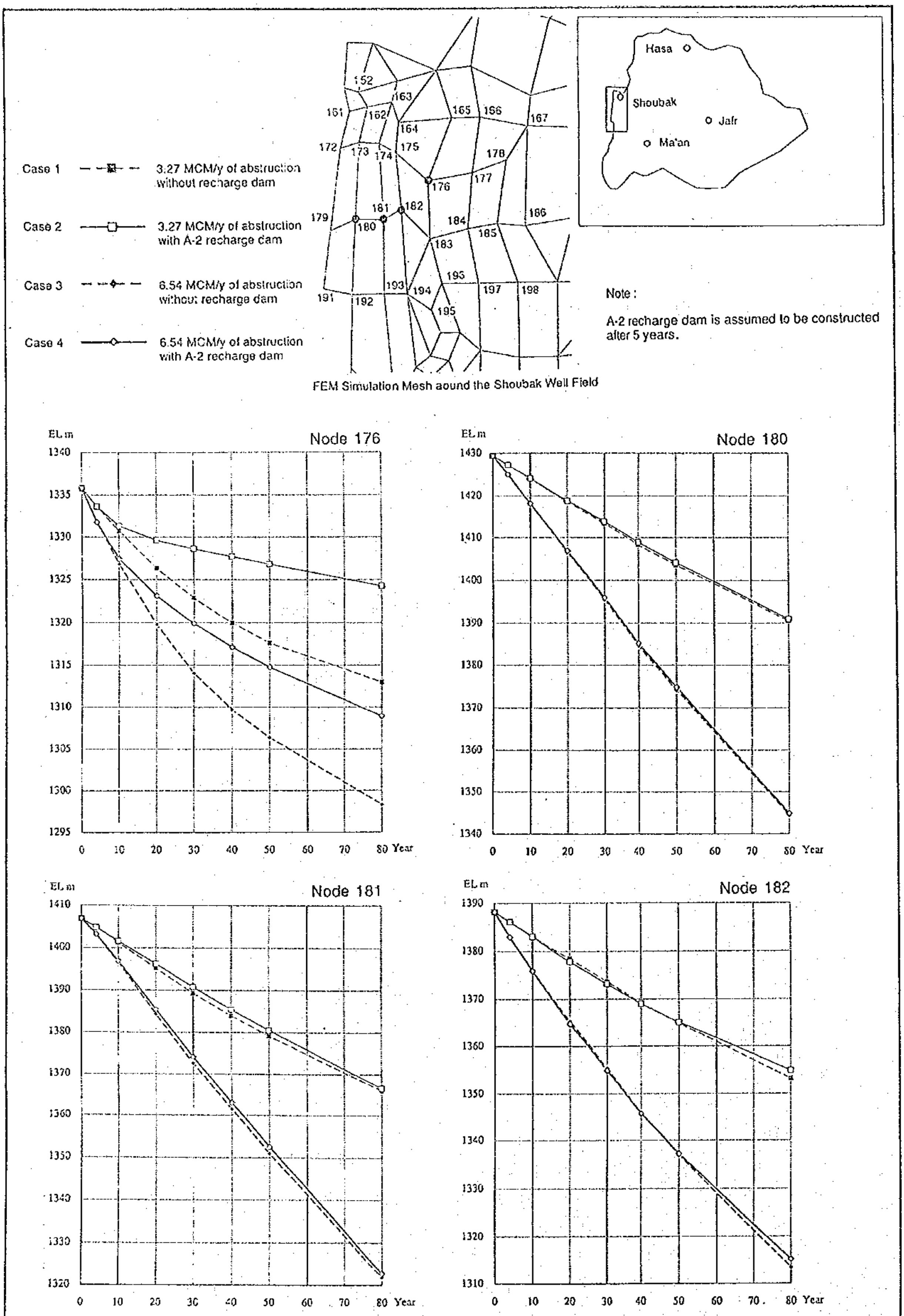

Fig.5.40

Predicted Piezometric Levels for the Mesh Nodes in the Shoubak Area (2/3)

THE HASHEMITE KINGDOM OF JORDAN

WATER RESOURCES STUDY OF THE JAFR BASIN

JAPAN INTERNATIONAL COOPERATION AGENCY

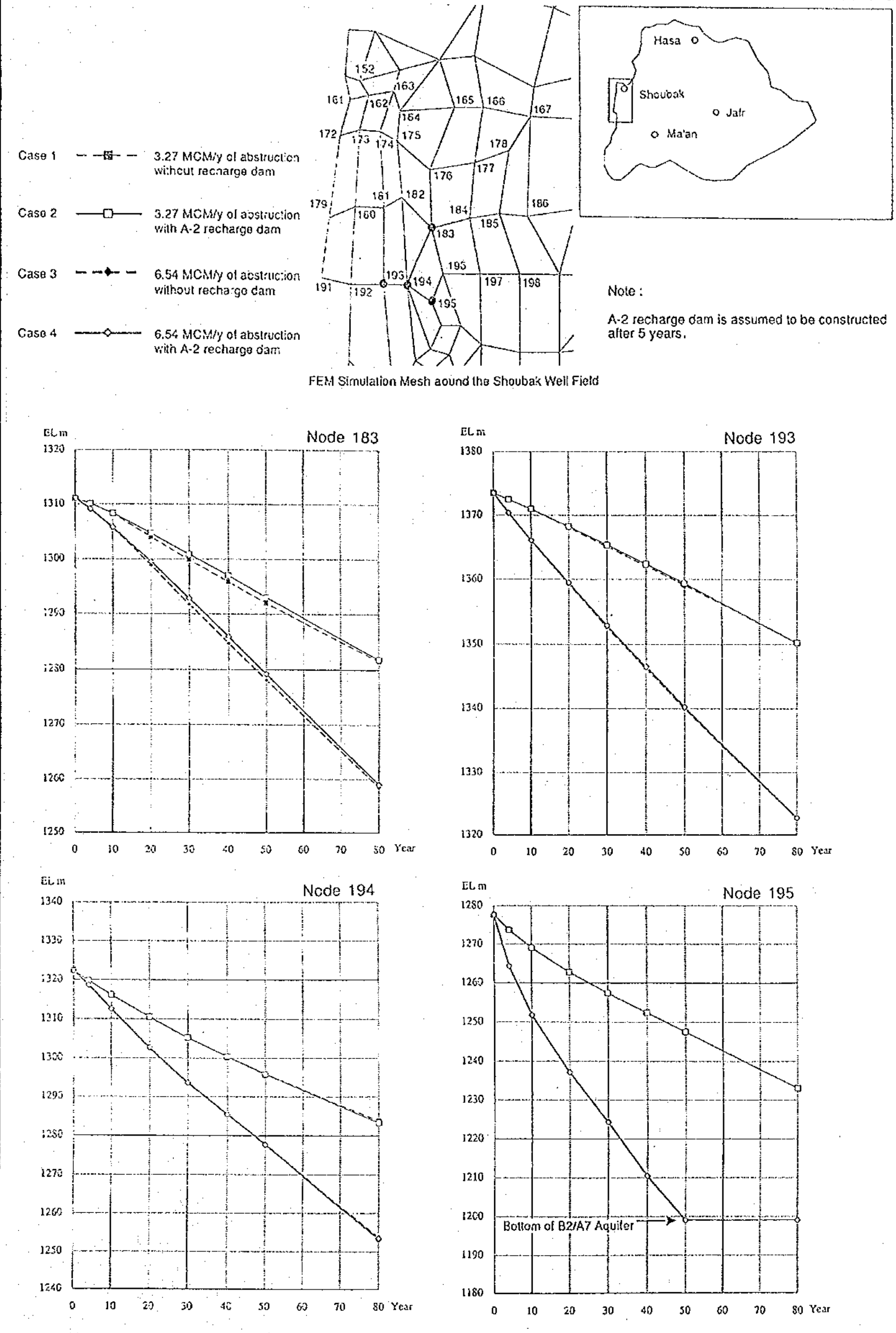

Fig.5.41

Predicted Piezometric Levels for the Mesh Nodes in the Shoubak Area (3/3)

THE HASHEMITE KINGDOM OF JORDAN

WATER RESOURCES STUDY OF THE JAFR BASIN

JAPAN INTERNATIONAL COOPERATION AGENCY

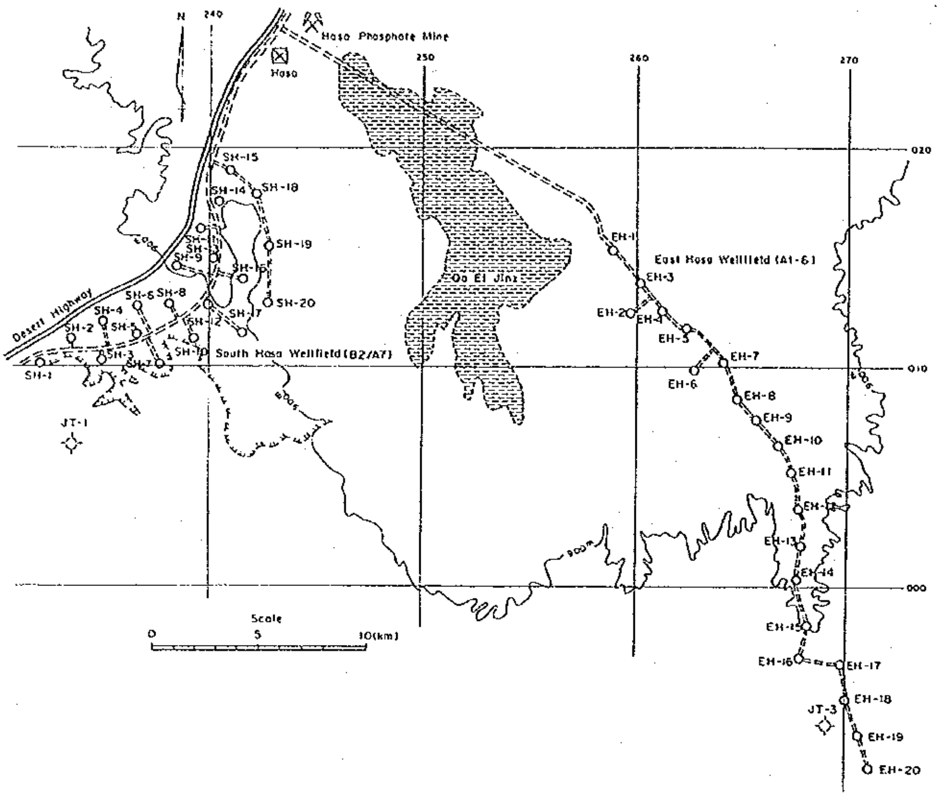

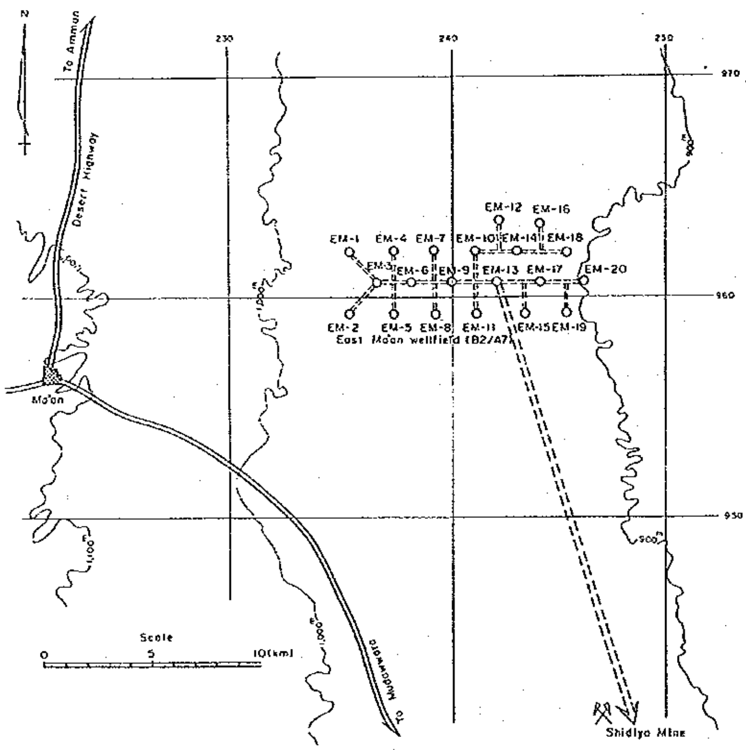

Fig.5.42

Preliminary Design of Proposed Wellfields

THE HASHEMITE KINGDOM OF JORDAN

WATER RESOURCES STUDY OF THE JAFR BASIN

JAPAN INTERNATIONAL COOPERATION AGENCY

VI. SALT ACCUMULATION PROBLEMS IN RIJAM (B4) AQUIFER

VI. SALT ACCUMULATION PROBLEMS IN RIJAM (B4) AQUIFER

6.1 Present Conditions

At Al Jafr town in the central Jafr basin, irrigation has been practiced by pumping groundwater from shallow unconfined aquifers in the Rijam (B4) formation since 1965. Since around 1971, salinity of the Rijam (B4) aquifer increased and its yield has already become unsuitable for irrigation use on farmland at Al Jafr town (See Fig.6.1 and Fig.6.2). At the Jafr No.17 well located in the farmland, salinity increased from 500 ppm to 2,000 ppm after 6 years of pumping and reached 3,400 ppm in 1975 (See Fig.6.2). Because of the saline contamination of the aquifer, two wells in the farmland have been temporarily abandoned and the pumping amount of other wells have been decreased.

6.2 Mechanism of Salinity Accumulation

Where saline contamination has become a serious problem, the Rijam (B4) aquifer is intercalated between the Alluvium layer and the impervious Mudawwara formation (B3). The part near the ground surface of the Alluvium layer is a root zone where plants are able to absorb water for growth (See Fig. 6.3).

With downward movement of irrigation water, salt is transported to the root zone. Once a year before sowing, initial leaching is conducted to remove concentrated salt from the root zone. Annually,about 10 % of leaching water is considered to reach the saturated Rijam (B4) aquifer as deep percolation. This is based on agronomic findings that 10 % in volume of the pore in the unsaturated soil layer below the root zone is pores of a the size larger than several microns through which free movement of pore water is possible, not being surrounded by capillary pores, and the remaining 90 % is capillary pores with the size less than several microns in which free movement of pore water is impossible due to capillary attractions. The remaining 90 % of leaching water is trapped in the unsaturated soil layer beneath the root zone.

The VLF (Very Low Frequency) survey conducted by JICA study team in 1988 has shown that the salinity-affected aquifer is known to be quite limited and stagnant in movement in the horizontal direction: transmissivities of adjacent salinity-less B4 aquifer which are situated west of the salinity-accumulated aquifer is 50 m^2/day and is considered to contribute to dilution of the salinity-accumulated aquifer

Accordingly, it is assumed that accumulation of salinity in the Rijam (B4) aquifer is caused by the annual 10 % of leaching water which transports salt accumulated at the root zone by irrigation water together with salt contained in the 10 % of leaching water itself, while the salinity-accumulated aquifer is continually diluted by adjacent salinity-less aquifers.

6.3 Simulation of Salinity Accumulation

Based on the conditions described in Section 6.2, a simulation model of salinity accumulation of the Rijam (B4) aquifer is constructed as shown in Fig.6.3. T.D.S. of the salinity-accumulated Rijam (B4) aquifer is derived from the equations as follows.

$$W31(i) = W32(i-1) + I2(i) + I3(i) + I4$$

$$W32(i) = W31(i) - I5(i)$$

$$H32(i) = W32(i)/A2/B/SY \times 100$$

and

$$I2(i) = Q1(i) \times A1 \times X1(i)$$

$$I3(i) = Q2 \times Y/100 \times X1(i) \times A1/1000$$

$$I4 = TR \times 365 \times W \times X4/10^6$$

$$I5(i) = (Q2 \times Y \times A1/100 + TR \times 365 \times W/1000) \times H31(i)/1000$$

where

W31(i) (ton) : Cumulative salt content of the salinity-accumulated Rijam (B4) aquifer before dilution at the end of i-th year

W32(i) (ton) : Cumulative salt content of the salinity-accumulated Rijam (B4) aquifer after dilution at the end of i-th year

H32(i) (ppm) : T.D.S. of the salinity-accumulated Rijam (B4) aquifer at the end of i-ty year

I2(i) (ton) : Transport of salt contained in irrigation water to the salinity-accumulated Rijam (B4) aquifer during i-th year

I3(i) (ton) : Transport of salt contained in leaching water to the salinity-accumulated Rijam (B4) aquifer during i-th year

I4 (ton) : Transport of salt contained in neighboring salinity-less aquifer to the salinity-accumulated Rijam (B4) aquifer during i-th year

I5(i) (ton) : Salt removed from the salinity-accumulated Rijam (B4) aquifer due to dilution

Q1(i)(m/year) : Irrigation water supply during i-th year

A1 (km^2) : Irrigation area

A2 (km^2) : Area of the salinity-accumulated Rijam (B4) aquifer

B (m) : Thickness of the salinity-accumulated Rijam (B4) aquifer

SY (%) : Specific yield of the salinity-accumulated Rijam (B4) aquifer

X1(i) (ppm) : T.D.S. of irrigation water during i-th year

X4 (ppm) : T.D.S. of neighboring salinity-less aquifer

Q2 (mm/year) : Amount of leaching water

Y (%) : Rate of leaching water transformed into deep percolation which transports salt to the salinity-accumulated Rijam (B4) aquifer

TR (m^2) : Transmissivity of salinity-less aquifer around the salinity-accumulated Rijam (B4) aquifer

W (m) : Width of an assumed groundwater channel through which salinity-less groundwater flows into salinity-accumulated aquifer for dilution

In the simulation, the following parameters are assumed.

a) A1 : Area of the irrigation area = 1 km^2

b) A2 : Area of the Rijam (B4) aquifer = 1 km^2

c) B : Thickness of the saturated Rijam (B4) aquifer = 22 m

d) SY : Specific yield of the saturated Rijam (B4) aquifer (Ref.6.1) = 10 %

e) Q1 : Annual irrigation water requirement :
  - Year 1966 to 1975 = 1.00 m/year
  - Year 1976 to 1983 = 0.31 m/year
  - Year 1986 to 1987 = 0.55 m/year

f) Q2 : Annual water requirement for initial leaching = 300 mm/year

g) Y : Rate of leaching water causing the salinity accumulation of the Rijam (B4) aquifer = 10 %

h) X1 : T.D.S. of irrigation water = 500 ppm

i) Initial value of T.D.S. of the saturated Rijam (B4) aquifer = 500 ppm

j) X4 : T.D.S of adjacent salinity-less Rijam (B4) aquifer = 500 ppm

k) TR : Transmissivity of adjacent salinity-less Rijam (B4) aquifer = 50 m^2/day

l) W : Width of an assumed groundwater channel through which salinity-less groundwater flows into salinity-accumulated aquifer for dilution = 4 m

It is also assumed that no leaching has been made at the irrigation area in year 1966, 1967,1968 and 1986,1987.

As a result of simulation, T.D.S.(Total Dissolved Solid) of the saturated Rijam (B4) aquifer is estimated as shown on Table 6.1.

The simulated T.D.S. values are plotted with actually recorded T.D.S. values of the Jafr No.17 well and average T.D.S. values over the irrigation area(See Fig.6.2).

According to the simulation, the salinity-accumulation of the irrigation area is expected to decline to T.D.S. of about 1,000 ppm in year 2000, which is considered acceptable for irrigation use.

REFERENCES

6.1 Stanley N.Davis, Roger J. M. DeWiest, John Wiley & Sons, "Hydrogeology"

TABLES

Table 6.1 Simulated TDS of 1-km2-Large Irrigation Area

Year	Simulated TDS at Year End (ppm)
1966	500
1967	500
1968	500
1969	715
1970	1,017
1971	1,208
1972	1,390
1973	1,564
1974	1,730
1975	1,888
1976	1,889
1977	1,890
1978	1,891
1979	1,892
1980	1,893
1981	1,894
1982	1,895
1983	1,895
1984	1,823
1985	1,753
1986	1,687
1987	1,624
1988	1,564
1989	1,506
1990	1,452
1991	1,400
1992	1,350
1993	1,303
1994	1,258
1995	1,215
1996	1,174
1997	1,135
1998	1,097
1999	1,062
2000	1,028
2001	995
2002	965
2003	935
2004	907
2005	880

FIGURES

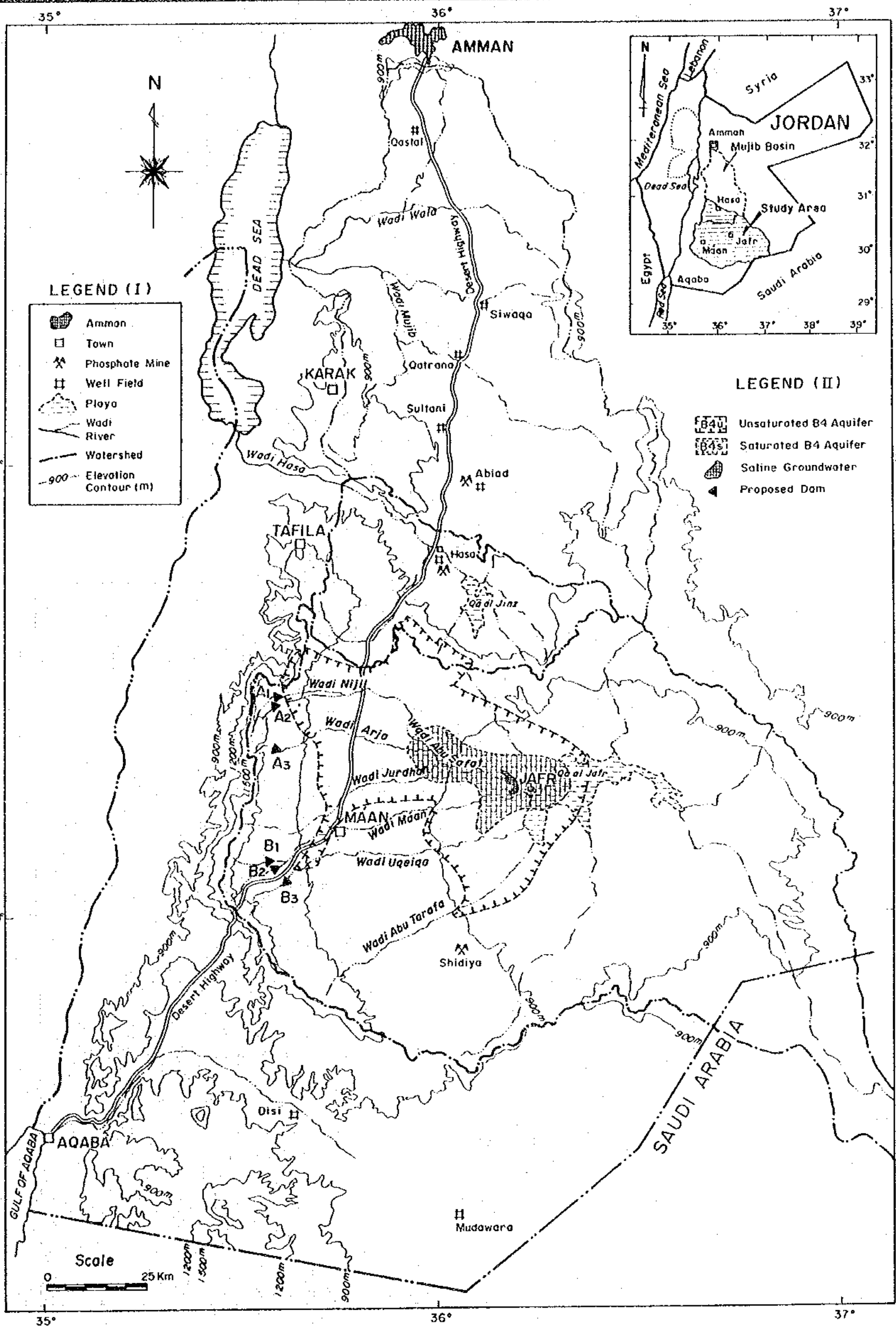

Fig. 6.1
Location of Salinity-Accumulated Area in Rijam (B4) Aquifer

THE HASHEMITE KINGDOM OF JORDAN
WATER RESOURCES STUDY OF THE JAFR BASIN
JAPAN INTERNATIONAL COOPERATION AGENCY

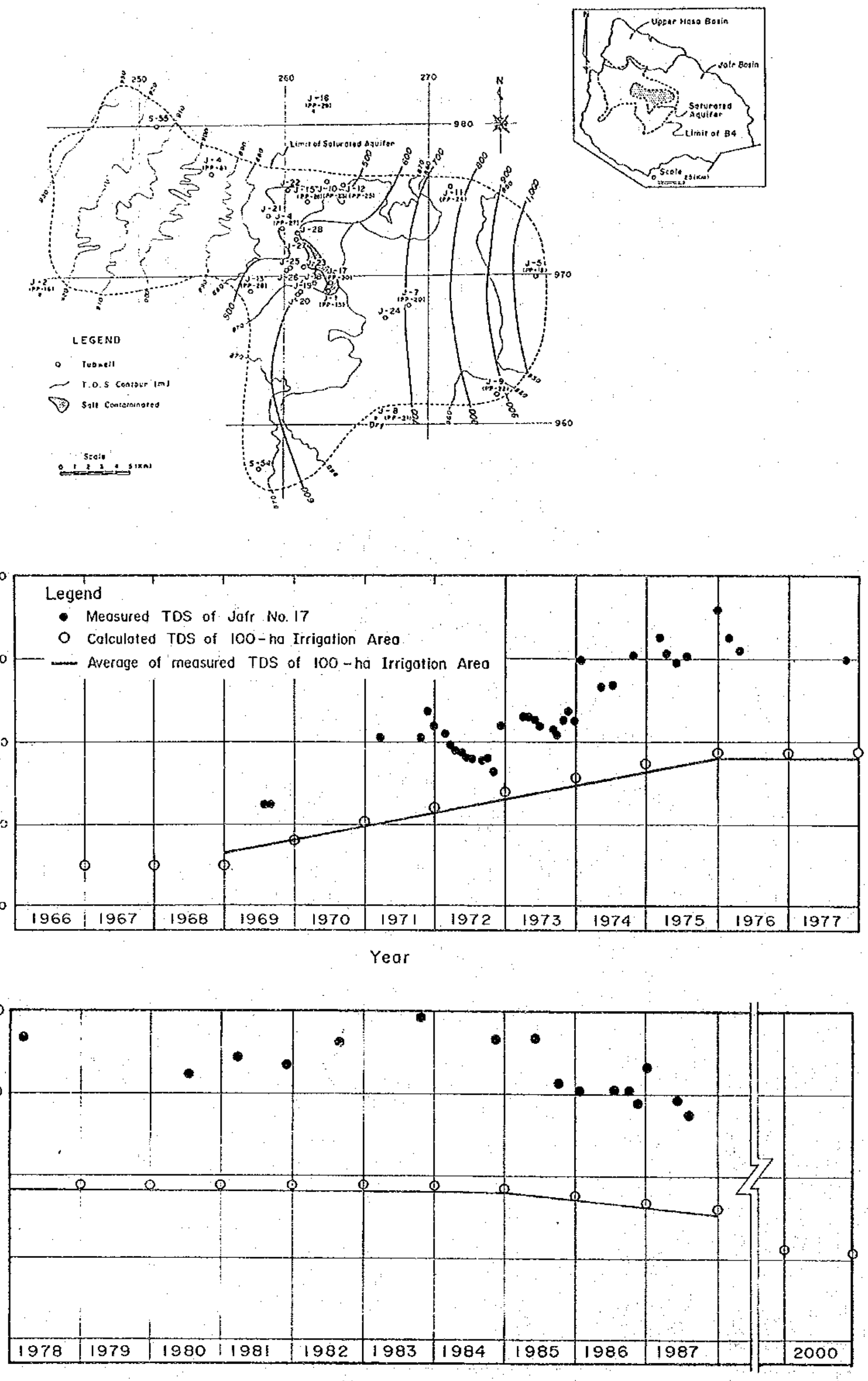

Fig. 6.2 Location of Salinity-Accumulated Area and Measured and Calculated TDS Values

THE HASHEMITE KINGDOM OF JORDAN
WATER RESOURCES STUDY OF THE JAFR BASIN
JAPAN INTERNATIONAL COOPERATION AGENCY

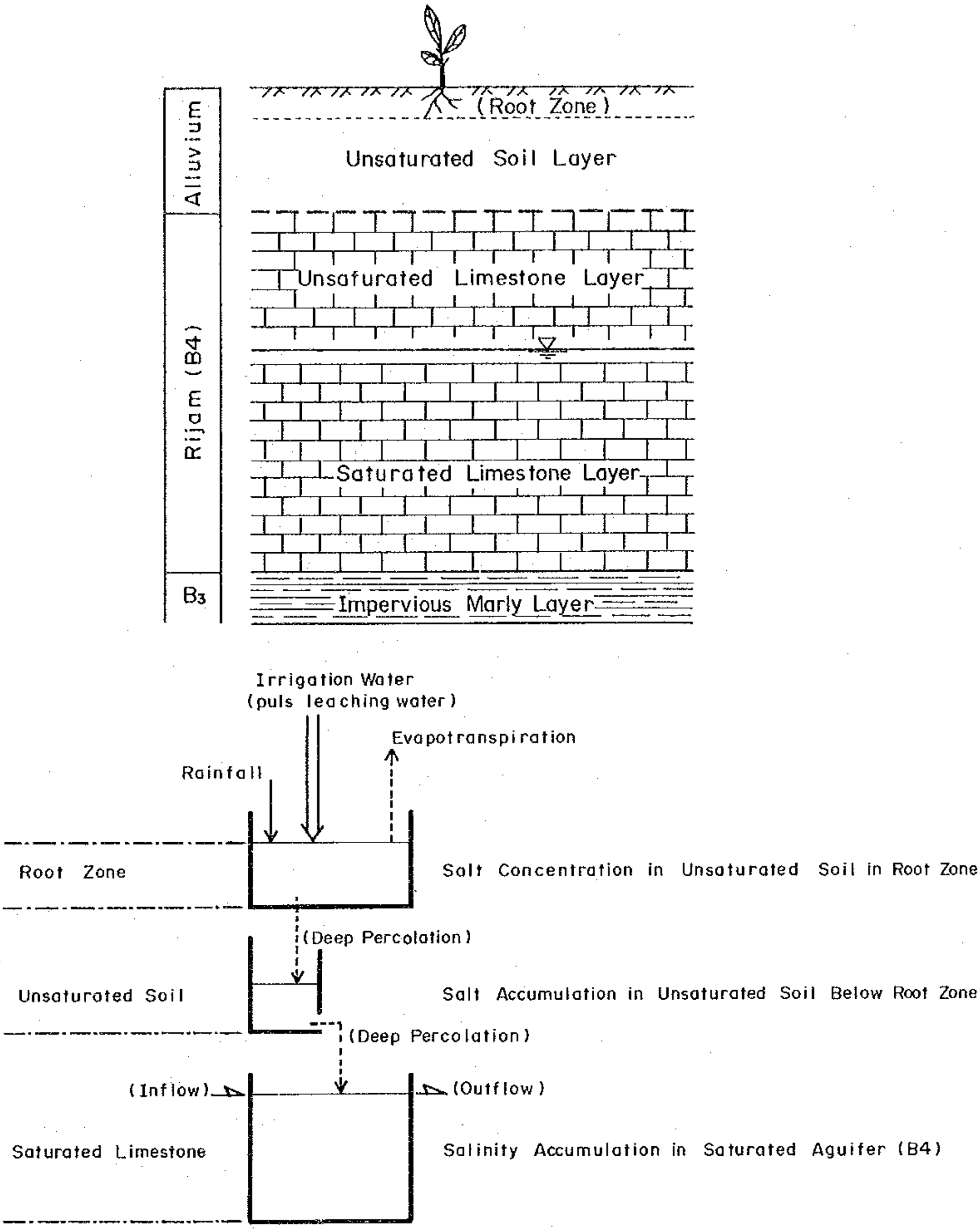

Fig. 6.3 Schematics of Salt Accumulation in Rijam (B4) Aquifer

THE HASHEMITE KINGDOM OF JORDAN

WATER RESOURCES STUDY OF THE JAFR BASIN

JAPAN INTERNATIONAL COOPERATION AGENCY

JICA